Institut für Medizinische Mikrobiologie, Immunologie und Hygiene
der Technischen Universität München

Development of immunological methods for detection of immunodeficiencies in mutant mice

Tobias Johannes Franz

Vollständiger Abdruck der von der Fakultät Wissenschaftszentrum Weihenstephan für Ernährung, Landnutzung und Umwelt der Technischen Universität zur Erlangung des akademischen Grades eines

Doktors der Naturwissenschaften

genehmigten Dissertation.

Vorsitzender:	Univ.-Prof. Dr. A. Gierl
Prüfer der Dissertation:	1. Univ.-Prof. Dr. M. Hrabé de Angelis
	2. Univ.-Prof. Dr. D. H. Busch

Die Dissertation wurde am 11.05.2005 bei der Technischen Universität München eingereicht und durch die Fakultät Wissenschaftszentrum Weihenstephan für Ernährung, Landnutzung und Umwelt am 20.06.2005 angenommen.

Die Ergebnisse dieser Arbeit sind zum Teil zur Veröffentlichung in „Infection and Immunity“ angenommen:

Pasche, B., Kalaydjiev, S., Franz, T.J., Kremmer, E., Gaius-Durner, V., Fuchs, H., Hrabé de Angelis, M., Lengeling, A., and Busch, D.H. (2005). Sex dependent susceptibility to *Listeria* infection is mediated by differential IL-10 production.

I TABLE OF CONTENTS

II INDEX OF FIGURES

III ABBREVIATIONS

Ab	Antibody
Ag	Antigen
AMP	Ampicillin
APC	Allophyco-cyanin
BHI	Brain-heart infusion medium
BSA	Bovine serum albumin
CBA	Cytometric bead array
CD	Cluster of differentiation
CFSE	Carboxy-fluoresceindiacetat succinimidyl ester
CFU	Colony forming unit
CTL	Cytotoxic T cell
Cy5	Cyanin 5
DNA	Deoxyribonucleic acid
ELISA	Enzyme-linked immunosorbent assay
ENU	N-Ethyl-N-nitrosourea
EMA	Ethidiummonazid-bromide
FACS	Fluorescence activated cell sorting
FCS	Fetal calf serum
FITC	Fluorescein-isothiocyanat
FOP	Fibrodysplasia Ossificans Progressiva
GBF	German Research Center for Biotechnology
GMC	German Mouse Clinic
GSF	National Research Center for Environment and Health
IFN	Interferon
IL	Interleukin
IL-10R	Interleukin-10 receptor
i.p.	Intraperitoneal
i.v.	Intravenously
KO	Gene knockout
L.m.	*Listeria monocytogenes*
mAb	Monoclonal antibody
MHC	Major histocompatibility complex
mLN	mesenterial lymph node
MML	Mutant mouse line
PBMC	Peripheral blood mononuclear cell
PE	Phycoerythrin
PE-Cy5	Phycoerythrin-cyanin 5
PFA	Paraformaldehyde
SD	Standard deviation
S.p.	*Streptococcus pyogenes*
SPF	Specific pathogen free
TCR	T cell receptor
Th	T helper
THY	Thymus
TNF	Tumor necrosis factor
TUB	Technical University Busch
TUBV	Technical University Busch variant
wt	wildtype

1 Introduction

1.1 Immunogenetics

1.1.1 Inherited human immunodeficiencies

Immunogenetics has become an important field of research (van der Pouw Kraan et al., 2004) for understanding the pathogenesis of inherited human immunodeficencies and several inflammatory diseases. Developments over the past decades also lead to the identification of novel genes with distinct immunological functions (Fischer, 2001).

In 1952, Ogden C. Bruton described the first inherited human immunodeficiency disease in a male patient (Bruton, 1952), later called the Bruton's X-linked agammaglobulinemia (Bruton et al., 1952). With the help of genealogy studies it turned out that the genes responsible for many immunological deficiencies are located on the X chromosome and that the effects of defects in these genes are mainly recessive (Fischer, 2002). In addition to general defects of the entire immune system, e.g. X-linked severe combined immune deficiency (Leonard, 2001) (no B and T cells), a variety of different inherited immunodeficiencies have been described, affecting distinct parts of the immune system: Wiscott-Aldrich syndrome (Schutt et al., 1983) (impaired T cell activation), X-linked lymphoproliferative sydrome (Nichols, 2000; Purtilo et al., 1991) (B cell proliferation), INFγ- (Jouanguy et al., 1997) or IL-12-receptor deficiencies (Altare et al., 1998) (increased susceptibility to certain pathogens). In several cases, the responsible mutations have been uncovered, for example a defective CD40L in X-linked hyper-IgM syndrome (Seyama et al., 1998), lack of DAF and CD59 in paroxysmal nocturnal hemoglobinuria (Smith, 2004), or loss of Btk tyrosine kinase for X-linked agammaglobulinemia (Vihinen et al., 2000). However, the underlying genotype defects are still unclear for many other diseases like the common variable immunodeficiencies (Strober and Chua, 2000). Although much information about the complex network of genes regulating the immune system came and will come from the studies of inherited human immunodeficiency diseases (Fischer, 2004), ethic principles do not allow full understanding of pathophysiological mechanisms behind these entities. Therefore, the use of model organisms has proven to be very useful for basic research and subsequent adaptation of results to the human system present a very promising approach.

1.1.2 The mouse as model system

The practical use of animals as model system for resolving certain scientific questions has proven to be very useful. Decisions in favor of one or the other animal model are often guided by logistical and technical issues like cost factors, required housing conditions and animal handling, duration of generation times, or number of offspring. On the other side, it is important to choose experimental models where results can be successfully extrapolated to human physiology and diseases. Depending on the field of research, different organisms turned out to be appropriate. Well-known examples are found in the pioneering experiments of Thomas H. Morgan who used *Drosophila melanogaster* to define basics of contemporary genetics, and is still used nowadays (Joshi, 2003; Sokolowski, 2001). In addition, *Caenorhabditis elegans* is often utilized for neurological studies (Chalfie and Au, 1989; Zhang et al., 2002) or *Danio rerio* (zebra fish) for developmental research (Glass and Dahm, 2004; Traver et al., 2003). A very attractive model organism for nearly all areas of biological research became the mouse system (Boyse, 1977; Denny and Justice, 2000; Lee et al., 2001), as many technical requirements have been solved for undertaking genetic research and manipulations in this species. Main reason for why immunological studies performed in the mouse are so valuable is the high physiological homology between mouse and man (International-Human-Genome-Sequencing-Consortium, 2004). This similarity has recently gained a strong prove after the complete genomes of both these mammalian species were sequenced (Gregory et al., 2002; Venter et al., 2001). Comparative analysis between mouse and man revealed genomic sequence homology of approximately 40%, even up to 90% within the protein-coding regions, indicating that the obvious differences between both species are mainly not based on the DNA sequence level, but on species-specific regulation of gene expression, different splice variants or protein modifications after transcription (Waterston et al., 2002). The usefulness of this model has been demonstrated by numerous studies, including in the field of immunology (Rogner and Avner, 2003; Shultz, 1991). Important knowledge about crucial signaling pathways (Mak et al., 2001) and the regulation of the immune system during bacterial or viral infections, still a major cause of morbidity and mortality worldwide (World-Health-Organization, 2003), have been gained from infection studies using mouse models (Lengeling et al., 2001). These results significantly increased our understanding of host-pathogen interactions, and set promises for advances in human therapy or the development of more effective vaccination strategies.

Besides being a milestone in biological research, the decoding of entire genomic sequences of different species has facilitated approaches for the manipulation of the genome, providing

helpful tools for either generation or mapping of mutations, but also opening new directions of research, like investigations on epigenetics (Jiang et al., 2004). These examinations will in the future not only focus on the analysis of certain genes and the role of their corresponding proteins in an organism, but also include the genome itself (Van de Vijver et al., 2002). It becomes more and more clear that the organization of the genome, the complex regulation of its structure and therefore the accessibility for gene regulatory elements, like transcription factors, is one of the most important features for understanding the molecular mechanisms of gene expression (Lee, 2003). Thereby, this complex regulatory network of gene silencing or enhancement seems to have severe consequences for the susceptibility and development of certain diseases, including cancer (Egger et al., 2004).

1.2 Technologies for mouse model generation

In principle, one can distinguish between two main approaches for the generation of mouse mutants, either the targeted manipulation of certain genes or random mutagenesis.

1.2.1 Reverse genetics

The expression “reverse genetics” is attributed to gene-targeted methods to generate mutant mouse lines. For this approach, the central starting point is a defined gene of interest and main goal is to uncover its functional role *in vivo*. Several methods have been established to produce mice in which the expression and/or the amount of a certain gene products is altered as compared to the not manipulated organism. By subsequent analysis of the phenotype of those mice, conclusions can be made with respect to the function of the manipulated gene in a living organism.

Reverse genetic approaches became possible because of the discovery and use of the natural phenomenon of homologous recombination, implicating the ability for integration of foreign DNA into the genome of a host cell. Cloning of the gene of interest, followed by its alteration and afterwards introduction into embryonic stem cells (ES cells) can lead to the replacement of the intact gene through the modified DNA: by pairing of homologous regions, the DNA strain breaks and subsequently replaces the wildtype allele with the mutated gene. Recent advances in successfully culturing a variety of different ES cell lines and the development of more efficient techniques of blastocyst injection for ES cells further facilitated this technology.

Most commonly used is the generation of gene-knockout (KO) mice, in which the expression of a gene of interest is prevented, usually resulting in a complete loss of a certain gene product and its different splice variants in the entire organism at all stages of development. In addition, transgenic mice have been generated, in which the amount or the expression pattern of certain proteins is altered by the use of different promoters or regulatory elements. By application of the powerful tool of transgenic or KO mice, today used in all fields of medical and biological research, the *in vivo* functions of many different molecules and their involvement in distinct physiological pathways have been elucidated. This includes immunological research, for example to determine the important role of TNF receptor signaling for effective innate immunity (Plitz et al., 1999), the essential function of perforin in functional T cell proliferation and host resistance against viral infections (Badovinac et al., 2003), or the key role of MyD88 in TLR signaling (Kawai et al., 1999). However, this technology has certain limitations, as the complete KO of several genes is lethal during embryogenesis or in the early postnatal period (Hrabe de Angelis et al., 1997; Pandolfi et al., 1995), making it impossible to uncover the role of these genes in adults, distinct tissues or after challenge with environmental factors, e.g. pathogens. In addition, it has been reported for several KO mice that due to the gene manipulation, the physiology of these animals has dramatically changed, not allowing further discrimination between direct or secondary effects of the gene KO on the observed phenotype (Pandolfi et al., 1995).

In order to overcome these limitations, inducible (Kuhn et al., 1995) and conditional (Rajewsky et al., 1996) methods have been developed for tissue- or time point-specific gene KO. Most frequently used is the Cre/lox system, based on the ability of the enzyme Cre recombinase to delete these parts of the genomic DNA that are positioned in between its specific recognition sequences, the so called lox-p sites. Flanking of essential regions for proper gene transcription and translation of a gene of interest, e.g. the transcription start point or several exons with lox-p sites in combination with expression of the Cre recombinase under an inducible or cell-type specific promotor leads to the controlled and tissue-specific deletion of the gene. By this approach new *in vivo* functions have been annotated to several genes for which the complete KO has turned out to be lethal, for instance the influence of delta1 on the development of marginal zone B cells *in vivo* (Hozumi et al., 2004) or Gata3 on Th_2 differentiation (Zhu et al., 2004). It also helped to elucidate the different consequences of IL-10 in dependency of its cellular origin (Roers et al., 2004), an important feature that remained unclear in the complete IL-10 KO (Kuhn et al., 1993).

1.2.2 Forward genetics

In contrast to reverse genetics, starting with a gene of interest followed by its mutation and subsequent analysis of the phenotype, forward genetics describes an opposite approach to generate new mutant mouse lines, in which not a distinct gene but a defined phenotype is the starting point for further investigations, with subsequent focus on the identification of the genetic reason for the observed abnormality. In the beginning, this phenotype-driven approach was limited to naturally occurring mouse mutants, usually only identified by obvious morphological phenotypes, like changes in coat color or skeleton deformations (Jackson, 1994; Jackson and Bennett, 1990). In order to enlarge the pool of mutants, over the last decades several physical and chemical methods have been tested to artificially increase the natural mutation rate (approximately $1x10^{-6}$ in mice (Balling, 1998)) by application of mutagens like chlorambucil or irradiation with x-rays, mainly causing chromosomal deletions, translocations or inversions (Rinchik et al., 1990). One of the most potent inducer of point mutations (Noveroske et al., 2000) turned out to be N-ethyl-N-nitrosourea (ENU), increasing the mutation rate for specific genes up to $1x10^{-3}$ (Russell et al., 1979), which is why ENU has become the most frequently used and best characterized chemical substance for mouse mutagenesis (Justice et al., 2000).

Comparing the two strategies for the generation of new mutant mouse lines, the specific advantage of the forward over the reverse genetic approach is the already existing phenotype, whereas there are several examples known from the literature, like single KOs of several members of the chemokine receptor family, in which much effort was put in the generation of a KO mouse, which subsequently was either embryonic lethal or, most likely due to redundancy in the system, showed no phenotype. Furthermore, the forward genetic approach allows the assignment of new functions to genes in an unbiased manner independent from previous assumptions about the potential roles of a gene (Appleby and Ramsdell, 2003).

The main goal but also challenge for forward genetic approaches is to finally identify the genetic mutation responsible for a defined phenotype. Although many advances have been made to improve and facilitate the localization of the mutation like the sequencing and publication of the mouse genome (Gregory et al., 2002) or new strategies for the mapping (Beier and Herron, 2004), the procedure to produce enough phenotype bearing progeny in a mixed background is still very lengthy and presents a main bottleneck of the forward genetic approach.

1.3 The phenotype gap

Whereas the generation of mutant mouse lines has been well-established and even transferred to large-scale mutant production via ENU mutagenesis (Hrabe de Angelis and Balling, 1998; Justice et al., 1999), gene-trap (Wurst et al., 1995), or conditional knock-in/knock-out technologies (Austin et al., 2004), the main bottleneck turns out to be the detailed and standardized phenotypic analysis in order to identify defined alterations in the immune system. Even many existing mouse resources have never been fully phenotyped, leaving an enormous source for potential mouse models of human diseases almost untouched. In order to face the challenge of standardized phenotypic analyses, several research centers around the world have initiated the development of generally accepted protocols for most comprehensive examinations of the mouse like the German Mouse Clinic, Munich, Germany (http://www.mouseclinic.de), the Eumorphia research program (http://www.eumorphia.org), the Mouse Clinic Institute, Strasbourg, France (http://www.mci.u-strasbg.fr) or the Center for Modeling Human Disease, Toronto, Canada (http://cmhd.mshri.on.ca), which will in the future remarkably contribute to the progress of genetic and biological research.

1.4 Homestasis and challenge screens

ENU mutagenesis is a very powerful tool for the effective generation of novel mutant mouse lines, which help to improve our understanding in a variety of different fields of biological research (Nolan et al., 2000b), what is best indicated by the increasing number of research centers around the world, which carry out ENU mutagenesis (Figure 1).

Research center/ENU program	Website
German ENU-Mouse Mutagenesis Screen Project, Munich, Germany	http://www.gsf.de/ieg/groups/enu-mouse.html
Harwell Mutagenesis Programme, Mammalian Genetics Unit, Medical Research Council, Harwell, UK	http://www.mut.har.mrc.ac.uk
Large-scale Mutagenisis Project, Riken Genome Science Center, Yokohama, Japan	http://www.gsc.riken.co.jp/Mouse/main.html
Jackson Laboratories, Neuroscience Mutagenesis Facility, Reproductive Genomics, Bar Arbor, USA	http://www.jax.org
Mutagenesis Project, McLaughlin Research Institute, Great Falls, USA	http://www.montana.edu/wwwmri/enump.html
The Scripps Research Institute, La Jolla, USA	http://www.scripps.edu
The John Curtis School of Medical Research and Australian Phenomics Facility, Australian National University, Canberra, Australia	http://www.jcsmr.anu.edu.au/group_pages/mgc/immunogen.html

Figure 1: ENU mutagenesis projects in mice around the world.

Within most of these projects, the identification of mice with an abnormal phenotype, potentially inherited from a mutagenized founder, takes place under resting conditions on naïve animals, housed in a SPF facility. Although this way of screening ENU treated mice is very effective, as proven by the numerous variants and mutants described in the literature (Rastan et al., 2004), it is by no means sufficient to identify all potential mutants out of an ENU screen, especially not regarding immunological phenotypes, as many important immune functions or pathways are not active in naïve mice. The main task of the immune system is the effective recognition and elimination of invading pathogens, followed by a subsequent protection of its host against reinfection. To achieve this goal, a variety of different genes and complex interactions are required, starting with an alert of the immune system by receptors for pathogen detection, proteins for signal transduction and activation of certain cell types of the immune system, to finally initiate essential defense mechanisms like complement

activation, proliferation, Ab production, cytotoxicity or cytokine release. Measuring steady state parameters of naïve mice is limited to observations of certain parts of the immune system and does not allow evaluation of its functional status and capacity. Therefore, a different and maybe even more effective way of screening genetically manipulated mice for immunologically relevant phenotypes is the application of challenge conditions to activate more immunological relevant genes. Depending on the field of interest, one can think of a variety of different ways to challenge the immune system and to specifically examine defined immune functions or pathways, which would remain undetected under resting conditions. One example is the *in vitro* stimulation of peritoneal macrophages derived from ENU mutagenized mice with different TLR ligands and measuring their expansion and cytokine secretion. These kind of assays have the advantage of being repeatable for individual mice, and have been successfully implemented in the ENU screen at the Scripps Research Institute by the group of Bruce Beutler (Hoebe et al., 2005).

In order to simulate physiological conditions, immunological phenotyping can also focus on *in vivo* challenges, like infection or immunization. This approach allows intensive investigation of innate and/or adaptive immune mechanisms and their capability to cope with a defined dose of antigen or infection. The group of Chris Goodnow in Australia successfully uses immunization of ENU mice for the identification of immunological variants with abnormal humoral immune response (Jun et al., 2003). Major drawbacks of *in vivo* challenge experiments are possible interferences with subsequent investigations, and the limited possibility to repeat the challenge within the same individual mouse due to acquisition of protective immunity.

1.5 The *Listeria monocytogenes* infection model

In order to investigate the complex regulation and mechanisms for an effective innate and/or adaptive immune response, immunological research frequently uses live pathogens in experimental mouse infection studies. One of the most widely utilized organisms is the Gram-positive, facultative intracellular bacterium *Listeria monocytogenes* (*L.m.*)(Kaufmann, 1995), which is also a human pathogen that causes disease mainly in immunocompromised individuals and pregnant women, often with deleterious consequences for the fetus (Gellin and Broome, 1989). Besides the importance of early antigen-independent immune responses, like the crucial function of neutrophils in controlling replicating, intracellular pathogens (Conlan and North, 1991) or the essential role of TNF receptor signaling for the early immune

response (Plitz et al., 1999), *L.m.* is mostly applied to study antigen-specific T cell responses. Many immunodominant peptides derived from *Listeria* proteins are known, which are presented on murine MHC molecules and against which detectable frequencies of *Listeria*-specific T cells are induced (Busch and Pamer, 1998). With the help of MHC multimers, mainly MHC-I Tetramers (Altman et al., 1996; Busch et al., 1998b) or streptamers (Knabel et al., 2002), these antigen-specific $CD8^+$ T cells can be visualized and subsequently analyzed in more detail. Thus, major advances of contemporary T cell immunology like the kinetics of primary and secondary T cell response (Busch et al., 1998b) or the prerequisites for a long enough availability of antigen in lymphoid organs for efficient T cell priming (Wong and Pamer, 2003b) are based on results acquired in the murine *Listeria* infection system. Furthermore, mice, once infected with a sublethal dose of *L.m.*, develop very effective protection against reinfection mediated by $CD8^+$ memory T cells (Harty and Bevan, 1992). This is why *L.m.* is also extensively used for analysis of the generation and maintenance of memory T cells, and important findings concerning effective memory T cell responses are rooted in *L.m.* infection experiments, e.g. changed TCR repertoire composition and TCR affinity maturation by selective expansion of an antigen-specific T cell population during recall response (Busch and Pamer, 1999; Busch et al., 1998a), the differentiation between effector, effector memory and central memory T cells by the surface markers CD62L and CD127 (Huster et al., 2004), or the influence of regulatory T cells on the quality and amount of memory T cells (Kursar et al., 2002).

Yet, the genetics behind successful T cell priming, preservation of a constant pool of memory T cells and its reactivation after secondary infection are just poorly understood. Therefore, infection with *L.m.* might be an interesting option for a challenge screen of ENU treated mice to specifically identify mutants with defects in these pathways.

1.6 Aim of this PhD work

Although up to now many different mouse models have been generated with forward or reverse genetic techniques, there is an urgent need for more standardized and comprehensive characterization of mutant mice, which potentially can serve as models for human diseases or as tools to uncover distinct biological pathways or the physiological role of different molecules *in vivo*.

The main goal of this PhD thesis was the development, validation and realization of an immunological screen of naïve mice to successfully identify mutants out of an ENU screen

with immunological abnormalities, especially to identify mutations with specific alterations in the composition or amount of defined T cell subpopulations. For this purpose, meaningful parameters from the peripheral blood, applicable and detectable with high throughput technologies, had to be determined, including cellular components of the immune system as well as soluble factors, and subsequent screening of approximately 5000 mice from recessive and dominant screens, had been carried out.

Since many genes involved in the activation or regulation of a functional immune system are not active under resting conditions, and mutations in those genes would remain undetected in a steady-state screen, the second part of this work was dedicated to the development of an advanced screening approach, aiming on the identification of mutants with a functional defect in the immune system, namely in host defense mechanisms against a pathogen and the generation and maintenance of pathogen-specific protective immunity. Therefore, the basic requirements were tested for using *Listeria monocytogenes* infection of ENU treated mice as challenge system to specifically identify mutants with defects in those pathways. These investigations included the determination of the influence of endogenous and exogenous factors on the severity and outcome of disease in order to design a workflow for standardized and robust detection of mutant mice after *L.m.* challenge in a high-throughput screen.

Since the knowledge about newly identified mutant mouse lines, achieved from ENU screening approaches, are limited to the high-throughput screening results from the peripheral blood, more detailed phenotyping is necessary to fully elucidate the consequences of a certain mutation on the whole organism. For this reason, mice from the first established mutant mouse line, TUB001, were analyzed more extensively to check for potential correlations of their phenotype with existing human diseases.

The results of this PhD work have been accepted for publication in part (section 3.3.1-3.3.5):
Pasche, B., Kalaydjiev, S., Franz, T.J., Kremmer, E., Gaius-Durner, V., Fuchs, H., Hrabé de Angelis, M., Lengeling, A., and Busch, D.H. (2005). Sex dependent susceptibility to *Listeria* infection is mediated by differential IL-10 production. Accepted for publication in “Infection and Immunity”.

.

2 Materials and methods

2.1 Materials

2.1.1 Chemicals and reagents

The reagents, used in the experimental procedures of this thesis, were purchased from the following companies:

Reagents	Supplier
18-plex mouse cytokine kit	Bio-Rad, Munich, Germany
Amoniumchlorid (NH_4Cl)	Sigma, Taufkirchen, Germany
Ampicillin	Sigma, Taufkirchen, Germany
β-mercaptoethanol	Sigma, Taufkirchen, Germany
Bovine serum albumin (BSA)	Sigma, Taufkirchen, Germany
$CaCl*6H_2O$	Sigma, Taufkirchen, Germany
CFSE	Sigma, Taufkirchen, Germany
Diethanolamin	Sigma, Taufkirchen, Germany
Dimethylformamid (DMF)	Sigma, Taufkirchen, Germany
Ethanol	Pharmacy, Klinikum rechts der Isar, Munich, Germany
Ether	Merck, Darmstadt, Germany
Ethiummonazid-bromid (EMA)	Molecular Probes, Leiden, Netherlands
Fetal calf serum (FCS)	BiochromAG, Berlin, Germany
Formaldehyde	Sigma, Taufkirchen, Germany
Gentamycin	GibcoBRL, Karlsruhe, Germany
HCl	Roth, Karlsruhe, Germany
HEPES	GibcoBRL, Karlsruhe, Germany
Isopropanol	Roth, Karlsruhe, Germany
$MgCl*6H_2O$	Sigma, Taufkirchen, Germany
Mouse Th1/Th2 Cytometric Bead Array (CBA)	BD Pharmingen, Heidelberg, Germany
NaOH	Roth, Karlsruhe, Germany
Natriumazide	Roth, Karlsruhe, Germany

Reagents	Supplier
Penicillin	Roth, Karlsruhe, Germany
Phosphate buffered salt solution (PBS)	BiochromAG, Berlin, Germany
Poly-L-Lysin	Sigma, Taufkirchen, Germany
RPMI 1640	GibcoBRL, Karlsruhe, Germany
Streptomycin	Sigma, Taufkirchen, Germany
Streptavidin-PE (SA-PE)	Molecular Probes, Leiden, Netherlands
Tris-hydrochlorid (Tris-Hcl)	Roth, Karlsruhe, Germany
Triton X-100	Bio-Rad, Munich, Germany
Tween20	Sigma, Taufkirchen, Germany

2.1.2 Buffers and media

All buffers, used for FACS staining or acquisition, were filtered using a Stericup 0.22μm vacuum filtering system (Millipore Corporation, Bedford, USA) in order to avoid blocking of the FACS machine. Adjustment for the proper pH was done with NaOH or HCl.

Buffer	Composition	
FACS staining buffer	1x	PBS
	0.5% (w/v)	BSA
	0.02% (w/v)	NaN_3
	pH 7.45	
Cell culture medium	1x	RPMI 1640
	10% (w/v)	FCS
	0.025% (w/v)	L-Glutamine
	0.1% (w/v)	HEPES
	0.001% (w/v)	Gentamycin
	0.002% (w/v)	Streptomycin
	0.002% (w/v)	Penicillin

Buffer	Composition	
Sample buffer	1x	PBS
	0.02% (w/v)	BSA
	0.02% (w/v)	NaN_3
	0.05% (w/v)	$MgCl_2/CaCl_2$
	0.01% (w/v)	β-mercaptoethanol
Coating buffer	1x	PBS
	0.02% (w/v)	NaN_3
Blocking buffer	1x	PBS
	1% (w/v)	BSA
	0.5% (w/v)	Tween20
	0.02% (w/v)	NaN_3
Wash buffer	1x	PBS
	0.02% (w/v)	NaN_3
	0.5% (w/v)	Tween20
Substrate buffer	1x	Aqua double distillated
	0.1% (w/v)	Diethanolamin
	0.2% (w/v)	$MgCl_2$
	0.02% (w/v)	NaN_3
	pH 9	
Lysis buffer	0.3M	Tris
	0.17M	NH_4Cl
	pH 7.45	

2.1.3 Tetramers

MHC-I Tetramers for the detection of Ag-specific $CD8^+$ T cells were routinely produced at the laboratory of Prof. Busch according to well-established protocols (Busch et al., 1998b). Depending on the mouse inbred strain and the respective MHC-allele, the following peptide loaded MHC-I Tetramers were used: H2-K^bSIINFEKL (C57BL/6J), H2-$K^d$$LLO_{91-99}$ (BALB/c) and H2-$K^k$$p60_{117-125}$ (C3H). All peptides were purchased from Jerini (Berlin, Germany).

2.1.4 Antibodies

If not stated otherwise, all described Abs are directed against mouse antigens.

2.1.4.1 FACS and proliferation assay

All Abs for *in vitro* stimulation or FACS staining had been titrated for optimal dilutions. Titrations were repeated for each new batch of Ab. CD3 and CD11b Abs, received from Elisabeth Kremmer (GSF – Institute of Molecular Immunology), were conjugated to Cy5 fluorescence dye, using the Cy™5 mAb Labelling Kit from Amersham Biosciences according to the manufacture's recommendations.

Antibody	Clone	Supplier
B220-PE-Cy5	RA3-6B2	BD PharMingen
B220-APC	RA3-6B2	BD PharMingen
CD3	17A3	GSF - IMI
CD3ε	145-2C11	BD PharMingen
CD4-FITC	H129.19	BD PharMingen
CD4-PE-Cy5	H129.19	BD PharMingen
CD5-FITC	53-7.3	BD PharMingen
CD8α-FITC	53-6.7	BD PharMingen
CD8α-PE-Cy5	53-6.7	BD PharMingen
CD8α-APC	5H10	CALTAG
CD8β-PE	H35-17.2	BD PharMingen
CD11b	M1/70.15.11.5HL	GSF - IMI
CD11c-FITC	HL3	BD PharMingen
CD16/32	4G8	GSF - IMI
CD19-PE-Cy5	6D5	CALTAG
CD21/35-PE	7G6	BD PharMingen
CD23-FITC	B3B4	BD PharMingen
CD28	JJ316	BD PharMingen
CD25-PE	PC61	BD PharMingen
CD34-PE	RAM34	BD PharMingen
CD44-APC	IM7	BD PharMingen

Antibody	Clone	Supplier
CD45RA-PE	14.8	BD PharMingen
CD49b$^+$-FITC	DX5	BD PharMingen
CD62L-FITC	MEL-14	BD PharMingen
CD62L-APC	MEL-14	BD PharMingen
CD103-FITC	2E7	BD PharMingen
CD117-FITC	2B8	BD PharMingen
Gr-1-PE	RB6-8C5	BD PharMingen
I-A^k-PE	11-5.2	BD PharMingen
Anti-IgD-FITC	11-26c.2a	BD PharMingen
Anti-IgM-PE	R6-60.2	BD PharMingen
Ly-6C-FITC	AL-21	BD PharMingen
TCRβ-APC	H57-597	BD PharMingen
TCRγδ	GL3	BD PharMingen
Anti IFNγ-FITC	XMG1.2	BD PharMingen
Rat IgG_1 isotype	R3-34	BD PharMingen

2.1.4.2 ELISA and Bio-Plex

As standards for quantitative ELISA and Bio-Plex, highly purified mouse isotype controls were used, all purchased from BD PharMingen. For the semi-quantitative anti-DNA and rheumatoid factor ELISAs, plasma samples from approximately 6 months old female MRL/MpJ-Fas$^{(lpr)}$/J, were utilized as positive controls (Jackson Laboratories, Bar Harbor, USA).

Bio-Plex assays for IgG_1, IgG_{2a}, IgG_3, IgA and IgM were performed as competitive measurements, with defined amounts of biotinilated isotypes (BD PharMingen) as competitors for endogenous immunoglobulins. The following polyclonal sera or mAbs were used for ELISA or Bio-Plex assays.

Antibody	Clone	Assay/application	Supplier
Anti mouse IgM	Serum	ELISA/coating	Biozol
Anti mouse IgA	Serum	ELISA/coating	Biozol
Anti mouse IgG	Serum	ELISA/coating	Biozol
Anti mouse IgG_1-AP	Serum	ELISA/detection	Biozol

Antibody	Clone	Assay/application	Supplier
Anti mouse IgG_{2a}-AP	Serum	ELISA/detection	Biozol
Anti mouse IgG_{2b}-AP	Serum	ELISA/detection	Biozol
Anti mouse IgG_3-AP	Serum	ELISA/detection	Biozol
Anti mouse IgM-AP	Serum	ELISA/detection	Biozol
Anti mouse IgA-AP	Serum	ELISA/detection	Biozol
Anti mouse IgG_{2b}-biotin	R12-3	Bio-Plex/second	BD PharMingen
Anti mouse IgG_1	A85-1	Bio-Plex/coupling	BD PharMingen
Anti mouse IgG_{2a}	R11-89	Bio-Plex/coupling	BD PharMingen
Anti mouse IgG_{2b}	R9-91	Bio-Plex/coupling	BD PharMingen
Anti mouse IgG_3	R2-38	Bio-Plex/coupling	BD PharMingen
Anti mouse IgM	II/41	Bio-Plex/coupling	BD PharMingen
Anti mouse IgA	C10-1	Bio-Plex/coupling	BD PharMingen

2.1.5 Peptide library

Screening procedure for a peptide library spanning the entire protein sequence of LLO for *Listeria*-specific $CD8^+$ T cell epitope was designed as previously described (Kern et al., 2000). Briefly, individual peptides consisting of 15-amino acid residues of the original protein sequence were designed to cover the whole LLO protein. Thereby, neighboring peptides overlap by 11 amino acids. All peptides were synthesized as cleaveable peptide spots and purchased from Jerini (Berlin, Germany).

2.1.6 Mice

Mice derived from different facilities and with different genetic backgrounds were used. Regardless of their origin or the genetic background, all mice were housed under specific pathogen-free conditions.

The ENU homeostasis screen of F1 (dominant) and G3 animals (recessive) was carried out exclusively with blood samples of C3H/HeJ male and female mice at an age of 12 weeks. All mice for the screening procedure were obtained from the animal facility of the GSF (authorized and approved by the local government under permission numbers 211-2531-112/02, 211-2531-55/01, 211-2531-40/98).

Experiments for the establishment of the *L.m.* challenge screen were carried out with male C3H/HeJ mice from Harlan (Blackthorn, United Kingdom), housed in the S2 animal facility at the Institute of Medical Microbiology, Immunology and Hygiene. If not stated otherwise, primary infection experiments were performed with 6-8 week-old mice, subsequent recall infections were done at the age of 11-13 weeks. These animal experiments were authorized and approved by the local government under the permission number 211-2531-51/00.
Inbred strains C57BL/6J, BALB/c, C3H/HeN and CBA/J for investigations of sex dependent susceptibility to *Listeria* infection were purchased from Harlan-Winkelmann (Borchen, Germany) and housed at the animal facility of the GBF, Braunschweig. $Il10^{tm1\ Cgn}$-knockout mice were purchased from the Jackson Laboratory (Bar Harbor, USA). All animal experiments analyzing sex dependent susceptibility to infection were carried out at the Division of Microbiology of the GBF in Braunschweig.

2.2 Methods

2.2.1 Screening protocols

To obtain reliable screening results, standard operation procedures (SOP) for screening assays are a prerequisite. All FACS, ELISA and Bio-Plex blood screen data were achieved by application of SOPs, as briefly described in the following parts. Detailed versions of the SOPs of the immunology screen are available on demand via the administration of the GMC.

2.2.1.1 FACS staining of PBMCs

Mice were bled retro-orbitally or from the tail vein, and blood was collected into heparinized sample tubes. To separate cellular components of the blood from plasma, samples were centrifuged (530RCF, RT, 10 min) and plasma was further used in ELISA or Bio-Plex assays. PBMCs were resuspended in 900μl PBS (RT), carefully filtered through a nylon-net in a fresh sample tube, and equally distributed to 6 wells (150μl each) of a 96-well U-bottom plate (Becton Dickinson, Heidelberg, Germany). Remaining cells from all blood samples were pooled in 6 additional wells, stained and used as controls to set up the FACS machine. Plates were centrifuged (530RCF, 3min, 10°C) and supernatants were discarded by vigorous tipping over. For erythrocyte lysis, cell pellets were resuspended in 200μl NH_4CL-Tris (RT) and incubated for 10 min at RT on a plate shaker (Titramax 101, Heidolph Instruments, Schwabach, Germany). Cells were centrifuged as described above, and pellets were checked

for proper lysis. If the lysis was not complete, this step was repeated. Then the cells were washed in 200μl FACS buffer for 30 seconds on the plate shaker. After subsequent centrifugation and discarding the supernatant, unspecific binding of the staining Abs via Fc-receptors was blocked by preincubation with 50μl Fc-block Ab solution (anti CD16/CD32). In addition, life/death discrimination was initiated by adding EMA (1:1000 diluted in FACS buffer), which binds stable to DNA of dead cells after photo-cross linking through light exposure (40 W of approximately 50cm distance) for 20 min (O'Brien and Bolton, 1995). Cells were subsequently washed by addition of 150μl FACS per well, centrifuged and the pellets were resuspended in 50μl antibody staining mix 1-6, respectively (as outlined in Figure 2). After 20 min incubation on ice in the dark, cells were washed twice with 150μl FACS buffer and then fixed in 100μl 1%PFA for 30 min on ice in the dark. Finally, cells were pelleted, washed twice in 200μl FACS buffer, resuspended in 100μl PBS, and stored at 4°C in the dark. The 6 controls were transferred and stored in 1.2ml microtubes in 300μl PBS.
For data collection, $3x10^4$ leukocytes per sample were acquired on a FACSCalibur (Becton Dickinson) supported by a Multiwell AutoSampler (MAS) or High-Throughput Sampler (HTS) loader system. Analysis of raw data was performed with FlowJo software (Tree Star, Ashland, USA).

	FL-1 FITC	**FL-2 PE**	**FL-3 Cychrom**	**FL-4 APC/Cy5**
1	CD5	γδ TCR	CD19	CD3
2	IgD	Gr-1	B220	CD11b
3	DX5	MHC-II		CD3
4	CD103	CD25	CD8α	CD3
5	CD62L	CD45RA	CD4	CD3
6	Ly6C	CD8β	CD4	CD44

Figure 2: FACS screening panel for peripheral blood leukocytes.
Blood samples were stained with the outlined combinations of mAb against the described cell surface antigens to determine the cellular composition and frequency of main cell lineages and defined subpopulations in the peripheral blood.

2.2.1.2 Measurement of Ab subclasses/autoimmune Abs

Plasma concentrations of immunoglobulin isotypes were determined by standard sandwich ELISA or Bio-Plex. Tests for the presence of autoimmune Abs were carried out with indirect ELISA techniques.

2.2.1.2.1 Immunoglobulin ELISA

For coating of immuno-plates (Nunc, Wiesbaden, Germany), solutions of 10μg/ml of the respective goat anti-mouse immunoglobulin (capture Ab) in coating buffer were prepared (anti-mouse IgG for IgG_1, IgG_{2a}, IgG_{2b} and IgG_3, anti-mouse IgA for IgA and anti-mouse IgM for IgM) and incubated overnight at 4°C with 50μl/well in a moist chamber. Uncoated positions in the wells were blocked by addition of 100μl of blocking buffer for 30 min at RT. Before use, plates were washed three-times with 200μl washing buffer using an automated plate washer (Tecan, Austria).

For the ELISA, serum samples and standards were incubated for 90 min at RT in a moist chamber. For different isotype measurements, individual plasma sample dilutions in sample buffer were required: IgG_1: 1:3000; IgG_{2a}: 1:3000; IgG_{2b}: 1:1500; IgG_3: 1:10000; IgA: 1:5000; IgM: 1:15000; Standards of the respective immunoglobulin were titrated down by 7 consecutive serial dilutions, starting with 200ng/ml (all IgGs) or 100ng/ml (IgA and IgM). Two hundred μl/well of diluted plasma or standards were used for the assay, and all values were determined in duplicates. Plates were washed three-times with 200μl washing buffer and 100μl/well of the respective isotype-specific AP-conjugated detection Ab (1:2000 in sample buffer) was added for 90 min at RT. After three washing steps (200μl/washing buffer), development was initiated by adding 100µl/well of p-nitrophenyl phosphate in substrate buffer, incubated for 17 min, and finally the extinction at λ=405nm was measured using a sunrise ELISA reader (Tecan, Austria).

Analysis of the raw data and calculation into concentrations was performed with Magellan software (Tecan, Austria).

2.2.1.2.2 Autoimmune Ab ELISA

ELISAs for the detection of autoimmune Abs in the serum were carried out as described for immunoglobulin subclasses, besides the following differences.

Rheumatoid factor: plates were coated with 10µg/ml rabbit IgG (50µl/well), and plasma samples were diluted 1:200. As positive control, serially diluted serum (7 steps) from MRL/MpJ-Fas$^{(lpr)}$/J mice was used, starting from a 1:250 dilution. Extinction values measured at the 1:2000 dilutions were defined as a cut off above which samples were considered positive. Detection Ab (anti-mouse polyvalent immunoglobulin) was diluted 1:3000.
Anti-DNA Ab: Before coating, plates were treated for 1 h at RT with 50µl/well of a 50µg/ml aqueous solution of poly-l-lysine hydrobromide to enhance binding of DNA. To generate a mixture of ss- and ds-DNA, calf thymus DNA was dissolved in coating buffer (5µg/ml) (ds-DNA) and part of it was boiled for 10 min in a water bath, then immediately transferred on ice for 30 min (ss-DNA). All samples were stored at –20°C. Plates were coated with a 1:1 mixture of ssDNA/dsDNA (50µl/well). Plasma was diluted 1:100, and as positive control, plasma from MRL/MpJ-Fas$^{(lpr)}$/J mice was used in serially diluted serum (7 steps), starting from a 1:1250 dilution. Extinction values for the 1:10000 dilutions were defined as a cut off above which samples are considered positive. Detection Ab (anti-mouse polyvalent immunoglobulin) was diluted 1:3000.

2.2.1.2.2 Bio-Plex

The Bio-Plex assay was used for the simultaneous detection of IgG_1, IgG_{2a}, IgG_{2b}, IgG_3, IgM and IgA isotypes in blood plasma samples. Therefore, mAbs specific for the described immunoglobulin subclasses, were coupled to different beads according to manufacturer's recommendations using the Bio-Rad bead coupling kit (Munich, Germany). Briefly, beads were vortexed and sonicated for 30sec to prevent aggregation. One hundred μl (approximately $1.25x10^6$) were used in one coupling procedure. After the beads were pelleted (14,000g, 4min) and washed once with 100μl wash buffer, they were resuspended in 80μl activation buffer. Beads were activated by addition of 10μl EDC (50mg/ml; 1-ethyl-3-[3-dimethylaminopropyl]) and 10μl S-NHS (50mg/ml; N-hydroxysulfosuccinimide) for 20min. Beads were then washed once with 150μl PBS, resuspended in 100μl PBS, and subsequently the respective mAb was added (for concentrations see 3.1.2). Total volumes were adjusted to 500μl with PBS, and samples were incubated at RT for 2h. Coupled beads were washed once with 500μl PBS, and reaction was stopped by addition of 250μl blocking buffer 30min. After an additional washing step with 500μl storage buffer, the beads were resuspended in 150μl storage buffer. Bead loss during the coupling was determined by counting an aliquot of the coupled beads under a microscope. Efficacy of the coupling was validated by incubation of

the beads with a PE-labelled mAb, directed against the coupled mAb. The following bead regions were chosen for the different isotypes: IgG_1-27, IgG_{2a}-46, IgG_{2b}-44, IgG_3-43, IgM-24 and IgA-42.

For the assay itself, 25μl/well of the plasma samples (1:750 dilution in PBS) or standards were incubated together with 25μl/well bead mixture. The optimal amounts of each bead preparation were titrated out depending on the efficacy and loss during each coupling procedure. Incubation was performed in a MultiScreen filter plate (Millipore Corporation, Bedford, USA) at RT for 10min on a plate shaker at 300rpm in the dark. After vacuum filtration, 25μl of a mixture of the biotinilated isotypes (200ng isotype/ml) were added for the competitive measurement of IgG_1, IgG_{2a}, IgG_3, IgM and IgA, and incubated for 30min at RT in the dark on a plate shaker. Plates were washed three times by adding 100μl FACS buffer with subsequent vacuum filtration in between. Afterwards, 25μl biotinilated anti-IgG_{2b} mAb solution (200ng/ml) was added, followed by a 30 min incubation period. Before 50μl/well SA-PE solution was added (2μg/ml in FACS buffer), plates are washed again three times as described above. Beads were resuspended in 100μl FACS buffer plus 0.1%Tween and analyzed on a Luminex 100 (Bio-Rad, Munich, Germany). Acquisition was stopped when 50 beads per region (=immunoglobulin subclass) were acquired.

2.2.2 Cell and organ preparation

For examination of defined immunological cell populations in different lymphoid tissues, animals were sacrificed at the indicated ages by cervical dislocation, and organ preparations were performed as described below.

2.2.2.1 Peripheral blood

Peripheral blood was obtained from the tail vein just before the mice were sacrificed. To enlarge the vein and to enhance the blood flow, mice were warmed up for 5 min under red light. Bleeding was performed by carefully cutting the vein with a scalpel, and approximately 500μl of whole blood per mouse was sampled in heparin-coated 1.5 ml tubes. Separation of cells from blood plasma was performed by centrifugation for 10 min at RT with 530RCF.

2.2.2.2 Bone marrow

The bone marrow of both femurs of a mouse was prepared. Therefore, bones were cut on both sides, and bone marrow was collected via flushing the cavities of a femur with 2 times 5 ml PBS using Microlance 27G3/4 needles and 5 ml syringes, both from BD Falcon™ (Heidelberg, Germany).

2.2.2.3 Spleen

Spleens were removed and single cell suspensions generated by homogenization through a steel-net in 10 ml FACS buffer.

2.2.2.4 Mesenterial Lymph nodes

For the investigation of lymph node tissue, exclusively mesenterial lymph nodes were analyzed. The peritoneum was opened, the intestinal loops moved apart and the mLN were dissected and collected. Cell suspensions were generated by homogenization as described for spleen tissue.

2.2.2.5 Thymus

Thymus was obtained by opening the sternum and removal of both thymic lobi. Single cell suspensions were generated as described for spleen tissue.

2.2.3 Organ FACS staining

Cell suspensions of organs were treated similarly to blood cells for FACS analysis as described before, besides following differences:
Resuspension and washing steps were carried out in 10ml of FACS buffer; erythrocyte lysis was performed in 5ml NH_4Cl-Tris solution for 7 min at RT; absolute cell numbers were determined by counting an aliquot of the suspension, 1:20 diluted with PBS, by using a "Neubauer-Zählkammer", adjusting the amount of cells to approximately $6x10^6$ per FACS staining; EMA/Fc block treatment was executed in 500μl per organ; stained cells were kept in 200μl 1%PFA for acquisition. For spleen and thymus at least $1x10^6$, for mLN and BM $5x10^4$ living leukocytes were acquired.

For standardized and comprehensive phenotyping of the cellular composition of lymphoid tissue, complex FACS staining patterns were designed. The Ab-combinations were chosen with respect to cell populations that can be expected within the described organs. If not stated otherwise, the following staining patterns were applied (Figure 3).

A) Spleen

	FL-1 FITC	FL-2 PE	FL-3 Cychrom	FL-4 APC/Cy5
1	CD5	γδ TCR	CD19	CD3
2	IgD	Gr-1	B220	CD11b
3	DX5	MHC-II		CD3
4	CD103	CD25	CD8α	CD3
5	CD62L	CD45RA	CD4	CD3
6	Ly6C	CD8β	CD4	CD44
7	CD11c	MHC-II	CD8α	CD11b
8	CD11c	Gr-1	B220	CD11b
9	CD23	CD21		B220

B) Thymus

	FL-1 FITC	FL-2 PE	FL-3 Cychrom	FL-4 APC/Cy5
1	CD4	CD8β		CD3
2		CD25	CD4 + CD8α	CD44
3	CD4	CD8β		β TCR

C) Bone marrow

	FL-1 FITC	FL-2 PE	FL-3 Cychrom	FL-4 APC/Cy5
1	CD117	CD25		B220
2	IgD	IgM		B220
3		Gr-1		CD11b
4	CD117	CD34		CD90

D) Mesenterial lymph node

	FL-1 FITC	FL-2 PE	FL-3 Cychrom	FL-4 APC/Cy5
1	CD103		CD8α	CD3
2	CD4	CD25		CD3
3	CD8α	CD25		CD3
4	IgD	Gr-1	B220	CD11b
5	CD11c	MHC-II	CD8α	CD11b

Figure 3: FACS staining patterns for lymphoid organs.

To get a general overview of the cellular composition of distinct lymphoid organs in ENU mutant mice, the outlined staining combinations of mAbs were used.

2.2.4 Proliferation assay

Proliferation assays were carried out to determine the responsiveness of T lymphocytes derived from the peripheral blood to distinct stimuli.

For the determination of the extent of proliferation, Carboxy-fluoresceindiacetate succinimidyl ester (CFDA SE) was used as fluorescence dye, which spontaneously penetrates the cell membrane and is converted intracellularly to anionic CFSE. CFSE irreversibly couples to available amino-groups of proteins, leading to a stable fluorescence labeling of cells. During cell division, the dye is distributed equally to daughter cells, resulting in a 50% reduction of the fluorescence intensity with each cell division. The pattern of distinct levels of fluorescence intensity induced by a stimulus can be readily detected by flow cytometry (CFSE excitation/emission: 488 nm/525 nm).

If not stated otherwise, activation of T cells was performed by supplementing the culture media with 0.25 μg/ml of stimulatory α-CD3 and same amount of co-stimulatory α-CD28 Ab during the 72 h incubation period.

For high throughput proliferation assays, aliquots of already lysed and filtered blood cell samples were transferred to 96-well plates and labeled with 100 μl of 5 μM CFSE in PBS for 10 min at 37°C. The reaction was stopped by adding 150 μl RP10+ and incubation for 5 min on ice, followed by two washing steps with cell culture medium. Cells were subsequently transferred in 200 μl culture medium with or without stimulating Abs to 96-well flat bottom plates, and were incubated at 37°C with 5% CO_2. After 72 h of culture, cells were harvested, treated with EMA/Fc block and stained for surface expression of CD8β-PE, CD4-PE.Cy5, and CD62L-APC as previously described, and were directly analyzed by flow cytometry.

2.2.5 Intracellular cytokine staining

Intracellular cytokine staining was performed for functional detection of Ag-specific T cell populations. Readout was the ability of T lymphocytes to respond with the intracellular production of pro-inflammatory cytokines, mainly IFNγ, after incubation in the presence of a defined peptide. If not stated otherwise, 2 μl of the indicated peptide stocks with a concentration of 1 mg/ml in DMSO were used. Same concentrations or amounts of α-CD3Ab or DMSO served as positive or negative controls, respectively. The assays were carried out with the delivered buffers according to manufacturer's recommendations (PharMingen, San Diego, USA).

At day 7 after primary or day 5 after secondary infection with *L.m.*, spleens were collected, red blood cells were lysed and the cell numbers counted as described above. $2x10^7$ splenocytes in 2ml RP10+ were incubated with or without stimulus in a 24-well plate at 37°C, 5% CO_2. After 2 h, 4μl Golgi-Plug was added to inhibit secretion of produced cytokines, followed by additional 3 h of incubation. After transfer to 15 ml Falcon tubes and one washing step with 1 ml FACS buffer, cells were transferred to 96-well plates and EMA/Fc block treatment and staining for expression of distinct surface markers was carried out as outlined before. Subsequent fixation and permeabilization of the cell membrane was achieved by 20min incubation on ice with 100μl Cytofix/perm solution. Cells were washed 2 times with Permwash, before intracellular staining was applied by incubating the cells for 30 min on ice with the respective Abs, diluted in Permwash. After one washing step in Permwash and an additional in FACS buffer, cells were fixed in 200μl 1% PFA and analyzed by flow cytometry.

2.2.6 *L.m.* infection

For infection experiments either the isolates *L.m.* 10403s from the ATCC (Rockville, USA), or *L.m.* EGD from the Junior Research Group Infection Genetics of the GBF (Braunschweig, Germany) were used as indicated. For investigation of $CD8^+$ T lymphocyte responses in C57BL/6J, mice were infected with a recombinant *L.m.* 10403s strain expressing ovalbumin. Infections were performed intravenously (i.v.) or intraperitoneally (i.p.) with the indicated dosages of bacteria as stated in the text. For infection, 20µl glycerol stock of the respective *L.m.* strain was pre-cultured in 5ml BHI medium at 37°C untill bacteria cultures entered the exponential growth phase, as determined by OD measurement ($OD_{600}\approx0.1$). The amount of bacteria was either calculated referring to standard curves, or an aliquot was taken and living, bacteria were directly counted in a “Thoma-counting chamber” under the microscope. Bacterial concentrations were adjusted with PBS to the desired infection dose in 200μl.

The exact infection dose was further controlled by plating out different dilutions of the used *L.m.* suspensions on BHI plates, incubation overnight at 37°C, counting of CFU, and calculation of the original bacterial concentration.

2.2.7 Bacterial load

As indicator for the strength of infection, numbers of live bacteria in infected spleens and livers were determined.

Organs were harvested, homogenized and resuspended in 5 ml sterile PBS. 100μl of the cell suspensions were diluted 1:10, 1:100 and 1:1000 in Triton solution in dH_2O (0.1%) to release the intracellular bacteria from the cells. Aliquots of 10μl per dilution were plated out in triplicates on BHI plates and incubated overnight at 37°C. Colony forming units (CFU) were counted on the following day, and the amounts of *L.m.* were calculated per organ according to the respective dilutions.

2.2.8 Cytokine measurements

The levels of different cytokines in the blood plasma were measured after *L.m.* infection. Therefore, plasma samples were prepared at different time points after infection as described before. Two different bead-based technologies were applied to measure plasma cytokine concentrations.

In principle both assays, the Cytometric Bead Array (CBA, Becton Dickinson, Heidelberg, Germany) and the Bio-Plex (Bio-Rad, Munich, Germany), work similar to a standard sandwich ELISA, in which the analyte is first captured by a surface-coupled mAb. In the next step, the amount of captured substance is determined by a second, fluorescence-conjugated mAb, and analysis is performed by flow cytometry. Discrimination of the measured parameters is obtained by different bead sizes and/or color. The big advantage of these bead-based assays over ELISA is that they allow simultaneous detection of several substances/cytokines in the same sample. During this PhD work, the Mouse Th1/Th2 Cytokine Kit (Becton Dickinson, Heidelberg, Germany) for IL-2, IL-4, IL-5, TNFα and IFNγ or the Bio-Plex Mouse 18-Plex Assay for IL-1α, IL-1β, IL-2, IL-3, IL-4, IL-6, IL-10, IL-12(p40), IL-12(p70), IL-17, G-CSF, GM-CSF, IFNγ, KC, MIP-1α, RANTES and TNFα (Bio-Rad, Munich, Germany) was used. The CBA assay was acquired on a FACSCalibur, the 18-Plex Assay on a Luminex100.

2.2.9 X-ray and computer tomography

X-ray images and computer tomography (CT) scans were performed in collaboration with Dr. Helmut Fuchs from the Institute of Experimental Genetics, GSF Neuherberg. X-ray analysis

was carried out using a MX-20 Specimen Radiography System (Faxitron X-ray Cooperation, Wheeling, USA) combined with EZ 40 X-ray scanner (NTB GmbH, Dickel, Germany). Micro CT scans were taken on a Tomoscope 10010 (VAMP GmbH, Möhrendorf, Germany) and analyzed by Syngo Software (Siemens, Munich, Germany).

2.2.10 Histology

Histological examinations were carried out in cooperation with Sandra Kunder, Institute of Pathology, GSF, Neuherberg. Collected organs were fixed in 4% formalin, embedded in paraffin, and 2μm-thick sections were prepared followed by standard hematoxylin and eosin (HE) staining. Stained sections were analyzed by light microscopy with the indicated magnifications.

2.2.11 Liver enzymes

Determination of enzyme activities in blood plasma samples, namely the liver enzymes glutamat-oxalacetat transaminase (GOT) and glutamic-pyruvic transaminase (GPT), was carried out in cooperation with Dr. Martina Klempt from the Clinical Chemical Screen of the GMC, Neuherberg. The assays measure the catalysis of ketoglutarat and aspartat to oxalacetat and glutamat (GOT) (Bergmeyer and Horder, 1980) or ketoglutarat and alanin to pyruvat and glutamat (GPT) (Bergmeyer et al., 1986). Measurements were carried out using Olympus System Reagent kits for GOT and GPT (Olympus Diagnostica GmbH, Hamburg, Germany) and acquired on an Olympus AU 400 auto-analyzer.

2.2.12 Statistical analysis and outlier detection

The values of quantitative screening parameters, like percentages of defined cell populations, mean fluorescence intensities of certain surface stainings and concentrations of different immunoglobulin subclasses, were imported from respective analysis software into Excel (Microsoft Corporation, USA). Cohorts of mice from the same experiment and origin were grouped, a set of statistical parameters (mean, standard deviation, three times SD, mean +/- three times SD) was automatically calculated by previously written macros for each parameter. Outliers, defined by values higher/lower than mean +/- three times SD were automatically marked, and raw data was rechecked. For analysis of the semi-quantitative

parameters like α-DNA or rheumatoid factor Abs, cut-off levels were defined, and mice with higher extinction values were considered suspicious.

For all suspicious FACS-, ELISA- or bead array-values, a second sample was taken at least 2 weeks after the first bleeding. Mice with alterations in the same parameter in two independent experiments were catalogued as variants, and offspring were tested for germ line transmission of the mutation. If inheritance was proven, the mouse mutant line received a TUB number for final identification.

3 Results

3.1 Homeostasis screen

3.1.1 Set up and validation of assays for the measurement of leukocyte frequencies and immunoglobulin concentrations

The robustness of screening protocols and the reliability of their results is crucial for the successful identification of outliers within cohorts of ENU mutagenized mice, especially because the exact phenotype and its potential influence on distinct immunological parameters are unpredictable. There are several immunological techniques available, like staining of leukocyte subsets with fluorescence conjugated mAbs and subsequent analysis by flow cytometry or determination of immunoglobulin isotypes by ELISA, which have been well established and have proven to be suitable for immunological analysis. These assays were slightly modified to transfer them into the workflow of high-throughput measurements as described in Materials and Methods, in order to allow management of up to 200 samples per day.

FACS staining:

An important control for reproducibility of an assay system is an independent repetition of the assay with identical samples. Although it would be desirable to evaluate the reproducibility of the complete handling of PBMCs generation and staining, including the procedure of blood taking from the retroorbital plexus, the validations had to be limited to the comparison of blood staining results for aliquots derived from the same blood sample. This decision was necessary, because consecutive bleedings of mice can interfere with each other. For example, it is well known in the mouse that after reduction of the total blood volume by larger amounts (>100μl) hematopoiesis increases rapidly, and substantial changes in the composition of cellular contents of peripheral blood are typical (e.g. occurrence of reticulocytes (Houwen, 1992)). Therefore, blood samples from 10 individual mice were split into two aliquots and subsequent FACS staining and data acquisition was performed in parallel independently by different technicians, applying strictly the SOPs. Subsequent comparison of the results obtained for the same sample revealed a very high degree of similarity for several main cell lineage markers, like $CD19^+$ B cells, $CD3^+$ T cells, $CD4^+$ T helper-cells, $CD8\beta^+$ T killer-cells, $DX5^+$ NK cells and Gr-1^+ granulocytes. Correlation coefficients between 0.773 and 0.961 were calculated (Figure 4). The comparison of smaller subpopulations with total frequencies

below 6% of total leukocyte content, like $CD19^+CD5^+$ B1 cells or $CD3^+\gamma\delta TCR^+$ γδ-T cells, provided poorer results with indices of stability around 0.2 (Figure 4). Taking together, these findings indicate that the reproducibility of high-throughput FACS staining decreases with the size of the measured cell population, being less sensitive for cellular subsets with low frequencies (approximately 6% of total cell content). Nevertheless, measurements of main cell lineage frequencies are very reliable and also for small cell subsets, extreme outliers should be easily detectable.

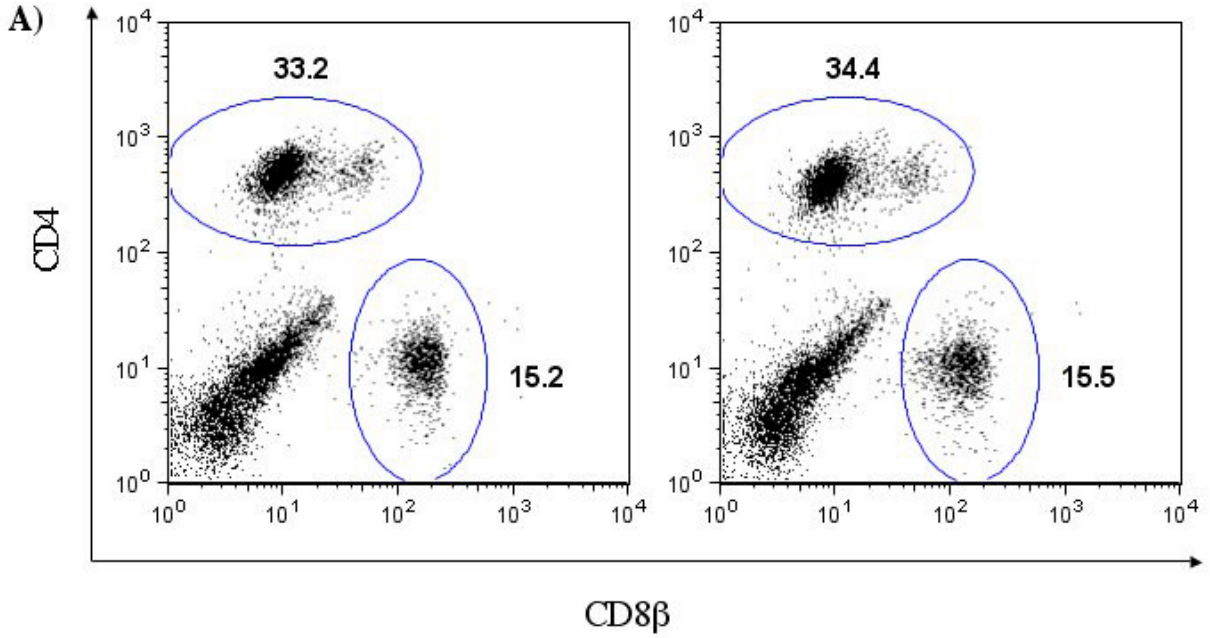

C)

Cell type	Average% of total blood cell content	Correlation coefficient
CD19⁺ B cells	24.6	0.930
CD19⁺CD5⁺ B1 cells	6.1	0.221
CD3⁺ T cells	37.7	0.961
CD3⁺γδTCR⁺ γδ T cells	0.7	0.208
CD4⁺ Th cells	28.2	0.881
CD8β⁺ CTL	11.9	0.823
DX5⁺ NK cells	20.1	0.773
Gr-1⁺ cells	28.1	0.951

Figure 4: Evaluation of high-throughput FACS protocols.

Blood samples of 10 C3H/HeJ males were divided in 2 aliquots and FACS staining was performed independently from each other. A) Representative dot plots for CD4 and CD8β staining. B) Plot of the results from first versus second measurement for percentage of $CD4^+$ cells plus corresponding correlation coefficient. C) Measured cell-populations, their contribution to total leukocyte content, and respective correlation coefficients.

ELISA:

We evaluated the intra-assay variability of ELISA by correlating values obtained for duplicate repetitions of the same plasma samples within an assay. The analysis demonstrated a high intra-assay reliability of the developed high-throughput ELISA protocols (Figure 5 and data not shown for indirect ELISA).

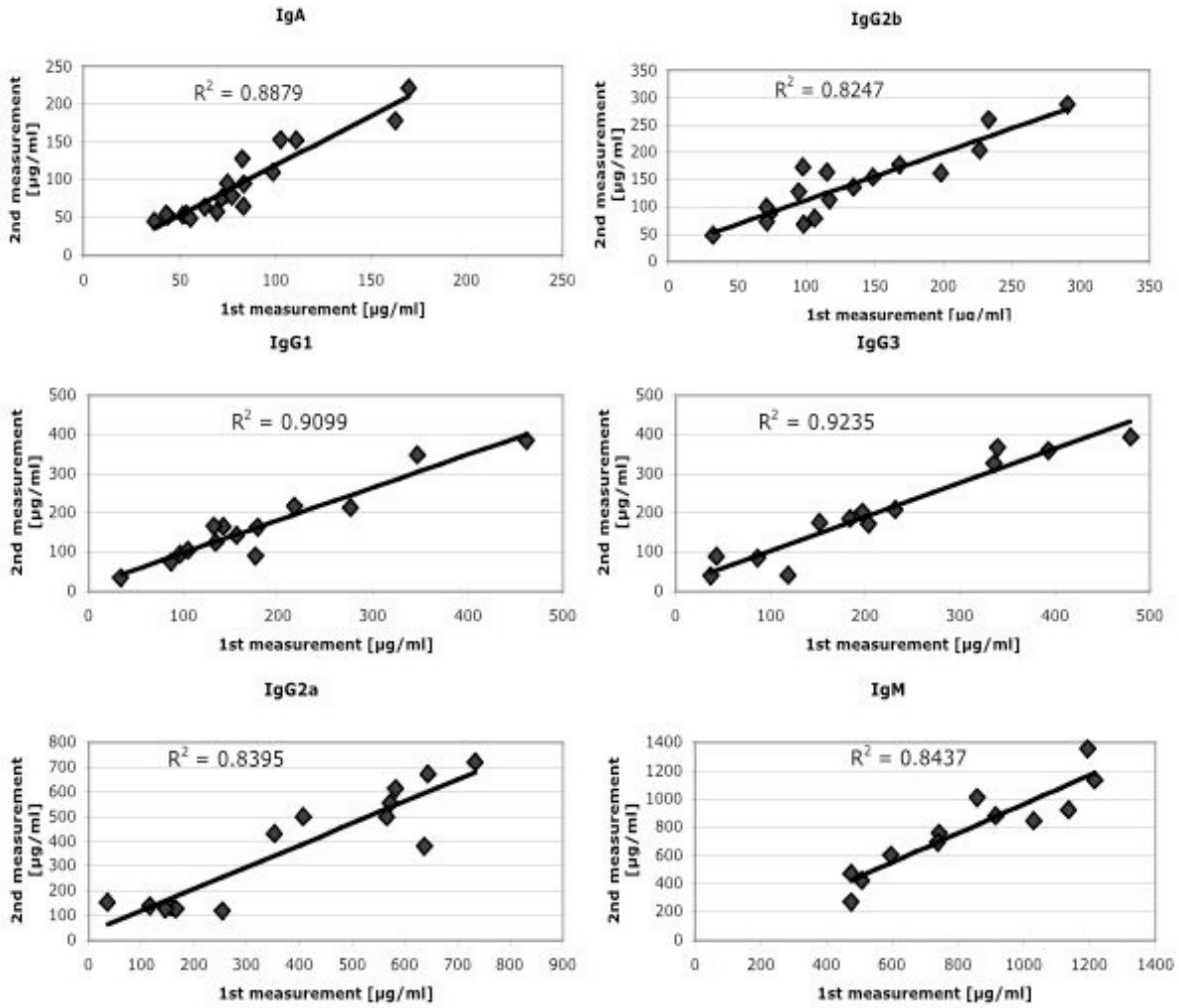

Figure 5: Intra-assay reproducibility of the high-throughput ELISA measurements. Comparison of 12-20 duplicate values for the outlined immunoglobulin subclasses, measured with the high-throughput SOP for ELISA. Numbers stand for the correlation coefficient for the respective immunoglobulin measurement.

Blood plasma samples can be stored at –20°C for longer periods of time, easily allowing the repetition of the assay on the identical samples. Comparison of the duplicate values (intra-assay variability) as well as of the repetitions of the measurement for several plasma samples in independent experiments (inter-assay variability) demonstrated high reproducibility and

sensitivity for high-throughput ELISA technology (Figure 6), although the indices compared to the intra-assay validation were slightly lower.

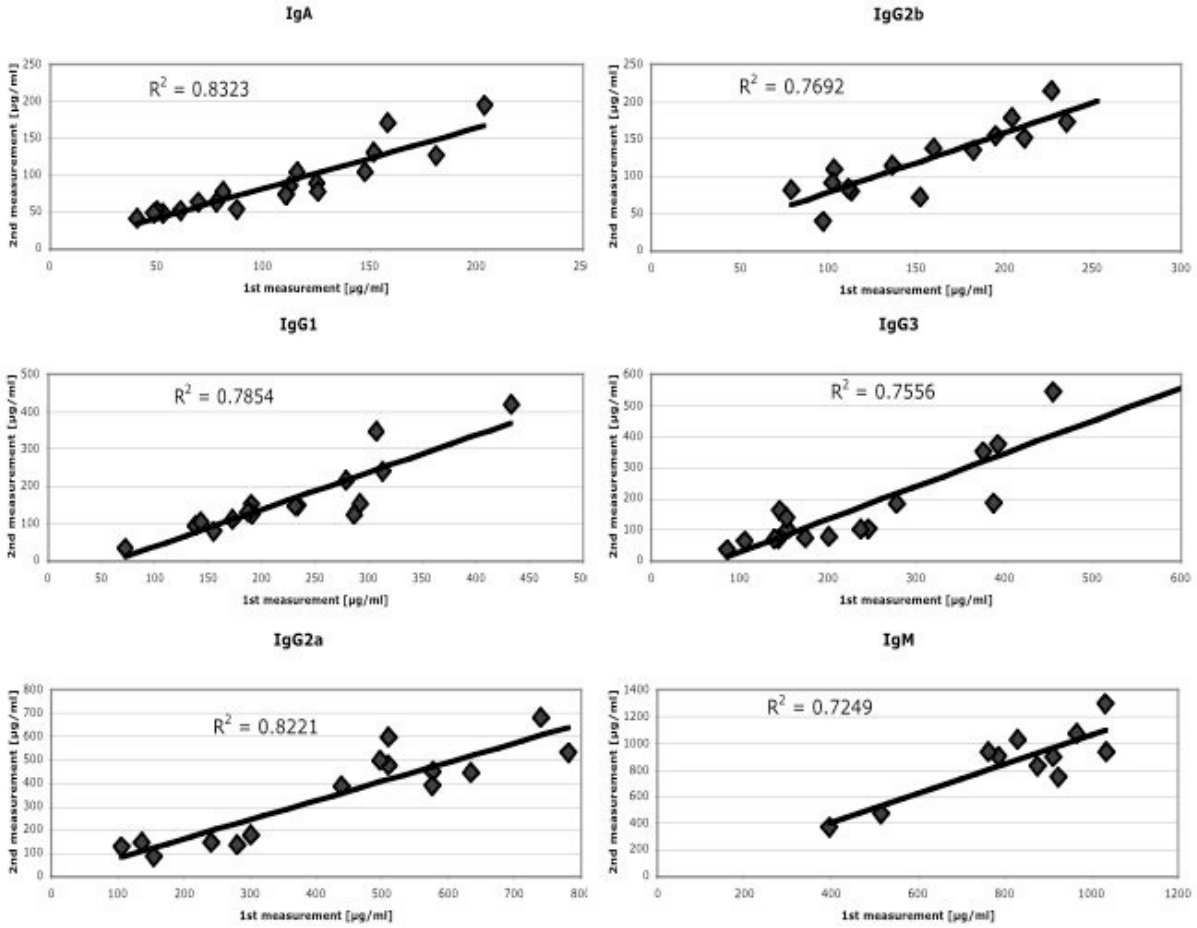

Figure 6: Inter-assay reproducibility of the high-throughput ELISA measurements. Concentrations of the indicated immunoglobulin subclasses in the blood plasma of 12-20 samples were measured in two independent experiments, applying the developed SOP for ELISA. Results were correlated and the values indicate the correlation coefficient for the 2 measurements.

Bio-Plex bead array:

As ELISA techniques are time consuming and need relatively high amounts of plasma because each parameter has to be determined separately, measurements of immunoglobulin subclass levels were transferred to bead array systems, allowing the simultaneous detection of different analytes in the same plasma sample. Since there are no commercially available kit systems for high-throughput bead array based immunoglobulin measurements in mice, this assay had to be newly established, including the production of beads coupled with mAbs (as described in Materials and Methods). Different concentrations of specific mAb against a

distinct immunoglobulin subclass were coupled to beads, efficiency of coupling was tested with an PE labeled mAb against the bound Ab, and standard curves were calculated to determine the ideal bead-Ab ratio. The following amounts of the specific Abs against the indicated immunoglobulin isotypes appeared to work best for binding to $1.25x10^6$ beads: IgA 15μg, IgM 15μg, IgG_1 30μg, IgG_{2a} 40μg, IgG_{2b} 10μg, IgG_3 15μg. Representative standard curves of a defined bead-mAb mixture are shown in Figure 7 for 2 independent coupling experiments. The quality of the coupling and comparability of the reagents was guaranteed by a SOP for the conjugation procedure, resulting in analogous standard curves, as depicted in Figure 7.

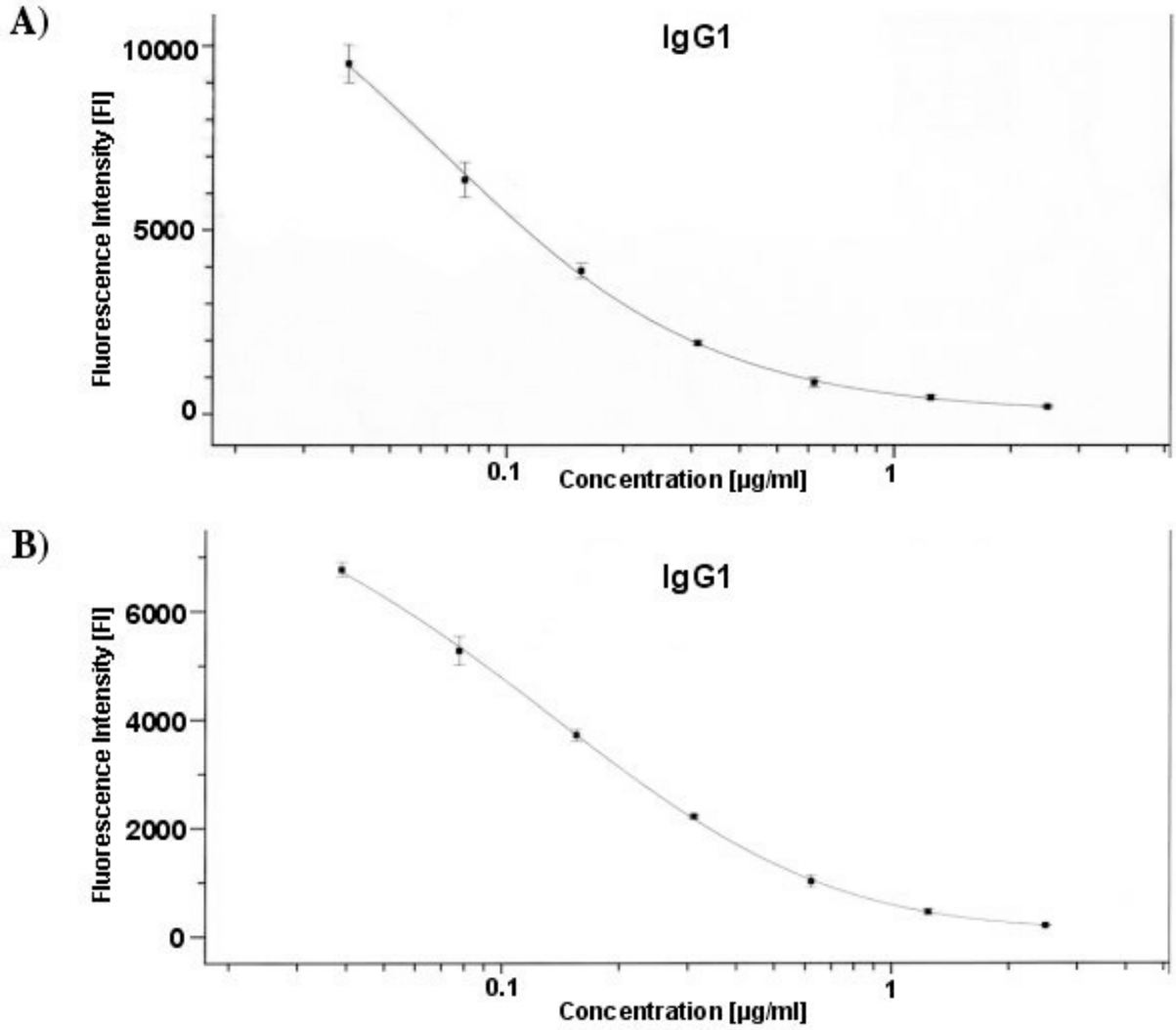

Figure 7: Quality control of the Bio-Plex bead coupling.
Representative standard curves after 2 independent coupling experiments are shown for IgG_1 (A+B). Differences in the maximum values of the absolute fluorescence intensities are most likely due to different batches of SA-PE or to slight variations within the absolute amounts of coupled mAbs per bead. Nevertheless, these minor changes in absolute fluorescence intensities do not alter the progression of the standard curves.

The specificity and sensitivity of self-coupled beads for immunoglobulin subclass measurements was evaluated by simultaneous measurement of all 6 immunoglobulin subclasses in PBS samples, which were spiked with defined amounts of different immunoglobulin isotypes. These results, summarized in Figure 8, demonstrated the functionality of the bead based technology and proved the quality of the laboratory-made reagents. At least within the range of 0.3125μg/ml to 1.5μg/ml per sample, the Bio-Plex assay was quite sensitive with medium deviations of actual to measured concentration between 9-

17%. Beyond this range, the sensitivity of the assay decreased significantly (data not shown). Nevertheless, plasma samples were usually diluted 1:750 to be within the reliable range for the Bio-Plex assay. No cross-reactivity was detectable between the measurements for each single immunoglobulin subclass.

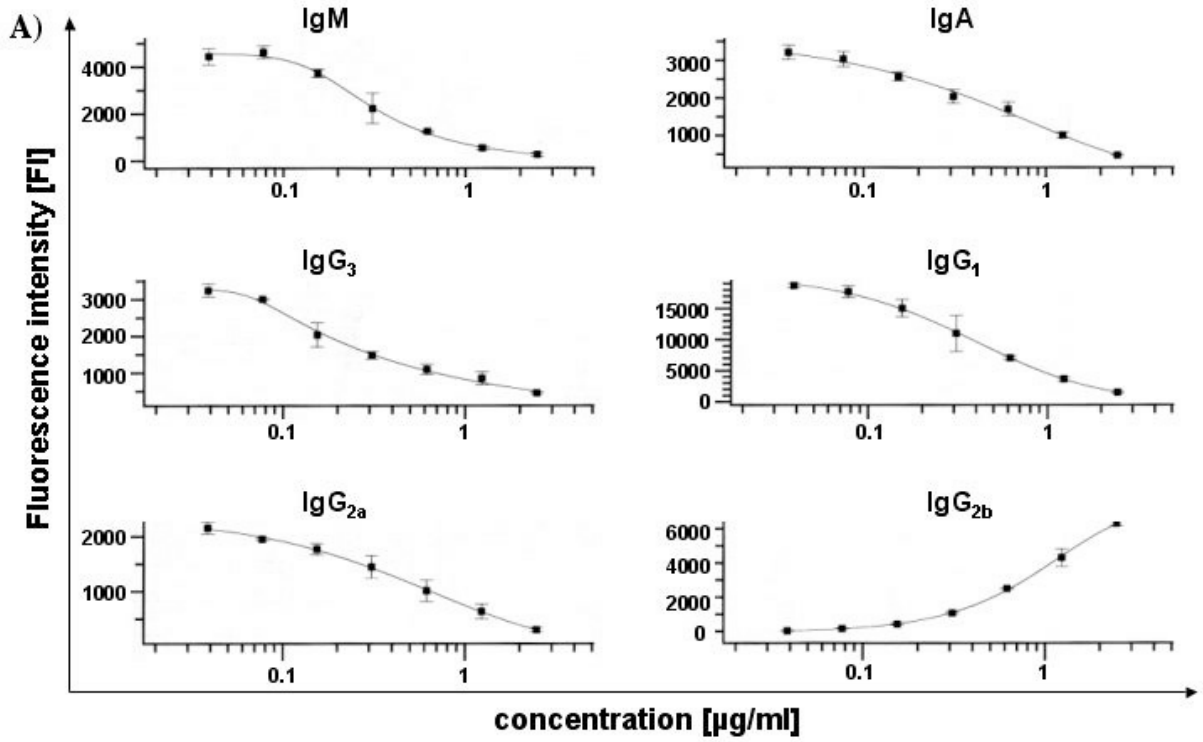

B)

Isotype	IgM	IgA	IgG_3	IgG_1	IgG_{2a}	IgG_{2b}
% deviation	9.13	17.04	13.60	12.48	10.05	15.40

Figure 8: Determination of immunoglobulin subclasses with Bio-Plex technology in spiked PBS samples.

PBS samples were spiked with defined amounts of immunoglobulin isotypes and subsequently the concentrations were determined by multiplex assay. A) Representative standard curves (0.039 – 2.5µg/ml) for each immunoglobulin subclass. With the exception of IgG_{2b}, assays were performed competitively, therefore the intensities decrease with increasing concentrations of the respective isotype. B) Measured concentrations of 15 spiked samples of the indicated immunoglobulin subclasses were compared with the inserted concentrations and the means for percentage deviations are shown.

Above summarized evaluation tests for bead based Bio-Plex technology were based on samples spiked with known concentrations of immunoglobulin isotypes, but this might not exactly reflect the sensitivity or specificity of the assay when performed in complex protein

solutions like blood plasma. Therefore, the immunoglobulin isotype concentrations of 10 individual plasma samples were determined in two independent experiments, using the high-throughput protocol described in Materials and Methods. As outlined in Figure 9, the comparison of both results revealed a high similarity between the measurements, reflected in indices of stability ranging from 0.7295 to 0.9255.

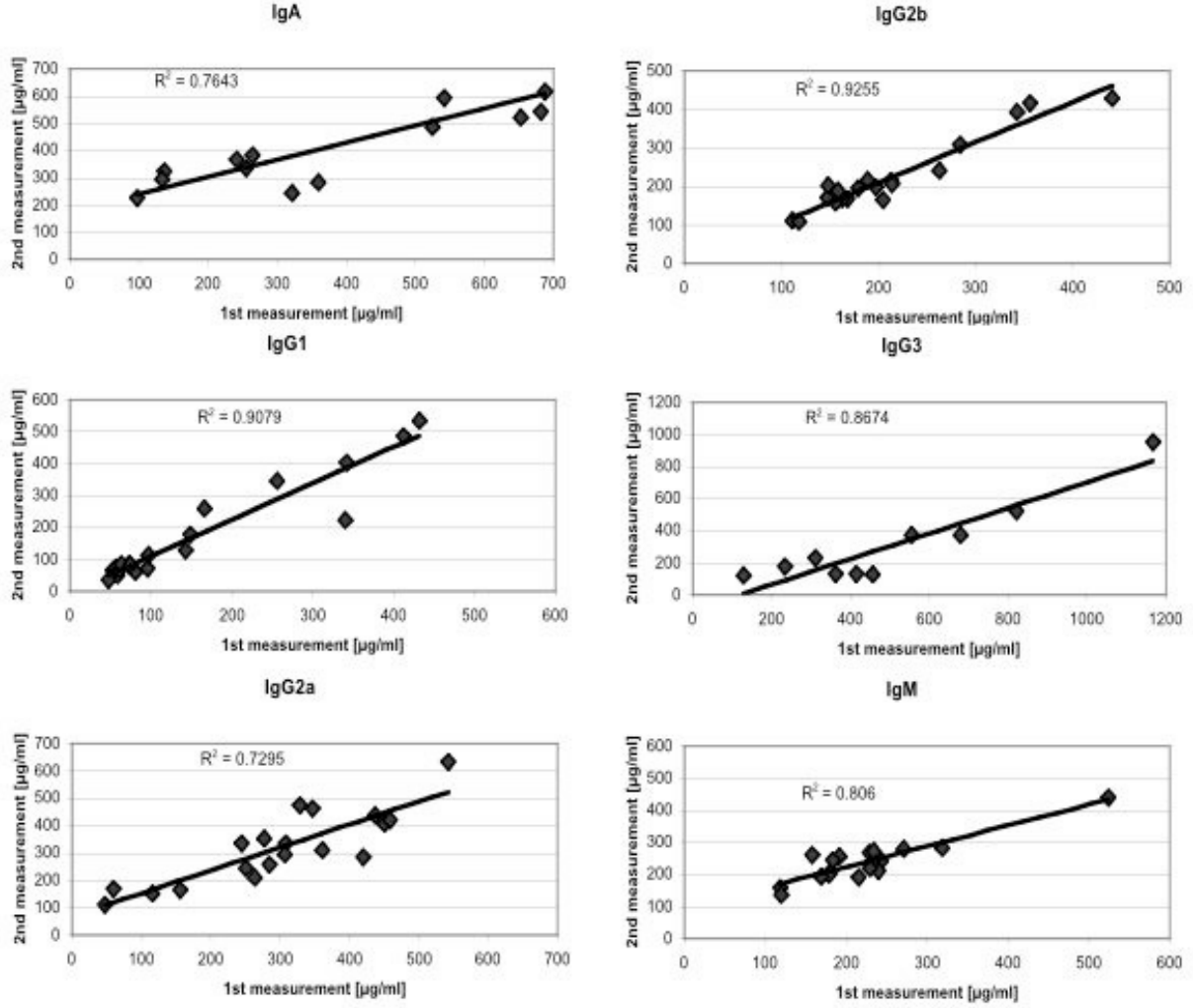

Figure 9: Evaluation of the reproducibility of multiplex assays for simultaneous measuring of six immunoglobulin isotypes.

10-20 blood plasma samples were split in two aliquots and the indicated immunoglobulin subclasses were determined independently from each other in a multiplex bead array assay. The graphs show the concentrations of the first plotted against the results derived from the second measurement; the values indicate the correlation coefficient for the respective isotypes.

These experiments illustrate the ability to apply bead array based assays like the Bio-Plex for standardized immunological phenotyping under high-throughput conditions. Meaningful results can be obtained measuring quantitative parameters, whereas semi-quantitative measurements like the determination of autoimmune Abs still requires ELISA techniques.

To further evaluate the FACS and ELISA/Bio-Plex-based high-throughput screening protocols, we newly determined the baseline values of defined immunological parameters (cellular frequencies and concentrations of the indicated immunoglobulin subclass) in the peripheral blood and blood plasma from several mouse-inbred lines (Figure 10). Subsequent comparison of the obtained results with depicted values for some of these parameters in age-, sex- and strain-matched mice, like IgG_1 IgG_{2a}, and IgG_{2b} (Ma et al., 1996) or IgM (Schubart et al., 2000) in C57BL6/J and IgG_{2a}, IgG_3 and IgM in BALB/c mice (Payet et al., 1999), revealed high consistency between measured and published data. Nevertheless, comprehensive and systematic reports concerning immunological baseline values for naïve mouse-inbred strains have not been described in the literature so far; therefore, most of our findings regarding the strain dependent differences of distinct immunological parameters are novel and represent an important new contribution to immunological mouse phenotyping.

	C57BL/6		C3HeB/FeJ		BALB/c	
Parameter	Male	Female	Male	Female	Male	Female
$CD19^+$(%)	59.2 ± 0.7	46.0 ± 3.2	39.6 ± 0.9	31.3 ± 1.2	44.5 ± 1.9	25.0 ± 2.5
$CD19^+CD5^-$(%)	98.7 ± 0.1	97.8 ± 0.4	97.5 ± 0.2	97.5 ± 0.2	97.8 ± 0.2	95.8 ± 0.7
$CD19^+CD5^+$(%)	1.3 ± 0.1	2.1 ± 0.3	2.5 ± 0.2	2.5 ± 0.2	2.2 ± 0.2	4.2 ± 0.7
$CD3^+$(%)	17.9 ± 0.7	22.0 ± 0.6	36.6 ± 0.7	33.4 ± 1.2	29.5 ± 1.4	42.2 ± 1.1
γ/δ TCR^+(%)	0.3 ± 0	0.6 ± 0.1	0.1 ± 0	0.1 ± 0	0.2 ± 0	0.1 ± 0
Gr-1^+(%)	14.6 ± 0.6	21.3 ± 3.8	26.8 ± 1.1	29.2 ± 1.1	22.4 ± 1	29.9 ± 2.6
$CD49b^+$(%)	19.8 ± 1.6	27.2 ± 3.9	34.8 ± 3.1	32.7 ± 3.2	53.9 ± 1.8	47.0 ± 2.5
$CD4^+$(%)	20.7 ± 0.8	21.4 ± 1.2	21.7 ± 0.4	22.8 ± 0.8	22.4 ± 1.0	32.1 ± 1.2
$CD8\beta^+$(%)	7.8 ± 0.2	8.4 ± 0.3	10.9 ± 0.2	11.6 ± 0.5	9.3 ± 0.3	10.7 ± 0.3
IgG_1(µg/ml)	147 ± 21.0	256 ± 34.0	103 ± 12.4	121 ± 14.7	170 ± 35.9	118 ± 28.8
IgG_{2a}(µg/ml)	n.a.	n.a.	323 ± 111	141 ± 44	115.7 ± 19	149 ± 30
IgG_{2b}(µg/ml)	155 ± 13	265 ± 8	34.6 ± 5	50.9 ± 9	62.2 ± 4.3	105.6 ± 7.7
IgG_3(µg/ml)	70.9 ± 7	107 ± 27	215 ± 40	173 ± 34	735 ± 123	639 ± 169
IgM(µg/ml)	1166 ± 109	1325 ± 176	212.4 ± 50	219.7 ± 67	202 ± 51.3	303 ± 99.3
IgA(µg/ml)	211 ± 12	184 ± 12	102 ± 23	83.8 ± 14	161.4 ± 28	156.3 ± 23
Anti-DNA Ab	n.d.	n.d.	n.d.	n.d.	n.d.	n.d.
Rheumatoid. Factor	n.d.	n.d.	n.d.	n.d.	n.d.	n.d.

Figure 10: Immunological blood baseline values.

Immunological baseline values for the cellular frequencies and plasma concentrations of defined cell populations and immunoglobulin isotypes in the peripheral blood of 14 weeks old C57BL/6, C3H/HeF and BALB/c. Mean values ± standard error are shown for 11-15 mice per strain and sex; n.d.: not detectable; n.a.: not available (B6 mice do not produce IgG_{2a} isotype).

3.1.2 Screening of ENU mutagenized mice

After establishment and confirmation of the screening assays, ENU mutagenized mice had been screened for immunological abnormalities in the peripheral blood, in order to discover

genetic mutations with consequences for the development, homeostasis or maintenance of the immune system. The screen was split into 2 parts, depending on the origin of the investigated mice, distinguishing between F1 animals to detect dominant mutations or G3 animals for recessive phenotypes.

Altogether, blood samples of approximately 5000 mice passed the immunology screen, 2600 from the dominant and 2400 from the recessive screen. In concordance with what has been described for other ENU screens, outliers were defined by a stronger variation in a certain parameter than mean ± 3 times standard deviation of the examined cohort of mice. Suspicious mice were declared as variants when the same phenotype(s) could be confirmed in an independent second experiment 2 weeks later. The principle of outlier detection and validation in a subsequent second blood sample is shown in Figure 11 for the identification of TUBV075 with increased percentage of $CD3^+$ T cells of more than 60%, compared to approximately 45% in normal mice.

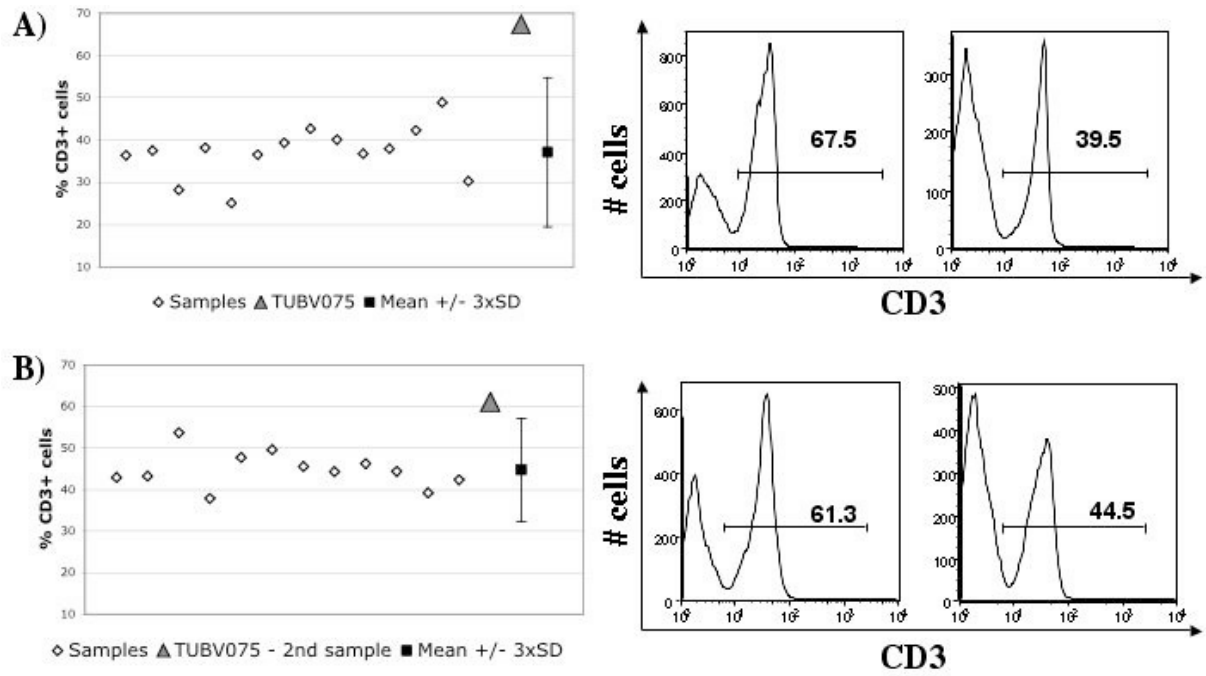

Figure 11: Principle of variant Identification.

Left panel: Relative frequencies of $CD3^+$ T cells in the peripheral blood of unsuspicious mice (open diamonds), TUBV075 (grey triangle) and mean ± 3xSD (filled square). Right panel: Staining histograms gated on EMA negative leukocytes of TUBV075 and a representative WT mouse. A) Fist measurement at an age of 12 weeks. B) Second measurement at 14 weeks.

3.1.3 Variants and mutant lines

Applying these criteria, 85 variants with immunological phenotypes and 9 with morphological alterations, were identified during the screening period (listed in Figure 12).

Variant number	Mouse ID	Phenotype	Screen
TUBV001	30001740	⇑IgG_1, IgG_{2a}, IgG_{2b}, IgM; ⇓$CD3^+$, $CD4^+$, $CD8^+$;	Dominant
TUBV002	40000173	⇑$MHC\text{-}II^+$	Dominant
TUBV003	40000240	⇓$CD4^-CD62L^+$	Dominant
TUBV004	10167174	⇑$Gr\text{-}1^+$; ⇓$B220^+$, $CD8^+$, $CD4^+$	Recessive
TUBV005	30003531	⇓$DX5^+$	Dominant
TUBV006	30003503	Kinky tail	Dominant
TUBV007	30003508	Kinky tail	Dominant
TUBV008	30004388	Kinky tail	Dominant
TUBV009	30003513	Kinky tail	Dominant
TUBV010	30003547	Cataract	Dominant
TUBV011	30004430	Abnormal eye	Dominant
TUBV012	40000264	⇑$Gr\text{-}1^+$; ⇓$CD19^+$, $CD3^+$, $CD8^+$, $CD4^+$	Dominant
TUBV013	40000265	⇑IgG_1, IgG_{2a}	Dominant
TUBV014	10168728	Rh-factor +	Recessive
TUBV015	40000627	⇓$CD19^+$, IgG	Recessive
TUBV016	40000629	⇓$CD19^+$, IgG	Recessive
TUBV017	40000628	⇓$CD19^+$, IgG	Recessive
TUBV018	20039854	Rh-factor +	Dominant
TUBV019	20043409	⇑$B220^+$, $MHC\text{-}II^+$	Dominant
TUBV020	20040053	⇑$CD19^+CD5^+$; CD44 expression	Dominant
TUBV021	40000689	$CD19^+$ absent	Recessive
TUBV022	40001168	⇑$CD8^+CD44^+Ly6C^+$; Ly6C expression	Dominant
TUBV023	40001173	⇓$CD19^+$	Recessive
TUBV024	40001341	CD11b expression	Recessive
TUBV025	40001699	CD8β expression	Dominant

Variant number	Mouse ID	Phenotype	Screen
TUBV026	10180064	⇑DX5	Recessive
TUBV027	10181596	⇓$CD19^+$, $B220^+$, $MHC\text{-}II^+$	Dominant
TUBV028	10183960	⇑ $CD8^+CD44^-Ly6C^-$	Dominant
TUBV029	10184028	⇑ $CD8^+CD44^-Ly6C^-$	Recessive
TUBV030	10185213	Rh-factor +	Dominant
TUBV031	20044709	⇑$CD19^+CD5^+$	Dominant
TUBV032	10185284	⇑$CD4^+CD44^+Ly6C^-$; CD44 expression	Dominant
TUBV033	30010236	Tremor	Dominant
TUBV034	10191275	⇑$CD3^+$	Recessive
TUBV035	10192888	Rh-factor +, αDNA-Ab +	Recessive
TUBV036	20040487	⇓$CD19^+$, $CD3^+$	Dominant
TUBV037	20040389	⇓$CD19^+$, $CD3^+$	Dominant
TUBV038	20040090	⇓$CD19^+$, $CD3^+$	Dominant
TUBV039	40002876	⇓$CD19^+$, $CD3^+$	Recessive
TUBV040	30014692	⇑$CD19^+CD5^+$, $CD8^+CD44^-Ly6C^-$	Dominant
TUBV041	10193325	⇑$CD11b^+Gr\text{-}1^-$	Recessive
TUBV042	10194640	⇑$CD19^+CD5^+$	Recessive
TUBV043	10194641	⇑$CD19^+CD5^+$	Recessive
TUBV044	10194642	⇑$CD19^+CD5^+$	Recessive
TUBV045	20053413	⇑$CD19^+CD5^+$	Dominant
TUBV046	10207835	⇑$CD8^+CD44^+Ly6C^+$	Dominant
TUBV047	20053014	⇑$CD19^+CD5^+$	Dominant
TUBV048	20052409	⇑$CD19^+CD5^+$	Dominant
TUBV049	10210150	⇓$CD3^+$; ⇑$CD44^+$	Dominant
TUBV050	10210903	⇑$CD19^+CD5^+$	Recessive
TUBV051	10198519	⇑$CD4^+CD25^+$, $CD11b^+Gr\text{-}1^-$, IgM; ⇓$CD19^+$, $CD4^+$	Recessive
TUBV052	10210480	⇑$CD19^+$	Recessive
TUBV053	40005907	⇑$CD19^+$; ⇓$CD3^+$, $CD8^+$	Recessive
TUBV054	40005908	⇑$CD19^+$; ⇓$CD3^+$, $CD8^+$	Recessive
TUBV055	40005321	⇑$CD19^+$	Recessive

Variant number	Mouse ID	Phenotype	Screen
TUBV056	40005658	⇑$CD8^+CD44^+Ly6C^+$	Recessive
TUBV057	10210151	⇓$CD19^+$	Dominant
TUBV058	10212339	⇑$CD8^+CD103^+$, $CD8^+CD62L^+CD45RA^+$; CD44 and Ly6C expression	Dominant
TUBV059	10212305	⇑$Gr\text{-}1^+$; ⇓$B220^+$	Dominant
TUBV060	10211683	⇑$CD19^+$	Dominant
TUBV061	10211911	⇓$CD19^+$, $CD4^+$	Dominant
TUBV062	10211936	⇓$CD19^+$; ⇑$CD19^+CD5^+$	Dominant
TUBV063	30016159	⇑$CD3^+$, $CD8^+$, $CD4^+25^+$	Dominant
TUBV064	30017287	⇑$Gr\text{-}1^+$; ⇓$CD3^+$, $CD19^+$	Dominant
TUBV065	30016186	⇑$CD8^+$	Dominant
TUBV066	40005988	Rh-factor +, αDNA-Ab +	Dominant
TUBV067	30018152	⇑$DX5^+$; ⇓$CD3^+$, $CD4^+$	Dominant
TUBV068	30018154	⇓$Gr\text{-}1^-$, $CD11b^+Gr\text{-}1^-$	Dominant
TUBV069	30018185	⇑$CD19^+$; ⇓$CD3^+$,	Dominant
TUBV070	30019082	⇑$CD3^+$, $CD4^+$	Dominant
TUBV071	30019081	Inflammation front limb	Dominant
TUBV072	30019091	Gut incidence	Dominant
TUBV073	10221534	⇑$CD19^+$; ⇓$CD4^+$	Recessive
TUBV074	30020098	⇑$CD4^+$, $CD8^+$	Dominant
TUBV075	30020107	⇑$CD3^+$, $B220^+$	Dominant
TUBV076	40007126	⇓$CD19^+$	Recessive
TUBV077	10221999	αDNA-Ab +	Recessive
TUBV078	10221320	⇓$CD3^+$; CD3 expression	Recessive
TUBV079	40006855	⇓$CD3^+$, $CD4^+$, $CD8^+$	Recessive
TUBV080	40007190	⇓$CD3^+$, $CD4^+$, $CD8^+$	Recessive
TUBV081	30021059	⇑$CD3^+$, $CD8^+$	Dominant
TUBV082	30022258	⇑$B220^+IgD^-$	Dominant
TUBV083	30022275	⇑$CD3^+$, $CD4^+$	Dominant
TUBV084	10220953	⇑$CD3^+$; ⇓$CD19^+$, $B220^+$	Dominant
TUBV085	10217892	CD8β expression	Dominant

Variant number	Mouse ID	Phenotype	Screen
TUBV086	40006381	⇑$CD19^+$, $CD19^+CD5^+$	Dominant
TUBV087	10218550	CD8β and DX5 expression	Dominant
TUBV088	10218521	B220 and Gr-1 expression	Dominant
TUBV089	10212456	⇑$CD8^+$, $CD19^+CD5^+$; ⇓$CD19^+$	Dominant
TUBV090	10212454	⇑$DX5^+$, $CD19^+CD5^+$; ⇓$CD19^+$	Dominant
TUBV091	30024228	⇑$CD19^+$; ⇓$CD3^+$	Dominant
TUBV092	30024177	⇑$CD3^+$, $CD8^+$	Dominant
TUBV093	10218726	⇓$CD3^+$	Dominant
TUBV094	10210149	⇓$CD3^+$; ⇑$CD44^+$	Dominant

Figure12: List of identified variants with mouse ID and phenotype.

If the mutation did not lead to enhanced lethality (e.g. TUBV082 and TUBV092) or sterility, (e.g. TUBV082) germ line transmission of the mutation and the corresponding phenotype was determined by setting up confirmation crosses. Subsequently, offspring were tested under the same conditions as the founder to confirm inheritance of the original phenotype. In 25 cases, offspring could be tested positive for the original phenotype, which gave rise to 25 new mutant lines, as listed in Figure 13.

Mutant line	Founder ID	Inherited phenotype	Screen
TUB001	40000264	⇑$Gr\text{-}1^+$; ⇓$CD19^+$, $CD3^+$, $CD8^+$, $CD4^+$	Dominant
TUB002	40001173	⇓$CD19^+$	Recessive
TUB003	40001168	⇑$CD8^+CD44^+Ly6C^+$; Ly6C expression	Dominant
TUB004	40001699	CD8β expression	Dominant
TUB005	10185284	⇑$CD4^+CD44^+Ly6C^-$; CD44 expression	Dominant
TUB006	20040487	⇓$CD19^+$, $CD3^+$	Dominant
TUB007	30003547	Cataract	Dominant
TUB008	20040053	⇑$CD19^+CD5^+$; CD44 expression	Dominant
TUB009	10193325	⇑$CD11b^+Gr\text{-}1^-$	Recessive

Mutant line	Founder ID	Inherited phenotype	Screen
TUB010	10184028	⇑ $CD8^+CD44^-Ly6C^-$	Recessive
TUB011	10194640	⇑$CD19^+CD5^+$	Recessive
TUB012	10210149	⇓$CD3^+$; ⇑$CD44^+$	Dominant
TUB013	10194642	⇑$CD19^+CD5^+$	Recessive
TUB014	10210151	⇓$CD19^+$	Dominant
TUB015	10207835	⇑$CD8^+CD44^+Ly6C^+$	Dominant
TUB016	30016159	⇑$CD3^+$, $CD8^+$, $CD4^+25^+$	Dominant
TUB017	40005321	⇑$CD19^+$	Recessive
TUB018	10212339	⇑$CD8^+CD103^+$, $CD8^+CD62L^+CD45RA^+$; CD44 and Ly6C expression	Dominant
TUB019	30019082	⇑$CD3^+$, $CD4^+$	Dominant
TUB020	10217892	CD8β expression	Dominant
TUB021	40005907	⇑$CD19^+$; ⇓$CD3^+$, $CD8^+$	Recessive
TUB022	10220953	⇑$CD3^+$; ⇓$CD19^+$, $B220^+$	Dominant
TUB023	10212456	⇑$CD8^+$, $CD19^+CD5^+$; ⇓$CD19^+$	Dominant
TUB024	30020107	⇑$CD3^+$, $B220^+$	Dominant
TUB025	10211911	⇓$CD19^+$; ⇓$CD4^+$	Recessive

Figure 13: Novel mouse mutant lines established during the first 2 years of screening.
List of newly identified and established mouse mutant lines with line name, mouse ID, inherited phenotype and type of mutation.

The generation of phenotype bearing offspring for recessive mutations is more time consuming. In theory, all F1 animals from the first mating are heterozygous for the mutation, and therefore, in most cases do not show penetration of the original phenotype. Subsequent brother-sister mating of these F1 animals is needed, to produce homozygous litters in the next generation, in which the original phenotype can be detected again. For this reason, the procedure of conformation cross for 24 variants is still ongoing, which potentially can lead to additional mutant lines (Status: 31.12.2004).

The main goal of ENU mutagenesis is not only the establishment of new mutant mouse lines, but also the identification of the mutated gene (genotyping) in order to gain new insights for

their function *in vivo*. Therefore, outcrosses for 4 lines to C57BL6/J background, TUB001, TUB005, TUB006, and TUB010, are already ongoing, in order to map the affected genes with the help of the SNP facility at the GSF.

3.2 Development of a *L.m.* infection screen

As demonstrated in 3.1, screening of ENU treated mice under resting conditions is a powerful tool for the identification of new mouse mutant lines, and analysis of those mouse lines can potentially lead to a better understanding of certain complex genetic networks and the diverse function of distinct gene products *in vivo*. Nevertheless, many genes involved in essential immune functions like innate and adaptive immune responses or the development and maintenance of protective immunity, won't be active under baseline conditions, and mutations in those will most likely remain undetected in steady-state screens. Therefore, the second part of this PhD work was dedicated to the development of an immunological challenge screen for ENU mutagenized mice using *L.m*. infection for the successful identification of mutants with defects in pathogen defense and establishment of protection against reinfection.

3.2.1 IFNγ and GOT plasma level correlate with strength of disease early after infection

Best-accepted parameters to determine the severity of listeriosis and the ability of the host to control a defined dose of pathogen, are survival curves or, to some extent, the determination of numbers of living bacteria in different organs. However, both methods are not suitable for a non-mouse consuming ENU screen, as each individual mouse theoretically carries a unique mutation and needs to survive the screening procedure. Therefore, to provide a founder for further breeding, a variety of different indirect parameters, which can be measured in a living mouse, were evaluated for their correlation with severity of disease and for monitoring the health status of *Listeria*-infected mice.

It is well known that *L.m.* mainly infects the spleen and liver of the host organism. Therefore, levels of certain liver enzymes in the plasma at day 3 after infection with different doses of *Listeria* (5,000-20,000 i.v.) were analyzed in order to investigate, whether the severity of hepatitis correlates with the overall severity of the systemic infection. It turned out, as illustrated in Figure 14 (upper panel) that there is a high correlation between the plasma

values of GOT and the number of *Listeria* in spleen, whereas this correlation is not as strong for other liver enzymes like GPT, Figure 14 (lower panel). Similar observations were made for the amounts of live *L.m*. in liver tissue (data not shown).

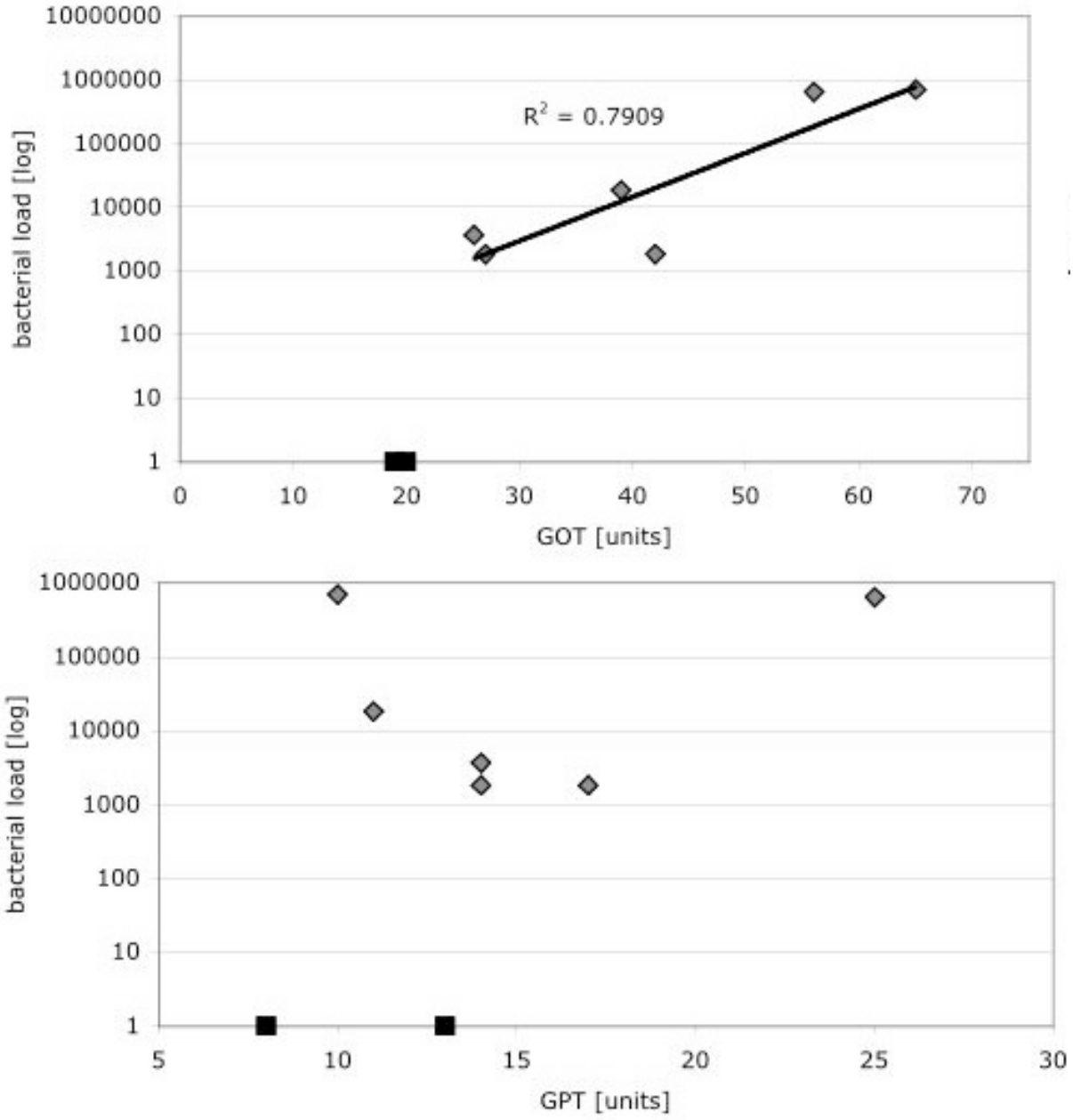

Figure 14: Severity of L.m. infection correlates with GOT plasma levels.
Bacterial load directly correlates with GOT plasma activity in mice on day 3 after infection (upper panel), but not with GPT levels (lower panel). Graphs show Listeria loads in spleen versus GOT/GPT values of infected (grey diamonds) and control (filled squares) C3H/HeJ males at an age of 12 weeks. Number in the upper histogram indicates the correlation coefficient between bacterial load and GOT activity.

Furthermore, the plasma level of certain chemokines and cytokines were promising candidates as indicators for the severity of disease, as the crucial role of pro-inflammatory cytokines for early control of *L.m.* infection has been described before. To address this

question, the concentrations of IL-2, IL-4, IL-5, IFNγ and TNFα in the plasma were determined in the same sets of experiments. Analysis of the data revealed that high plasma values of IFNγ correspond to high numbers of bacteria in the spleen, indicating that IFNγ values are also a suitable parameter for immunomonitoring in a *L.m*. infection screen (Figure 15, upper panel). In contrast, bacterial burden is not reflected by TNFα amounts (Figure 15, lower panel), and IL-2 concentrations were below the detection limit of the assay (data not shown) As expected in a Th1 driven infection system, amounts of the typical Th2 cytokines IL-4 and IL-5 were not altered in infected compared to uninfected mice (data not shown).

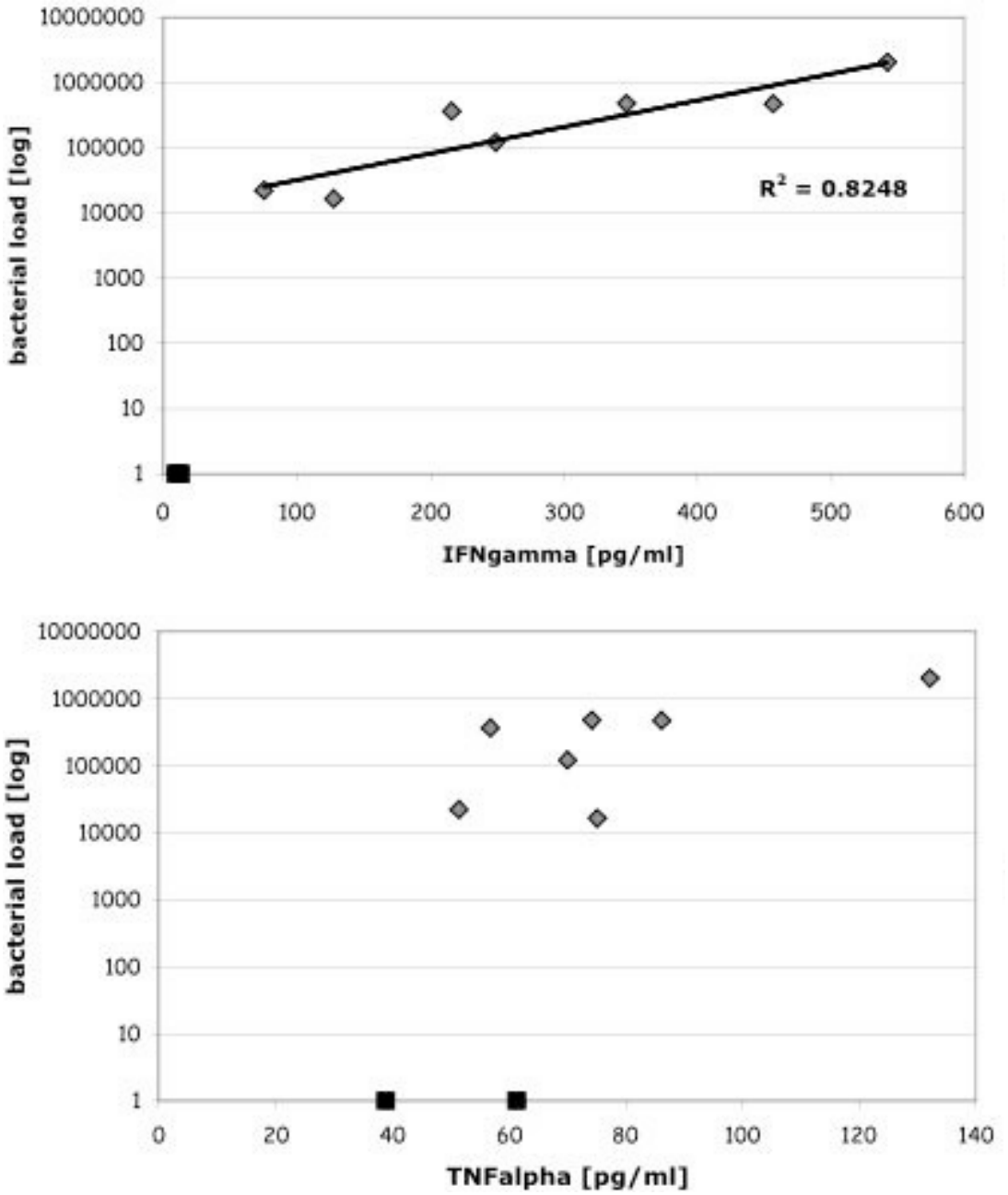

Figure 15: Direct correlation between the amounts of INFγ in the blood plasma and bacterial load in the spleen at day 3 after infection of C3H/HeJ males.

Blood plasma concentrations of the Th1 cytokine IFNγ (upper panel), but not of TNFα (lower panel), reflect the severity of Listeria infection in male 12 weeks old C3H mice at day 3 after infection. Grey diamonds represent mice infected with different doses of L.m. (5,000-20,000 i.v.), filled squares PBS injected control males.

3.2.2 Detection of *L.m.*-specific CD4$^+$ and CD8$^+$ T cell populations in C3H mice

Since the plasma level of GOT or IFNγ measured during the early phase of infection at day 3, most likely reflect the innate immune response and the ability of early control of replicating bacteria, next step was to find suitable parameters for the quality of the adaptive immune response. Although there are some reports for a minor involvement of Abs in this infection model, the adaptive immune response against the facultative intracellular bacteria mainly consists of T cells, especially of CD8$^+$ T cells. A substantial number of CD8$^+$ T cells, directed against distinct peptides derived from WT or genetically modified *L.m.* are detectable at day 7, peak of the primary T cell response, in BALB/c or C57BL6/J. Until now, no epitopes were described for C3H mice, the mouse strain which is used in the Munich ENU screen.

To test for the presence of Ag-specific CD4$^+$ or CD8$^+$ T cells in C3H mice, splenocytes at day 7 after primary infection with $2x10^3$ *L.m.* were stimulated *in vitro* with either *Listeria* epitopes, predicted to bind on H2-K^k of C3H mice like $p60_{117-125}$ (Pamer et al., 1997; Sijts et al., 1997), or peptides derived from a peptide library (Maecker et al., 2001) of listeriolysinO, and the frequencies of peptide-responsive T cells was determined by intracellular cytokine staining for IFNγ. LLO had been chosen because it has been demonstrated before that LLO is readily accessible to the proteasome of infected host cells, as the peptide LLO_{91-99} derived from this protein is presented on MHC-I in BALB/c mice and induces strong immunodominant CD8$^+$ T cell population (Busch and Pamer, 1998).

Concerning the predicted MHC-I peptide $p60_{117-125}$, a remarkable CD8$^+$ T cell responses of around 0.7% of all CD8$^+$ T lymphocytes in the spleen could be observed in C3H mice against this epitope, Figure 16, upper panel, whereas no significant CD8 T cell response was detectable against peptides out of the LLO library (data not shown). Nevertheless, analysis of CD4 response to LLO peptides revealed a consistent CD4$^+$ T cell population of approximately 0.5% after primary infection specific for $LLO_{215-234}$, as illustrated in Figure 16, lower panel.

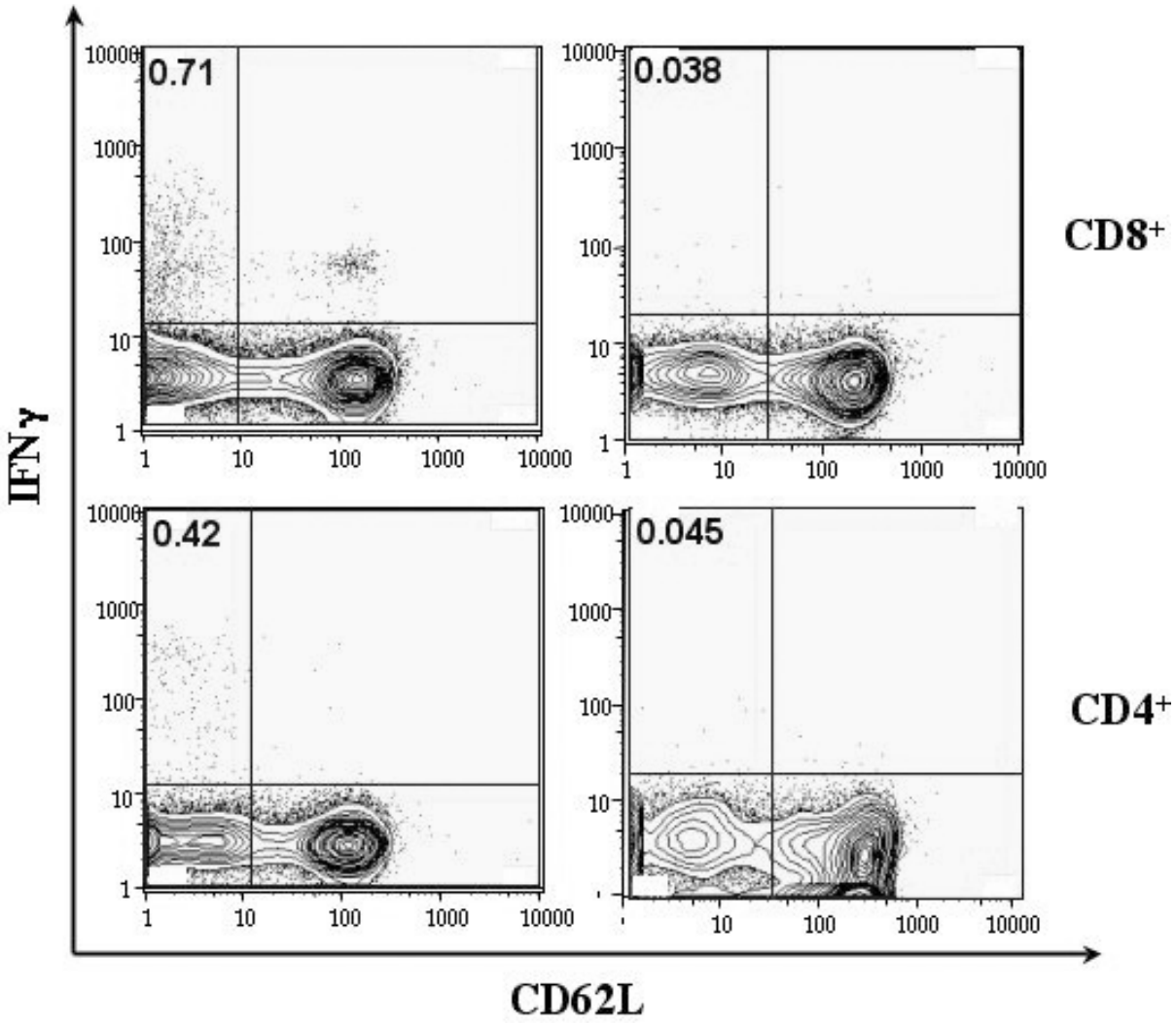

Figure 16: Listeria-specific CD8$^+$ and CD4$^+$ T cells detectable in spleens of C3H mice after primary infection.

Measurable frequencies of IFN responsive CD8$^+$ (upper) or CD4$^+$ (lower) T cells in spleens of C3H/HeJ mice at day post primary infection and in vitro stimulation with p60$_{117-125}$- (upper left) or LLO$_{215-234}$-peptide (lower left) compared to stimulation with irrelevant peptides (right side). Contour plots are gated on CD8$^+$ (upper) or CD4$^+$ (lower) cells. Numbers represent the percentage of CD62L$^-$IFNγ producing CTL or Th cells.

To further confirm the presence of the described *Listeria*-specific CD8$^+$ and CD4$^+$ T cell populations in C3H, mice were reinfected with a high dose of 1x10^5 *L.m.*, 5 weeks after primary infection. This induces a secondary T cell response, which, at least shown for CD8$^+$ T cells, results in higher frequencies of Ag-specific cells at day 5, the peak of the recall response. Indeed, for both populations, the p60$_{117-125}$ class-I restricted epitope as well as for the class-II restricted LLO$_{215-234}$, a 2-4 fold increase compared to primary frequencies could be observed by ICS in spleens of secondary infected C3H mice (Figure 17).

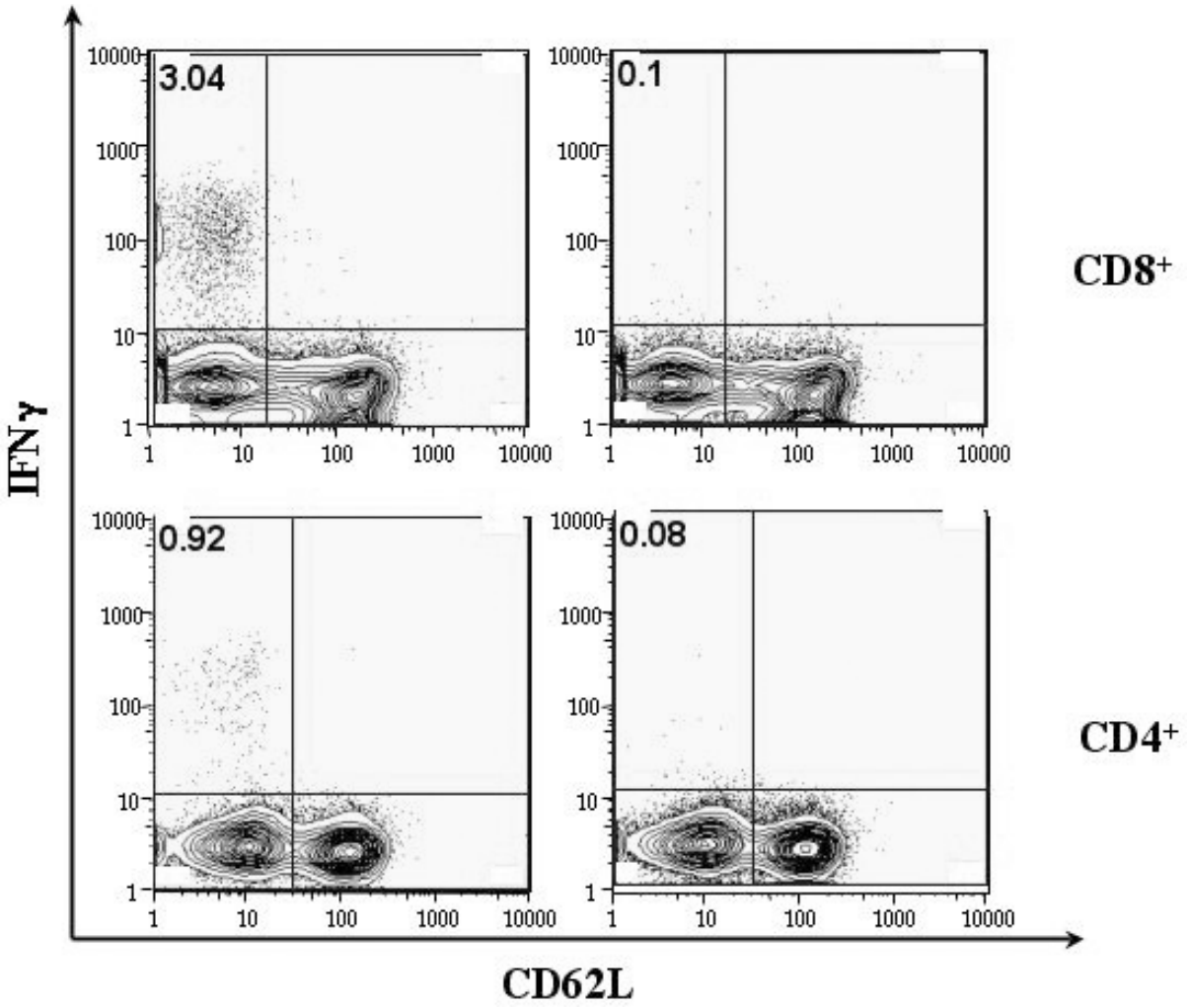

Figure 17: Stronger CD8⁺ and CD4⁺ T cell response after recall infection with L.m..
Increased frequencies of $p60_{117\text{-}125}$ responsive CD8⁺ (upper left) and $LLO_{215\text{-}234}$ CD4⁺ (lower left) T cells as compared to stimulation with irrelevant peptides (right) after recall infection. Representative ICS results after in vitro stimulation of bulk splenocytes at day 5 after infection with respective peptides. Images are gated on live CD8⁺ (upper) or CD4⁺ (lower) cells. Numbers indicate the frequency of activated T cells, responding with IFNγ production to peptide stimulation.

3.2.3 Detection of Ag-specific CD8⁺ T cells *in vivo* with H2-K^k $p60_{117\text{-}125}$ Tetramers after primary and secondary infection

Since ICS is a quite time- and work-intensive assay for which the mouse has to be sacrificed, as it is usually performed with LN-cells or splenocytes, this method is not suitable for measuring acquired immunity in a non-mouse consuming, high-throughput screen. To circumvent this problem, the MHC multimer technology was used in order to generate

Tetramers for the detection of Ag-specific T cells, also applicable for measurements in the peripheral blood. Although the successful construction of MHC-II Tetramers has been described in the literature, the focus laid on the construction of class-I H2-K^kp60$_{117-125}$ Tetramers, as this technology is well established in our laboratory. In addition, it has been reported in several articles, that protective immunity against *Listeria* is mediated via $CD8^+$ T cells, what makes the monitoring of *Listeria*-specific $CD8^+$ T cells, especially during recall response, the most important parameter to identify mutants with defects in the adaptive immune response as well as in the generation or maintenance of protective immunity.

Therefore, Tetramers were generated as described and blood samples were stained with H2-K^kp60$_{117-125}$ at day 7 after primary or day 5 after secondary infection, respectively. As shown in Figure 18, substantial p60$_{117-125}$-specific $CD8^+$ T cell populations could be detected in the peripheral blood of C3H mice after first and second infection, supporting the idea that p60$_{117-125}$ Tetramers might be a useful tool to screen for proper induction of acquired immune responses in C3H mice.

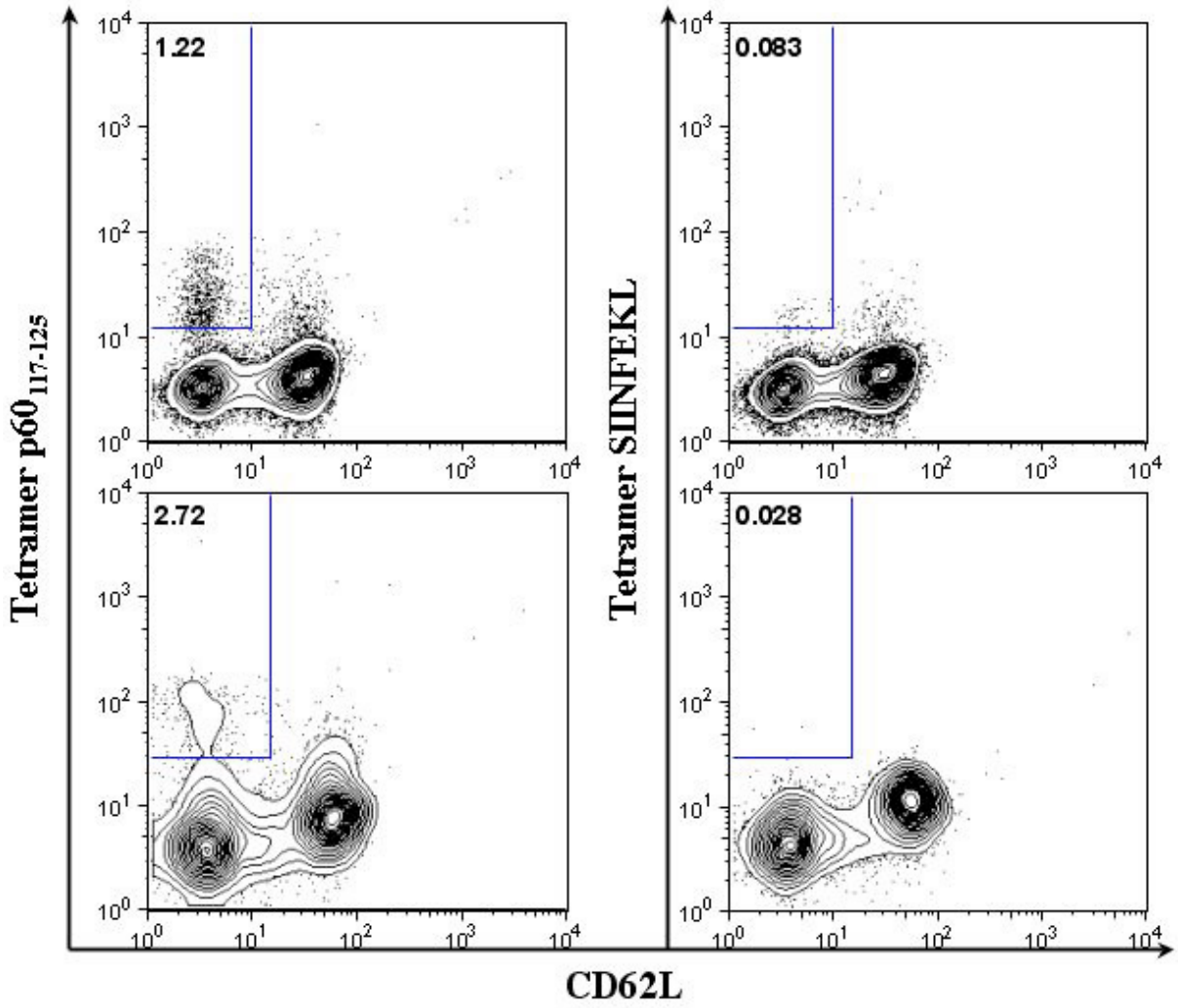

Figure 18: $p60_{117-125}$ Tetramer staining of peripheral blood lymphocytes after primary and secondary L.m. infection.

Substantial frequencies of Listeria-specifc $CD8^+$ T cells are detectable in the peripheral blood of C3H mice after primary (upper left) and secondary (lower left) infection. Representative contour plots, gated on live $CD8^+$ T cells, are shown. Numbers represent the frequency of $CD8^+CD62L^-Tetramer^+$ cells. Staining with the irrelevant H2-Kb SIINFEKL Tetramer (right panel, upper: after secondary-, lower post primary-infection) served as negative control.

3.2.4 Standardized screening protocol

Besides the need for robust parameters for innate and adaptive immune responses, additional requirements have to be fulfilled to be able to use *Listeria* infection as an immunological challenge screen. As demonstrated before and also described in the literature, the severity of disease is tightly connected to the infection dose. In an ENU challenge screen, with the target

to identify single individuals out of a cohort of mice with defects in the immune response, control of the infection dose with minimized variations is crucial to reduce the number of false positive mice. Therefore, although i.v. infection is often used in the literature for *Listeria* infection and can be handled relatively consistent by trained personal, application of the pathogen i.p. is according to our experience less error-prone and therefore the preferred route of infection for ENU screening.

Furthermore, whereas WT mice can handle the chosen doses for primary or recall infection, animals with mutations in genes responsible for effective immune response may not and eventually even die after infection. The big advantage of *L.m.* is the fact that *L.m.* is a bacterium, which can be treated very effectively with antibiotics in order to rescue the potentially most interesting mice with severe disorders in immunity. In addition, it was recently demonstrated by others that treatment with antibiotics early during the infection does not significantly influence the *Listeria*-specific $CD8^+$ T cell response and subsequent memory T cell generation. Similar findings could be observed for C3H mice (Figure 19).

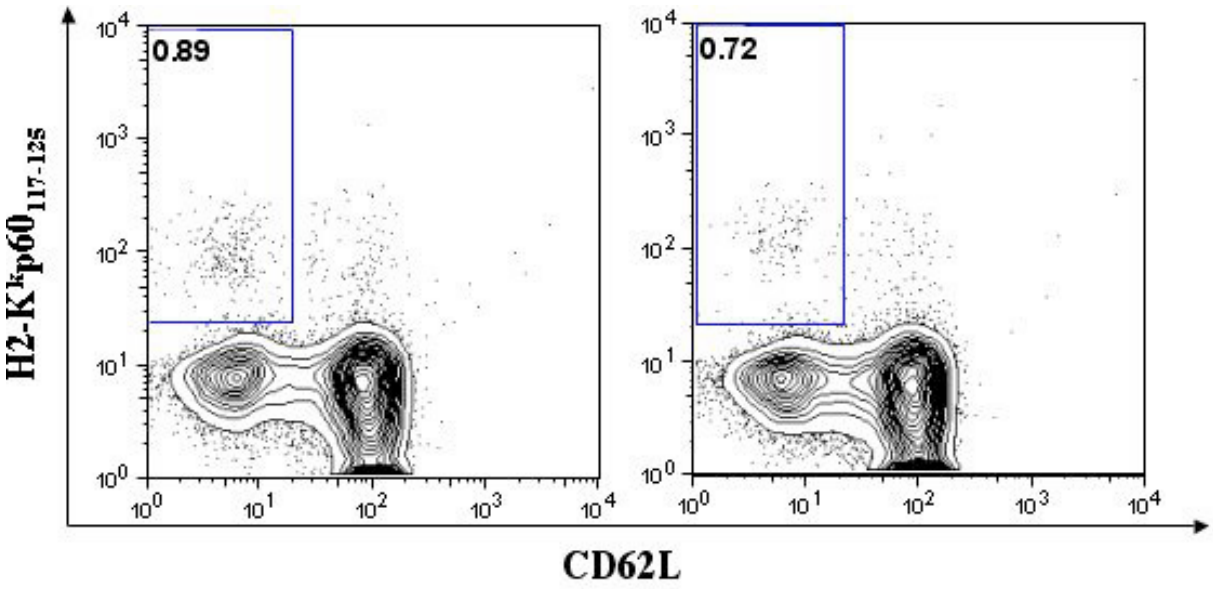

Figure 19: Antibiotic treatment does not influence the adaptive $CD8^+$ T cell response. Comparable frequencies of $p60_{117-125}$-specific T cells are detectable at day 7 after primary infection in the peripheral blood of C3H mice, either treated (right) or not treated (left) with 2mg/ml ampicillin in the drinking water. Medication was started 48h after infection. Plots are gated on live $CD8^+$ T cells and values indicate the percentage of $CD8^+CD62L^-Tetramer^+$ cells.

Combining the practical requirements with the results for robust parameters, a *Listeria* challenge screen for ENU mutagenized mice could be designed as followed:

I.p. infection of C3H males with $2.5x10^4$ *L.m.* is performed at day 0. First blood taking is done at day 3 to determine GOT activities and IFNγ concentrations in the blood plasma. Subsequent application of 2mg/ml ampicillin in the drinking water, in order to rescue mutant mice that would not survive primary infection doses. Second bleeding should be performed at day 7 to monitor primary T cell response in the peripheral blood.

Recall infections could be given five weeks later with $1x10^6$ *L.m.* i.p.. Blood taking is then carried out at day 2 for GOT and IFNγ measurement, followed by ampicillin treatment. Final bleeding is conducted at day 5 to calculate the frequencies of $p60_{117-125}$–specific T cells in the peripheral blood during the memory T cell response.

3.3 Sex dependent susceptibility to *L.m.* infection

During the work on the establishment of *L.m.* infection as challenge screen for ENU mutagenized mice, the influence of gender had to be determined for the progress and severity of listeriosis. It has been described in the literature, that in many experimental models, females show higher resistance against certain pathogens than males, nevertheless this issue had never been clarified for *L.m.* infection, although this organism is extensively used to study innate and adaptive immune responses in mice.

3.3.1 Increased lethality of female mice after *L.m.* infection

To address this question, cohorts of age-matched male and female BALB/c mice were infected with $1.5x10^4$ *L.m.*, and survival was followed for a period of 14 days. As positive control served male and female BALB/c mice infected with $1x10^5$ *S.p.,* for which a clear sex dependency had been shown before. As expected *S.p.*-infected male showed an increased lethality compared to females, with all males dying until day 4, whereas half of the females survived the whole observation period (Figure 20, left panel). In contrast, an exactly opposite sensitivity pattern was observed against *L.m.* infection, as 40% of the females died up to day 4, and nearly all males survived the experiment (Figure 20, right panel).

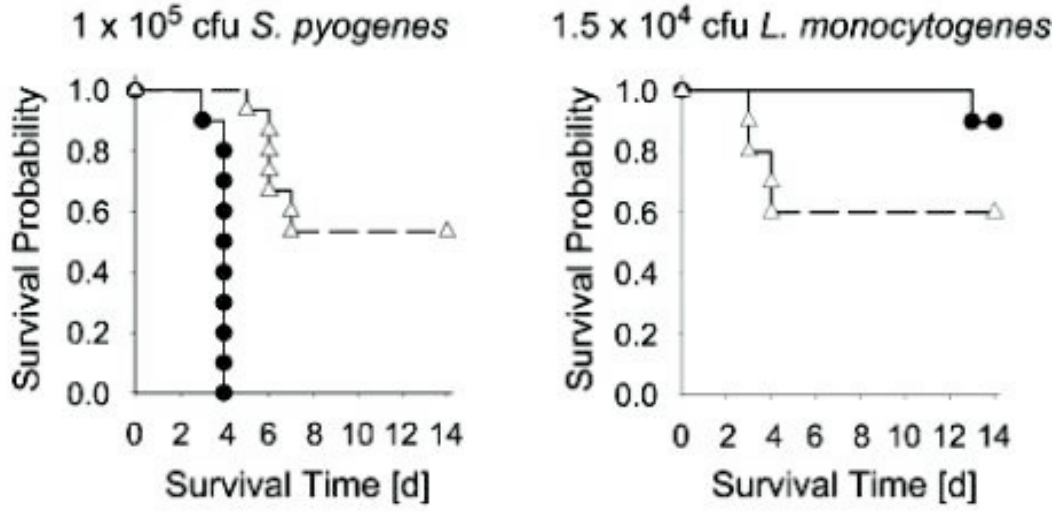

Figure 20: Infection of BALB/c mice with L.m. reveals increased lethality in females.
Kaplan-Maier survival curves for male (filled circles) and female (open triangles) BALB/c mice after infection with L.m. (right) or S.p. (left) with the indicated doses. Seven mice per group were monitored for a period of 14 days.

As it is known that susceptibility to *L.m.* infection is partly dependent on the mouse strain, it had to be ruled out that the observed sex difference is a BALB/c specific phenomenon. Therefore, age- and sex-matched groups of 4 different mouse strains, C57BL6/J, BALB/C, C3H/HeN and CBA/J were infected with $2x10^4$ *L.m.*, and survival was monitored over 14 days. A slightly increased infection dose was used, as it is well documented for C57BL6/J to be more resistant against *L.m.* infection than other mouse strains. For BALB/c, similar results were obtained as described above. Thereby, the difference between the sexes was even more pronounced due to the higher infection dose (Figure 21). In addition, female mice of all other 3 mouse inbred strains showed poorer survival curves compared to the males, demonstrating that increased susceptibility of females is a general feature of *L.m.* infection in mice (Figure 21). Also differences between the strains in susceptibility towards *L.m.* can be seen in Figure 21, with C57BL6/J and BALB/c being most resistant, followed by C3H/HeN and CBA/J mice are most sensitive against *L.m.* infection.

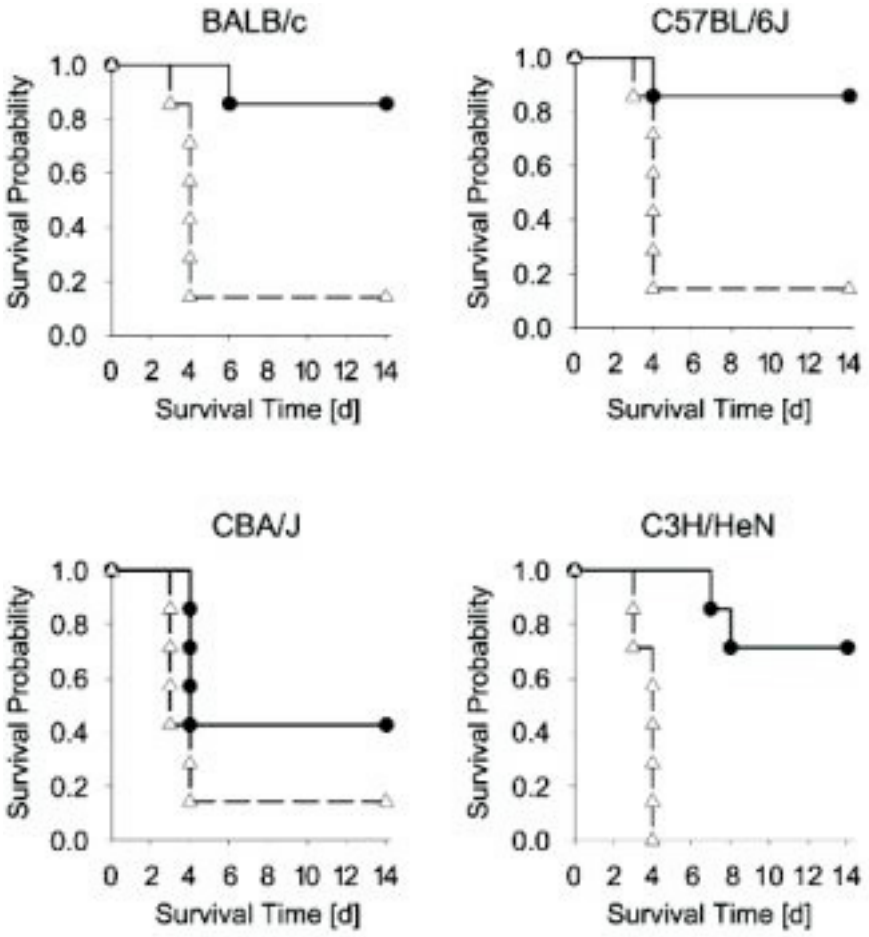

Figure 21: Increased susceptibility of female mice against L.m. infection is strain independent.

Kaplan-Maier survival curves for 4 different mouse inbred strains (BALB/c, C57BL/6J, CBA/J, C3H/HeN), infected with 2x10^4 L.m. i.v.. Survival of seven mice per group was monitored for 14 days.

3.3.2 Higher bacterial load in spleen and liver of infected mice

To elucidate the underlying mechanisms for the sex dependent susceptibility pattern to *L.m.*, on day 3 after infection bacterial loads of spleen and liver, the 2 mainly affected organs during *L.m.* infection, were determined. As shown in Figure 22, significantly higher bacterial loads were counted in spleens of infected females compared to their male counterparts. Similar tendencies were obtained from calculating values of CFU in the liver (data not shown). However, CFU values are clearly influenced by the genetic background of the mice, as higher values for living bacteria in spleen or liver do not always reflect higher susceptibility. For

example, the resistant C57BL6/J males or females have equal or even higher amounts of *L.m.* in spleens than the sensitive CBA/J.

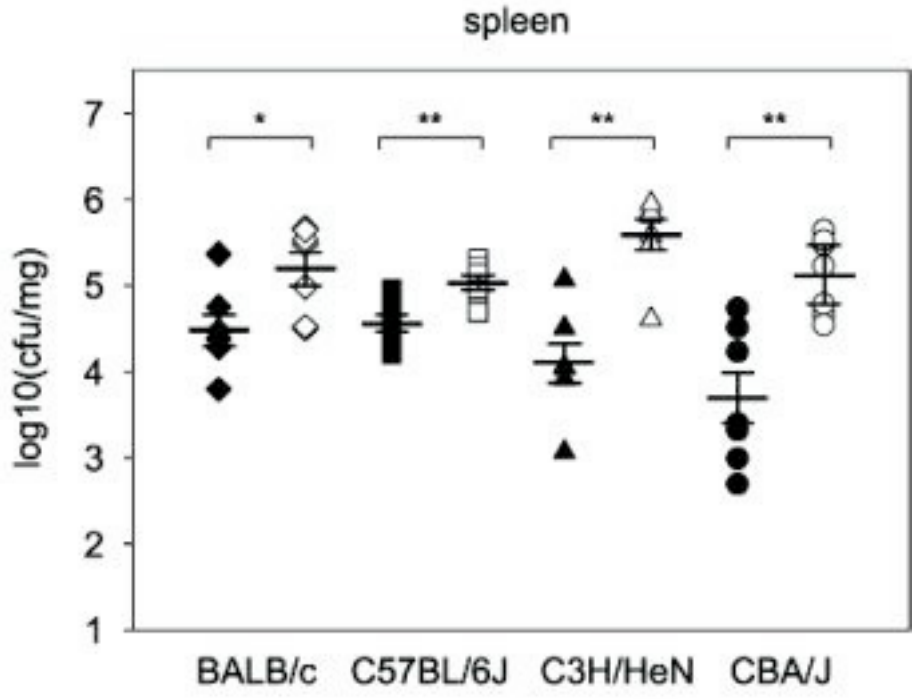

Figure 22: Bacterial load of male and female mice of 4 different inbred strains after L.m. infection.

Amount of live L.m. in the spleen of male (filled symbols) and female (open symbols) mice of the indicated mouse inbred strains at 3 after i.v. infection with $2x10^4$ L.m..

3.3.3 More severe lymphopenia in the peripheral blood of female mice

As previously reported, *L.m.* infection is characterized by a tremendous reduction of lymphocytes (lymphopenia) in the periphery. To address the question, whether there is a correlation between the intensity of lymphopenia and sex dependent resistance against *L.m.*, the cellular content and constitution of the peripheral blood was intensively analyzed by flow cytometry at the GMC at day 3 after infection. This time point was chosen, since susceptible mice usually die around day 4. As shown exemplarily for $CD4^+$ T cells in Figure 23, lymphopenia was statistically significantly different in nearly every gender and strain after *L.m.* infection. However, no statistically significant differences between sexes were detected with respect to the degree of lymphopenia.

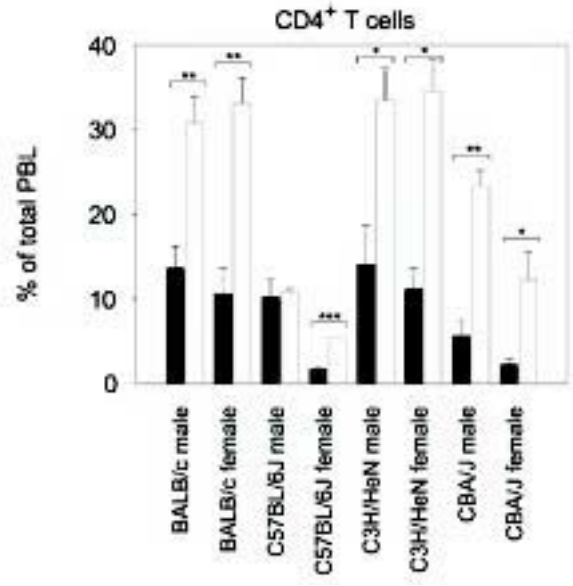

Figure 23: Lymphopenia in the peripheral blood after L.m. infection.
*Lymphopenia, shown at the example of reduced CD4⁺ Th cells, in the peripheral blood of infected (filled bars) compared to uninfected control mice (open bars) at day 3 after infection with $2x10^4$ L.m.. Histograms represent the means of 3-7 animals per group ± standard error of mean. Significant differences are shown as: *p<0.05, **p<0.01, ***p<0.001.*

3.3.4 Differences in plasma levels of IFNγ and IL-10

In order to find other explanations for the differences between male and female mice in resistance against *L.m.* infection, the cytokine response of the different sexes and strains was determined in the plasma, as there could be shown by others that several cytokines play a crucial role especially in the early control of the infection. Therefore, the concentrations of 18 different cytokines or chemokines were measured in the peripheral blood, showing several typical changes already known for this infection model (Figure 24 and data not shown). Most interestingly, although male littermates had lower bacterial loads, there was a clear tendency or in some strains even a statistically significant increase in the level of pro-inflammatory IFNγ in male mice (Figure 24, left). A contrary picture was found for IL-10 values in the blood plasma, being statistically significantly higher in the more susceptible females (Figure 24, right). Keeping in mind that IL-10 has the capacity of down-regulating IFNγ, a very important cytokine for early control of infection, these results indicate a crucial role of IL-10 for the sex dependent susceptibility pattern to *L.m.* infection.

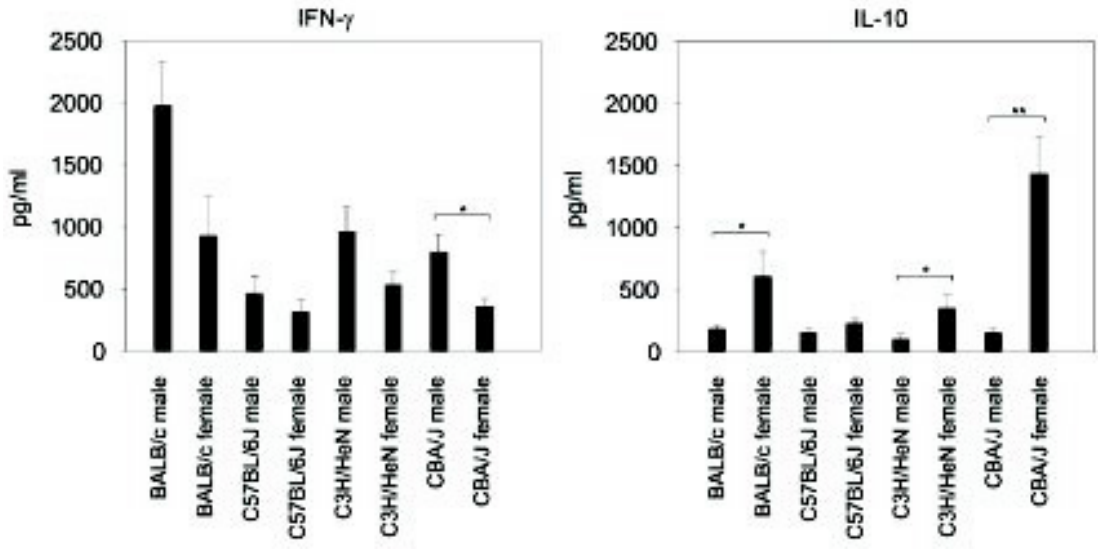

Figure 24: Lower IFNγ and higher IL-10 blood plasma concentrations in more susceptible female mice.

*Blood samples were taken at day 3 after infection from males and females of the indicated mouse inbred strains and blood plasma concentrations for IFNγ (left) and IL-10 (right) were determined. The mean results obtained from 3-7 mice per group (± standard error of mean) are shown. Significant differences are indicated as: *p<0.05, **p<0.01.*

3.3.5 Loss of sex dependent susceptibility to *L.m.* infection in IL-10 deficient mice

To test the hypothesis that the immunosuppressive cytokine IL-10 is involved in the increased susceptibility of female mice towards *L.m.* infection, IL-10 deficient mice and their littermate controls were infected with $1.5x10^4$ *L.m.* and subsequent survival was monitored. As shown in Figure 25 A, the sex dependent difference in survival of WT mice disappears in IL-10 deficient mice, where females survive as well as their male counterparts. Furthermore, as described in Figure 25 B, the IFNγ level of female IL-10 deficient mice reach similar values compared to male WT controls, both being statistically significantly higher than in IL-10 sufficient females. Therefore, these results support the interpretation for a crucial role of IL-10 in gender specific resistance against *L.m.* by down-regulating IFNγ in the more susceptible female mice.

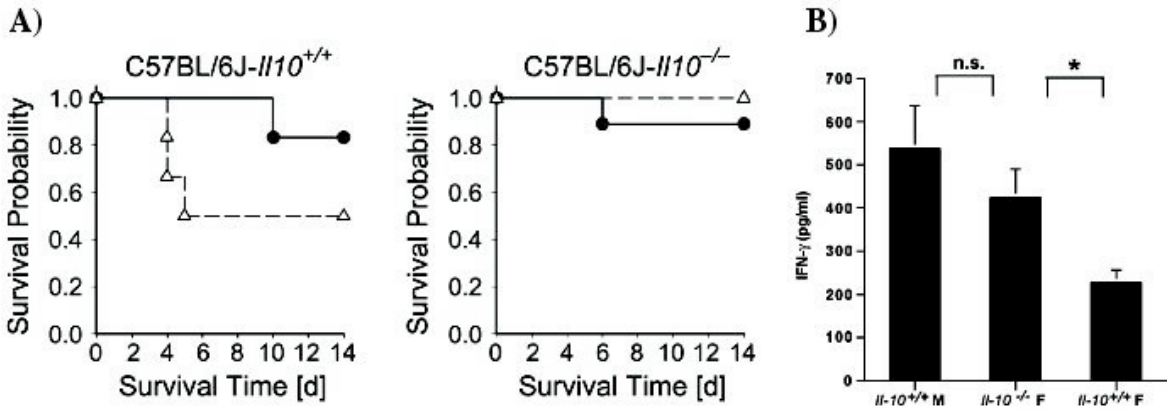

Figure 25: Absence of sex-specific susceptibility pattern in IL-10 KO mice after L.m. infection.

*A) Kaplan-Maier survival curves for L.m.-infected male (filled circles) and female (open triangles) control (left) and IL-10 KO (Il10$^{-/-}$, right) mice. Seven mice per group were monitored for a period of 14 days. B) Female IL-10 KO mice show IFN levels comparable to concentrations found in WT males after L.m. infection. Seven mice per group were sampled on day 3 post-infection. Level of significance is indicated as: *p<0.05, n.s. = not significant.*

3.3.6 Different susceptibility to *L.m.* does not reflect different T cell responses in male and female mice

In order to search for additional differences between the sexes in the regulation and efficiency of immune responses against *L.m.*, which could further contribute to the observed differences in susceptibility, the adaptive T cell response in males and females was investigated in more detail. For this reason, male and female C57BL6/J mice were infected with a sublethal dose of $2x10^3$ ovalbumin expressing *Listeria*, allowing a simultaneous investigation of the SIINFEKL-specific $CD8^+$ and $LLO_{188-201}$-specific $CD4^+$ T cell responses with MHC-I Tetramers and/or with ICS staining for IFNγ producing, peptide-responsive T cells. Interestingly, analysis of frequencies and absolute numbers of SIINFEKL $Tetramer^+$ T cells in the spleen revealed no significant differences in the amount of Ag-specific $CD8^+$ T cells between males and females (Figure 26), although resistance to *Listeria* infection turned out to be so different between sexes during early phase after infection.

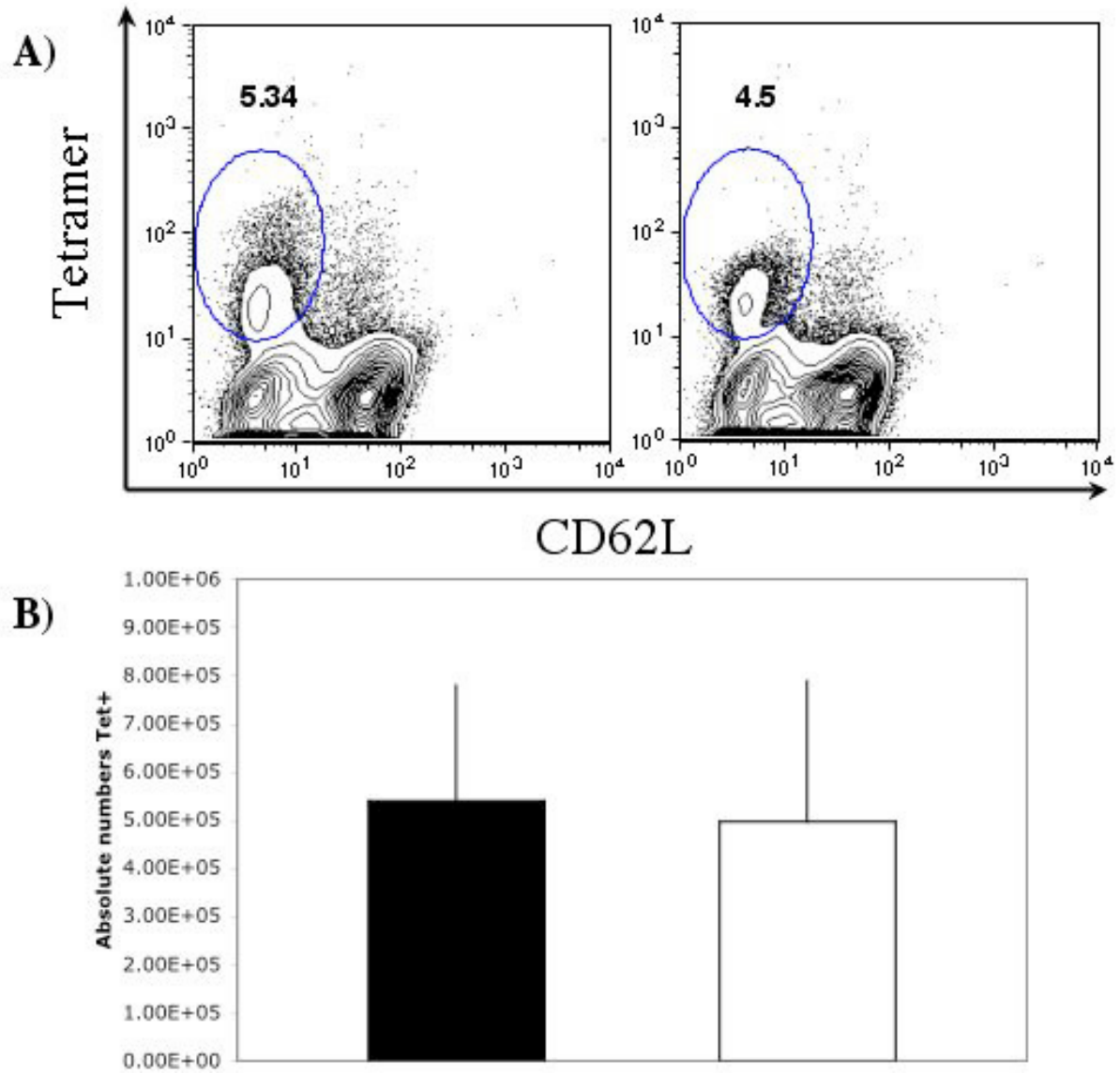

Figure 26: Comparable amounts of CD8$^+$ Tetramer$^+$ T cells in male and female mice after infection with L.m..

A) Representative plots of a male (left) or female (right) mouse, gated on live CD8$^+$ splenocytes on day 7 after infection. Numbers indicate the frequency of SIINFEKL-Tetramer$^+$ CD62L$^-$ cells within the CD8 population. B) Histograms show the mean of 4-5 animals per gender ± SD of the absolute numbers of Tetramer$^+$ cells per spleen of male (black bars) and female (open bars) C57BL/6J on day 7 post-infection.

This finding was further confirmed by results based on ICS, Figure 27, which confirmed that there are no substantial differences in the cytotoxic T cell response against SIINFEKL. The same is true for $LLO_{188-201}$-specific T helper cell responses (data not shown), suggesting comparable adaptive immune responses in both sexes, without any correlation to the different susceptibility pattern after *L.m.* infection.

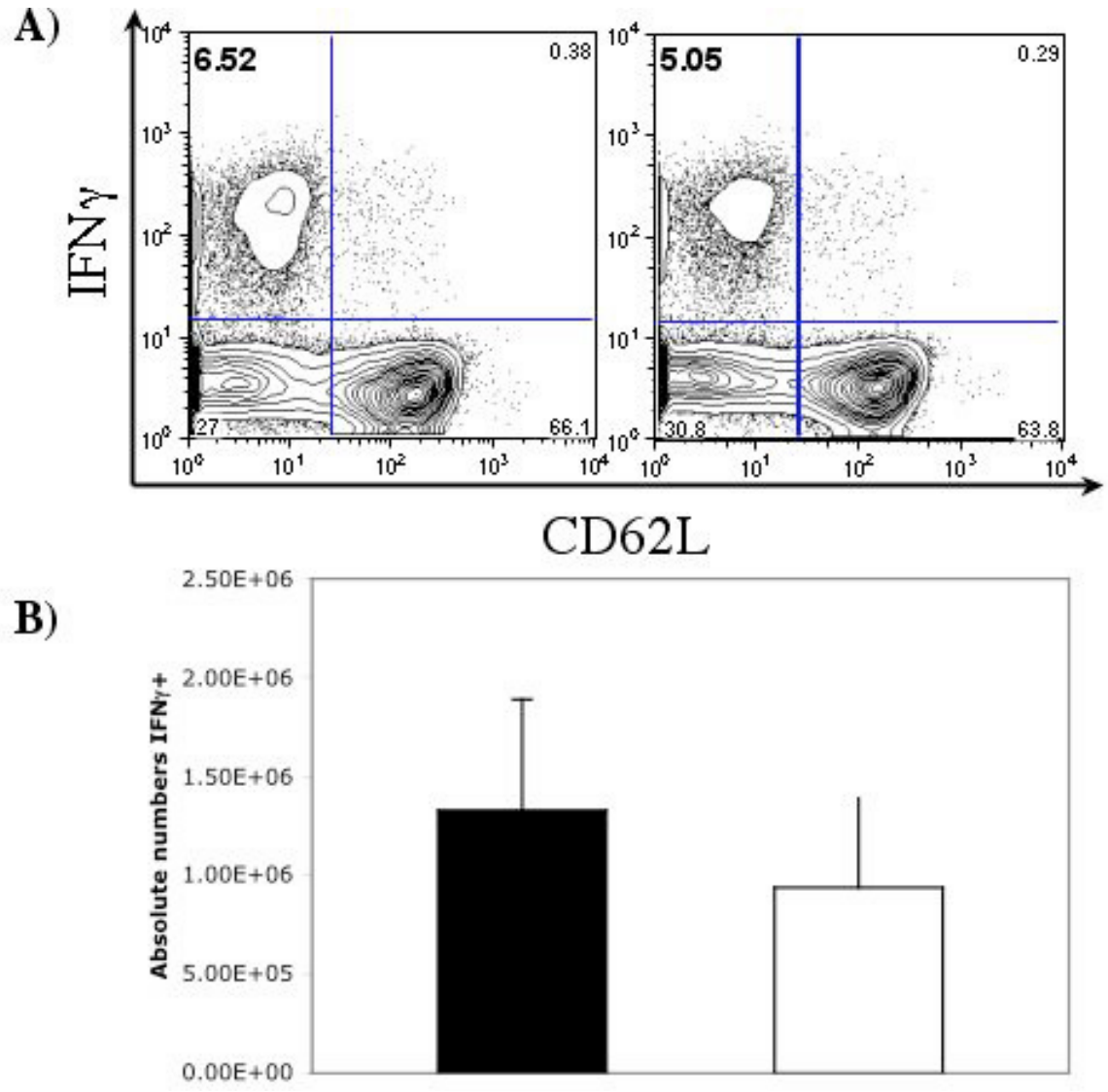

Figure 27: Similar frequencies of antigen-specific CD8⁺ T in male and female mice.
A) Representative contour plots (gated on live CD8⁺ cells) after 5h SIINFEKL peptide stimulation of bulk splenocytes at day 7 after L.m. infection. The numbers indicate the percentage of activated CD8⁺CD62L⁻ T cells that produced IFNγ due to stimulation (left: male; right: female). B) Comparable absolute numbers of IFNγ producing cells in spleens of male (black bars) and female (open bars) C57BL6/J mice. Histograms represent the means ± SD of IFNγ⁺ cells per spleen in 4-5 mice per group.

3.3.7 Higher resistance leads to impaired T cell response in IL10 KO mice

It has been reported for many infection models that deficiency for the immunosuppressive IL-10 leads to higher resistance, which might be partially explained by enhanced T cell responses. To test whether a similar correlation could also be found in our experimental

setting, Tetramer staining and ICS of WT and IL10$^{-/-}$ mice at day 7 after infection with 2x10^3 ovalbumin expressing *L.m.* was performed to investigate the consequence of IL-10 deficiency on the Ag-specific T cell response. Surprisingly, our data revealed reduced numbers and frequencies for SIINFEKL-specific Tetramer$^+$ T cells in IL10$^{-/-}$ males and females (Figure 28). Similar results were obtained for ICS assays upon SIINFEKL stimulation (Figure 29). Concerning the LLO$_{188-201}$-specific CD4$^+$ T cell population, no significant differences in the T cell response was detected in IL10$^{-/-}$ mice (data not shown).

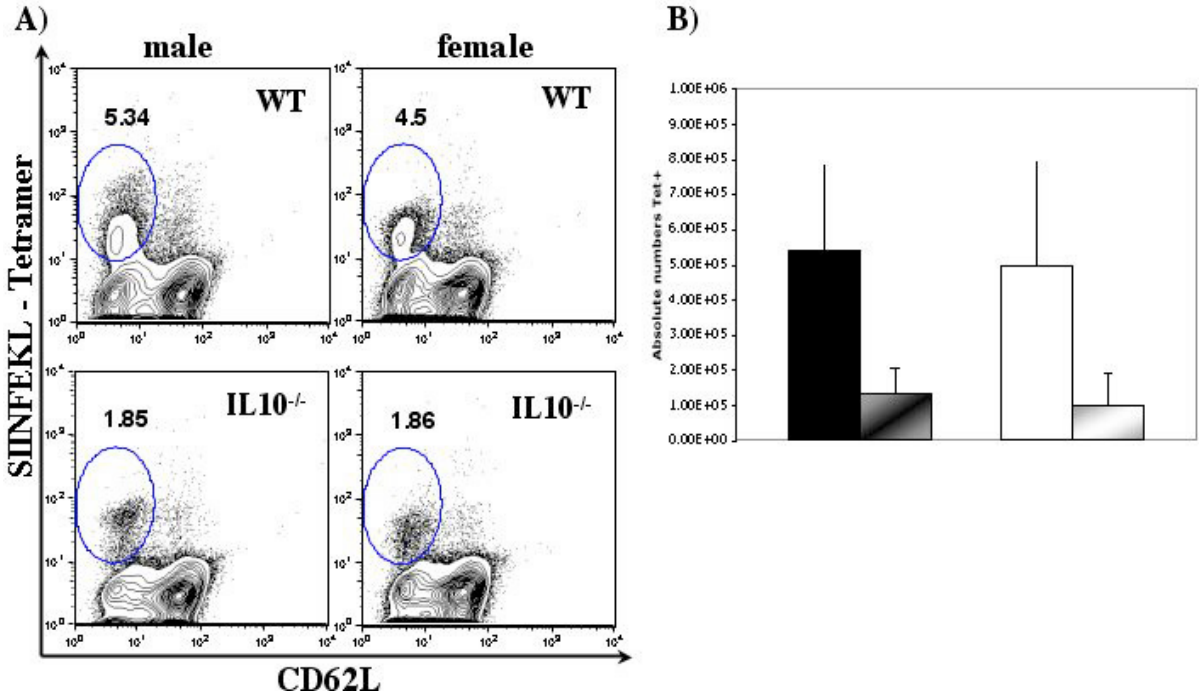

Figure 28: Reduced frequencies of antigen-specific T cells in IL-10 KO male and female animals.

A) Representative dot plots of male (left panel) and female (right panel) IL-10 sufficient (upper row) and IL-10 deficient (lower row) C57BL6/J mice. Images are gated on live splenocytes, numbers indicate the frequency of CD8$^+$CD62L$^-$Tetramer$^+$ T cells on day 7 after L.m. infection. B) Graph illustrates absolute numbers of CD8$^+$CD62L$^-$Tetramer$^+$ T cells per spleen in WT males (black bars) and females (open bars), as well as in IL10 KO males (grey/black bars) and females (grey/white bars). Shown are the means of 4-5 mice per group ± SD.

In summary, these observations suggest that higher resistance of IL-10 KO mice is not caused by an enhanced T cell response, as the frequencies and amounts of Ag-specific T cells are even lower in IL-10 KO mice. Therefore, it is more likely that deficiency for IL-10 results in

a more effective innate immune response against *Listeria*, which subsequently leads to a reduced time period for successful T cell priming and lower numbers of *Listeria*-specific T cells.

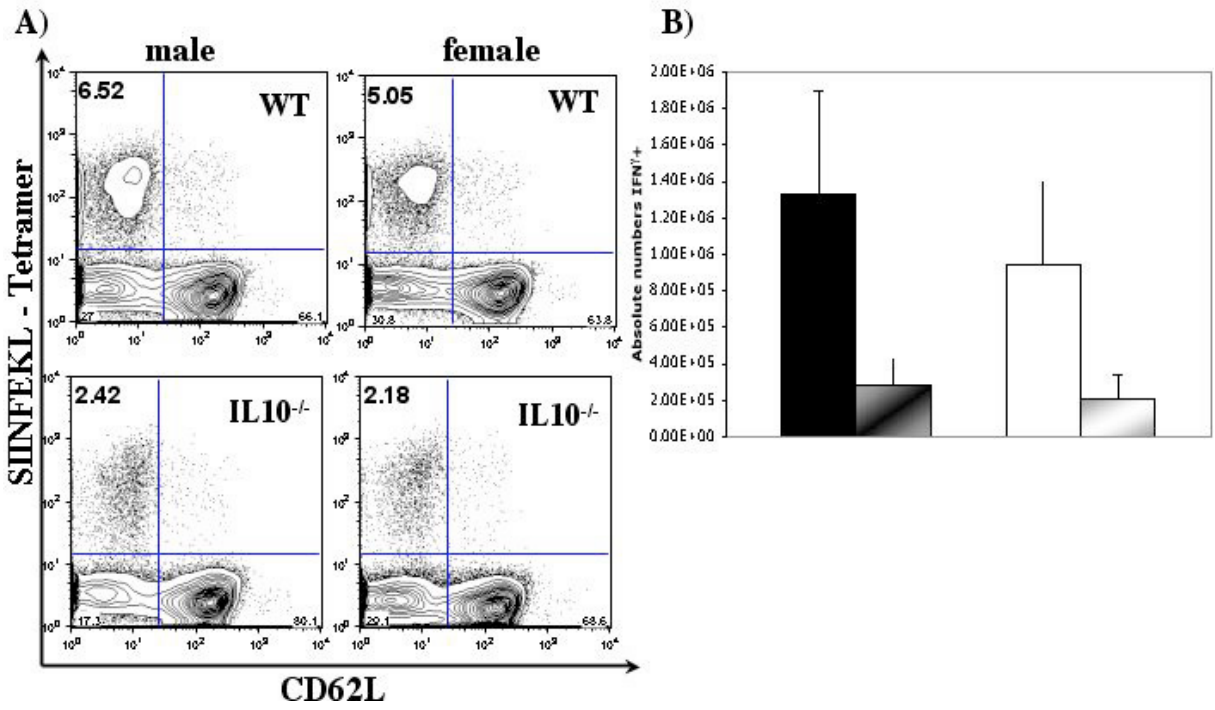

Figure 29: Reduced frequencies of antigen-responsive CD8$^+$ T cells in spleens of IL-10 KO mice.

A) Representative staining results of male (left panel) and female (right panel) IL-10 sufficient (upper row) and IL-10 deficient (lower row) C57BL6/J mice on day 7 after L.m. infection. Images are gated on live CD8$^+$ splenocytes and the numbers represent the frequency of CD8$^+$CD62L$^-$ T cells, producing IFNγ$^+$ after in vitro stimulation with SIINFEKL peptide. B) Histograms show the absolute numbers of IFNγ$^+$ producing CD8$^+$CD62L$^-$ T cells per spleen in WT males (black bars) and females (open bars) as well as in IL10 KO males (grey/black bars) and females (grey/white bars). Shown is the mean of 4-5 mice per group ± SD.

3.4 Phenotyping of TUB001

As demonstrated before, ENU mutagenesis and subsequent screening for abnormal phenotypes, either of naïve mice as well as after *in vivo* challenge, is a powerful tool to generate new mutant mouse lines. Besides the cloning of the mutated genomic region, the next step in the analysis of ENU mutants is a more detail characterization of the phenotype in

order to uncover all implications of a certain mutation on the entire organism. Therefore, the first established mutant line, TUB001, was characterized more intensively during this thesis.

3.4.1 TUB001 mice develop heterotopic calcifications and pseudotumors with age

The founder of this mouse line, 40000264, had been identified out of the dominant screen because of abnormally high values of IgG_1 and IgG_{2a} in both measurements at 12 and 14 weeks, and 7 out of 20 offspring from the conformation cross were showing the same phenotype (data not shown). Even more impressive than the original screening result was the fact, that with age, approximately at 8-10 months, heterozygous TUB001 mice developed a severe morphological phenotype, characterized by a crippled back and the formation of inflammatory pseudotumors around the chest and upper abdomen, as illustrated in Figure 30.

Figure 30: Crippled back and formation of pseudotumors in TUB001 mice.
Representative pictures from an affected heterozygous male TUB001 mouse at the age of 10 months. Left: lateral view. Right: Abdominal view with inflammatory pseudotumors around the chest.

To elucidate the origin of these alterations, X-ray measurements of the thoracic region were performed with affected TUB001 animals and littermate controls. Obtained images showed many sites of tissue calcification, randomly distributed around the chest region. Additionally, to some extent the cartilage between vertebrae of the spinal cord were affected by calcification, giving first explanations for the stiffness of the back and the existence of inflammatory pseudotumors in TUB001 animals, Figure 31.

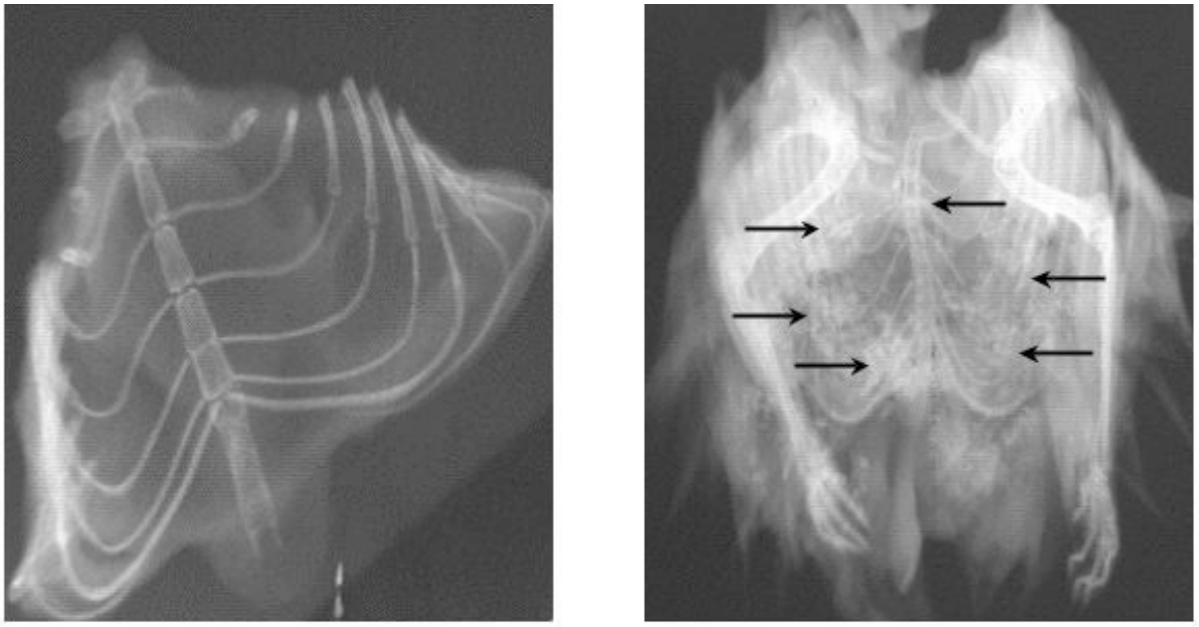

Figure 31: X-ray analysis of TUB001 animals.
X-ray of the chest region of affected TUB001 male (right) or unaffected littermate (left) at an age of 10 months. Black arrows indicate sites of calcification within the chest or of the cartilage of the sternum.

Further analysis of mice showing the abnormal appearance via computer tomography confirmed the X-ray results, even providing evidence for the formation of whole plates of heterotopic calcifications, spanning from the chest down to the abdomen (Figure 32). These findings indicate that the mutation in TUB001 mice leads directly or indirectly to inflammation and ectopic calcium formations throughout the body.

Figure 32: 3D computer tomography of a TUB001 mouse.
3D CT images of a 10 months old affected heterozygous TUB001 male (lower panel) and of an age- and sex-matched littermate control (upper panel). White arrows show the calcium plate around the sternum in TUB001 animals.

3.4.2 Cell degeneration and granulocytosis in tissue

Since macroscopic examinations revealed dramatic alterations in TUB001 mice, histology of the sick animals had been carried out to elucidate the cellular bases for this kind of disease. Results of tissue sections and subsequent HE staining showed mainly in muscle tissue several sites of inflammation or even tissue lesions with an abnormally strong infiltration of granulocytes, ending up in fibroblast degeneration, followed by calcification of the affected region, delivering an explanation for the observed calcifications in TUB001 mice, Figure 33.

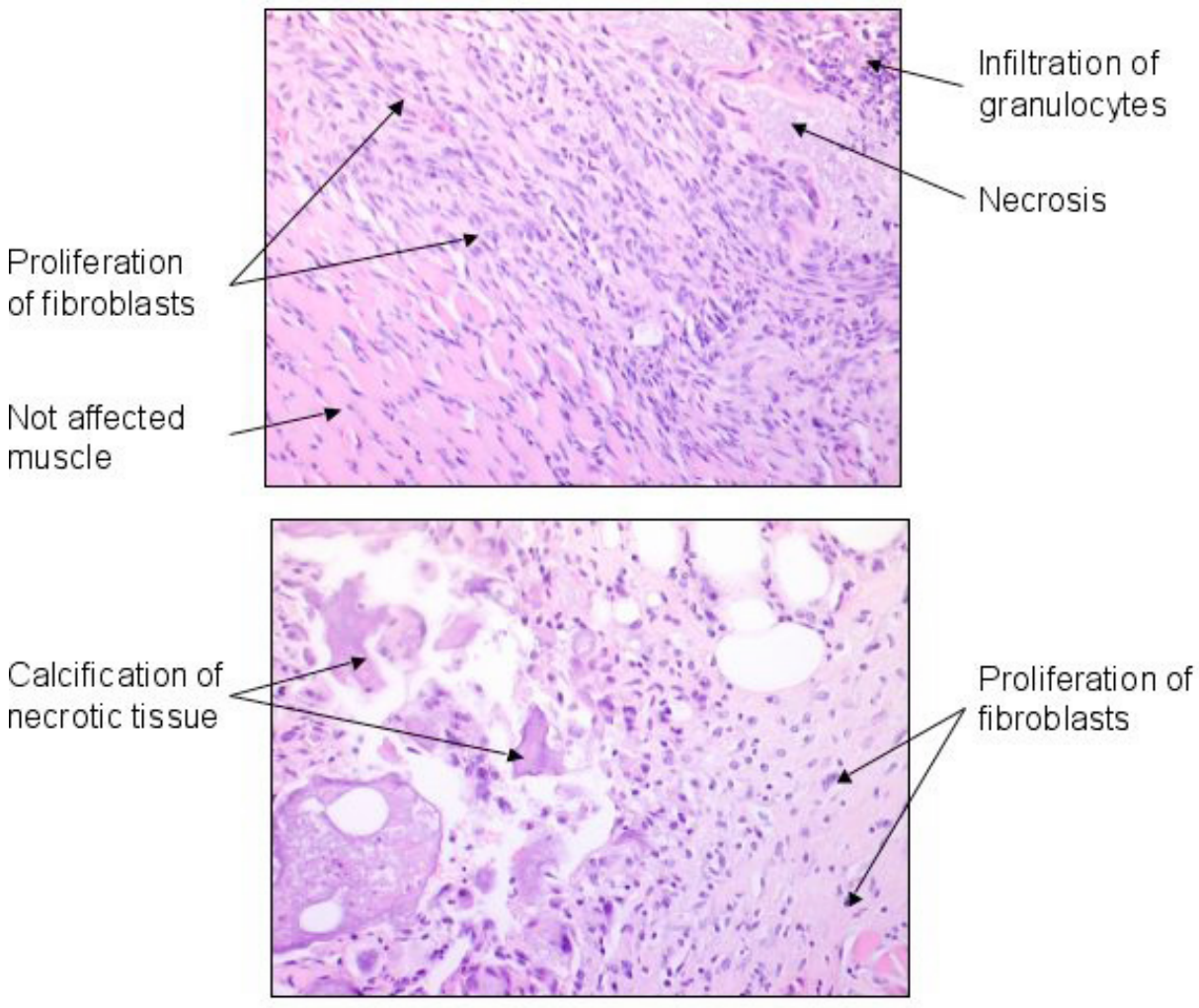

Figure 33: Cellular degeneration of muscle tissue in TUB001 skeletal muscle.
Images represent representative histological findings of fibroblast proliferation, granulocyte invasion necrosis, and subsequent calcification in muscle tissue of an affected heterozygous TUB001 male (10 months old). Images show skeletal muscle sections with subsequent HE staining at a magnification of 200.

3.4.3 Lymphopenia and granulocytosis in peripheral blood and spleen

Based on these findings, several organs had been investigated in sick, heterozygous animals for abnormalities in the content or composition of the immune system, which could provide an explanation for the systemic inflammation. It could be shown that affected TUB001 mice have higher frequencies of Gr-1$^+$ cells and a decrease of CD19$^+$ B- and CD3$^+$ T-lymphocytes in blood (Figure 34) and spleens (Figure 35), pointing towards an acute granulocytosis and lymphopenia in the mutants.

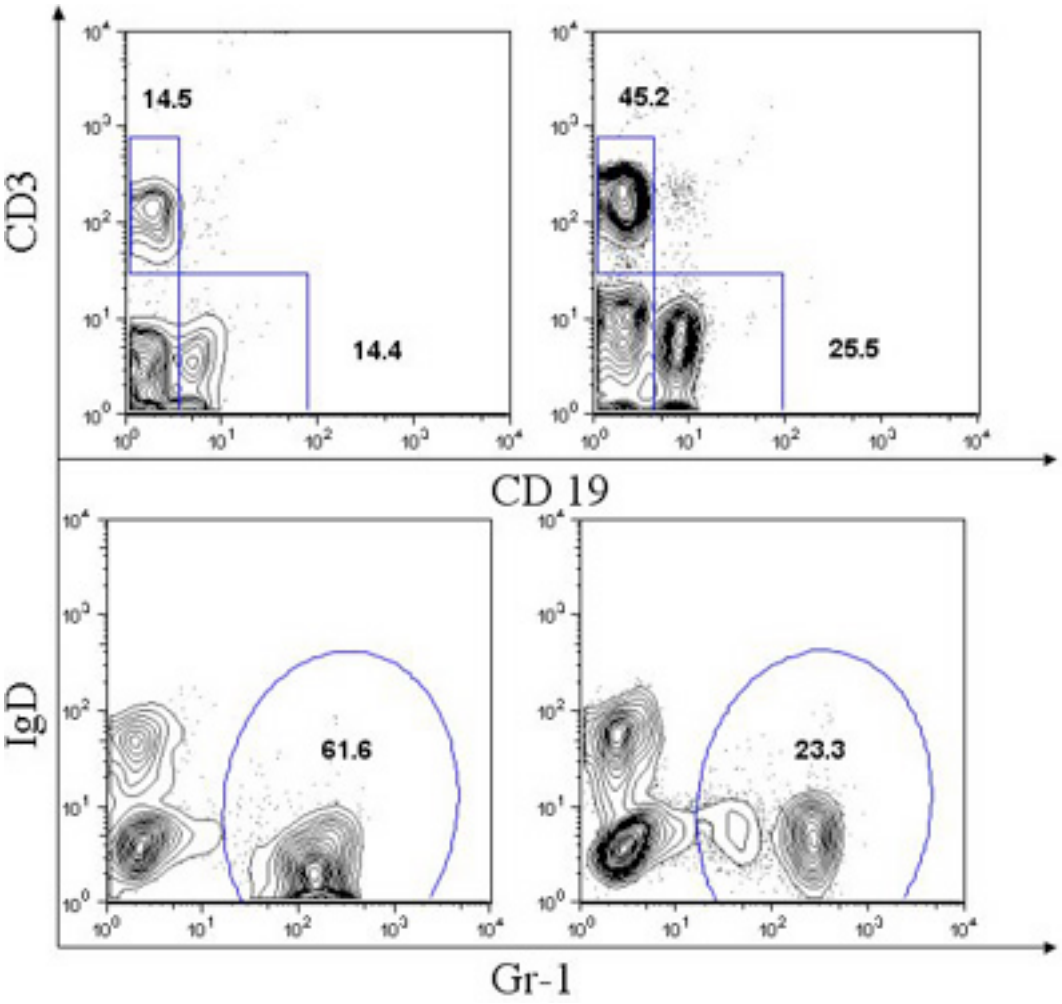

Figure 34: Granulocytosis und lymphopenia of TUB001 animals in the peripheral blood. Representative FACS staining results of 8 months old heterozygous male TUB001 (left) and age- and sex-matched control mouse (right). Contour plots are gated on live leukocytes and the numbers represent the percentage of the respective gates.

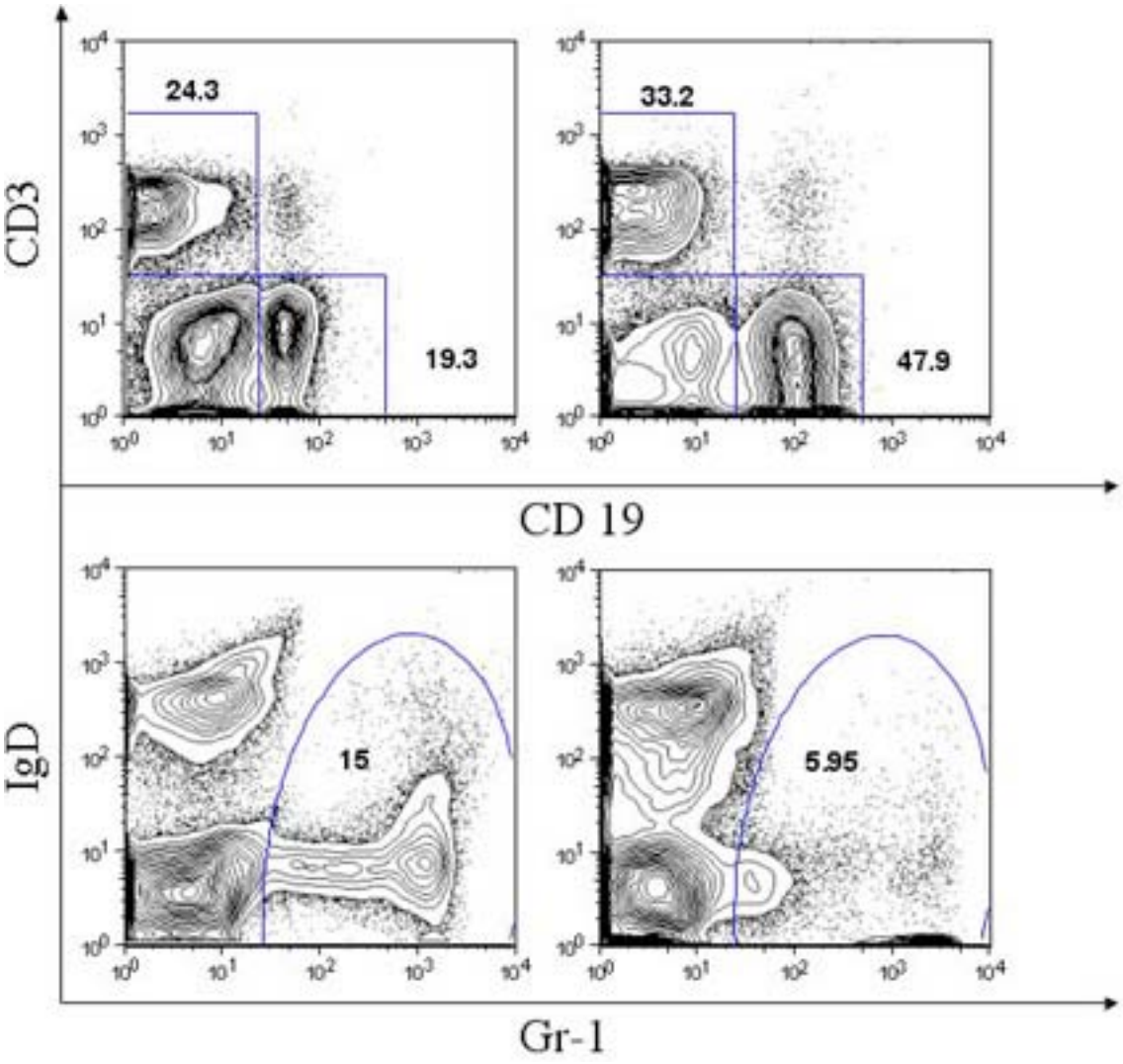

Figure 35: Granulocytosis und lymphopenia of TUB001 animals in the spleen.
Representative FACS staining results of 8 months old heterozygous male TUB001 (left) and an age- and sex-matched control mouse (right). Contour plots are gated on live splenocytes and the numbers represent the percentage within the indicated gates.

As heterozygous animals for the TUB001 mutation develop the disease relatively late, around the age of 8-10 months, examinations limited to those animals would have been very time consuming. Therefore, brother-sister mating of TUB001 heterozygous mice was performed in order to obtain homozygous animals for analysis. Indeed, some of these offspring (approximately 20%), potentially homozygous for the mutation, developed the same kind of phenotype much earlier, around week 8-14, which served as source for further analysis.
Similar results were obtained from blood and spleens comparing hetero- and homozygous TUB001 animals, with even stronger granulocytosis and lymphopenia in homozygous mice. As shown in Figure 36 for absolute cell numbers in the spleen, a nearly 6-fold increase of Gr-1^+ cells was seen in homozygous TUB001 mice compared to not affected littermates, whereas

the numbers of $CD19^+$ and $CD3^+$ lymphocytes were decreased to a similar extent. Furthermore, a closer investigation of the CD8 and CD4 compartment indicated that the reduction of T cells is more pronounced in the cytotoxic T cell compartment than in the T helper-cell compartment. Taking together, the enhanced severity and earlier outbreak of the disease in homozygous animals underlines once more the direct influence of the mutation on the disease, as well as a correlation between the progress of illness and the degree of granulocytosis and lymphopenia.

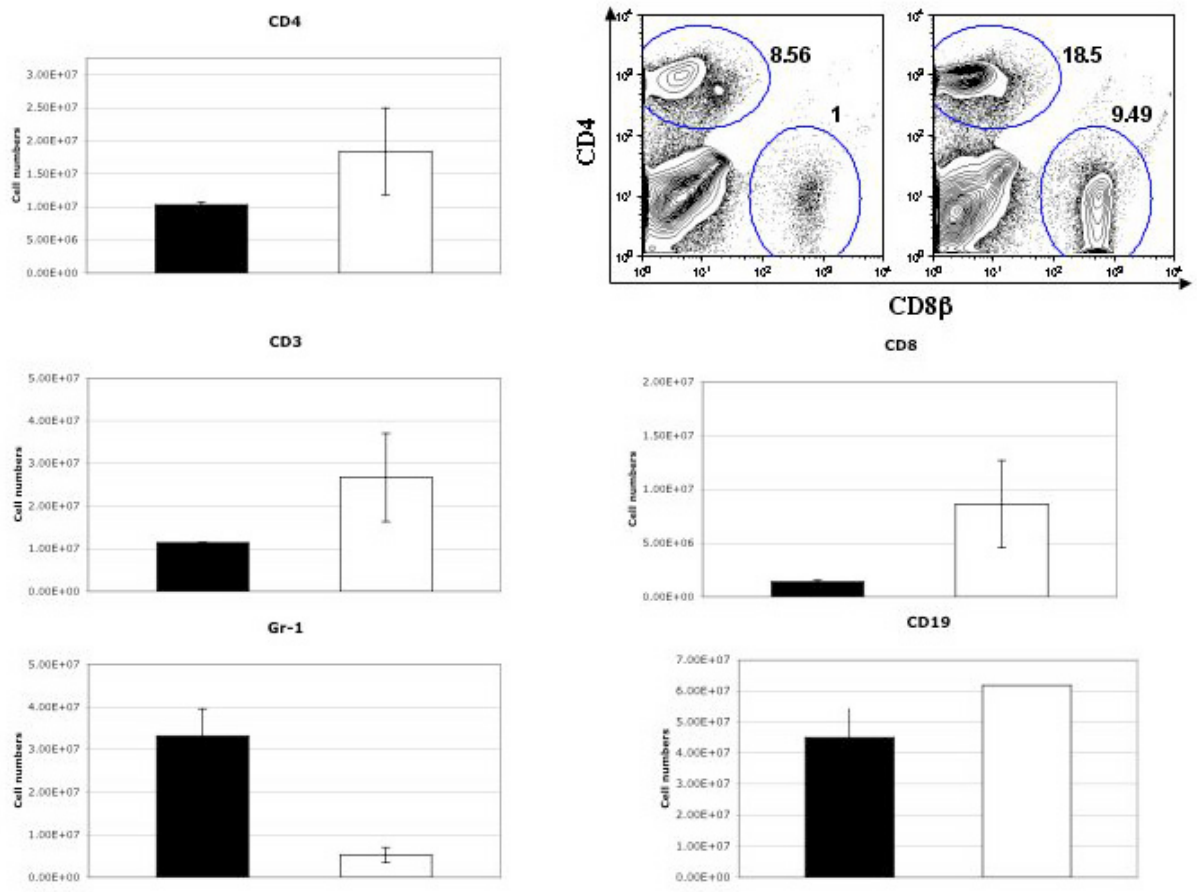

Figure 36: Comparison of absolute cell numbers in the spleen between TUB001 and WT animals.

Upper right: Representative contour plot for $CD4^+$ and $CD8\beta^+$ T cells in the spleen, gated on live leukocytes (left: TUB001, right: WT). Histograms: Absolute numbers of $CD4^+$, $CD3^+$, $CD8^+$, $Gr\text{-}1^+$ and $CD19^+$ splenocytes of 3 homozygous male TUB001 (filled bars) or 3 male WT controls (open bars) at the age of 10-14 weeks ± SD.

3.4.4 Higher frequencies and numbers of $CD8^+CD25^+$ and $CD4^+CD25^+$ T cells in spleen and lymph node

T cells can be further characterized by surface expression of certain molecules, like activation or differentiation markers. Since the T cells appeared to be severely diminished in TUB001 mice, a more precise analysis of the T cell compartment in different organs was carried out in homozygous TUB001 mice.

The most striking difference observed for TUB001-derived T cells was an increase in IL-2 receptor α-chain expression, CD25. T cells up-regulate surface expression of CD25 short after TCR-antigen engagement, as its ligand IL-2 triggers T cell proliferation. Nevertheless, it has been shown by others (Sakaguchi, 2000) that a certain subset of $CD4^+$ T cells constitutively expresses $CD25^+$ and that these T cells can mediated suppressive effects on other T lymphocytes , giving them also the name “regulatory T cells”. In spleens of TUB001 homozygous animals, the proportion of $CD4^+CD25^+$ cells was largely increased in frequency and number, as shown in Figure 37. In addition, the same difference in frequency was found in mLN for both, $CD8^+$ and $CD4^+$ T cells, Figure 38. These results could indicate that in TUB001 mice many T cells are in an activated status, which is perhaps related to the ongoing inflammatory process. However, our experiments did not yet address the question whether the large fraction of $CD25^+$ T cells in TUB001 mice also contains T cells with regulatory functions.

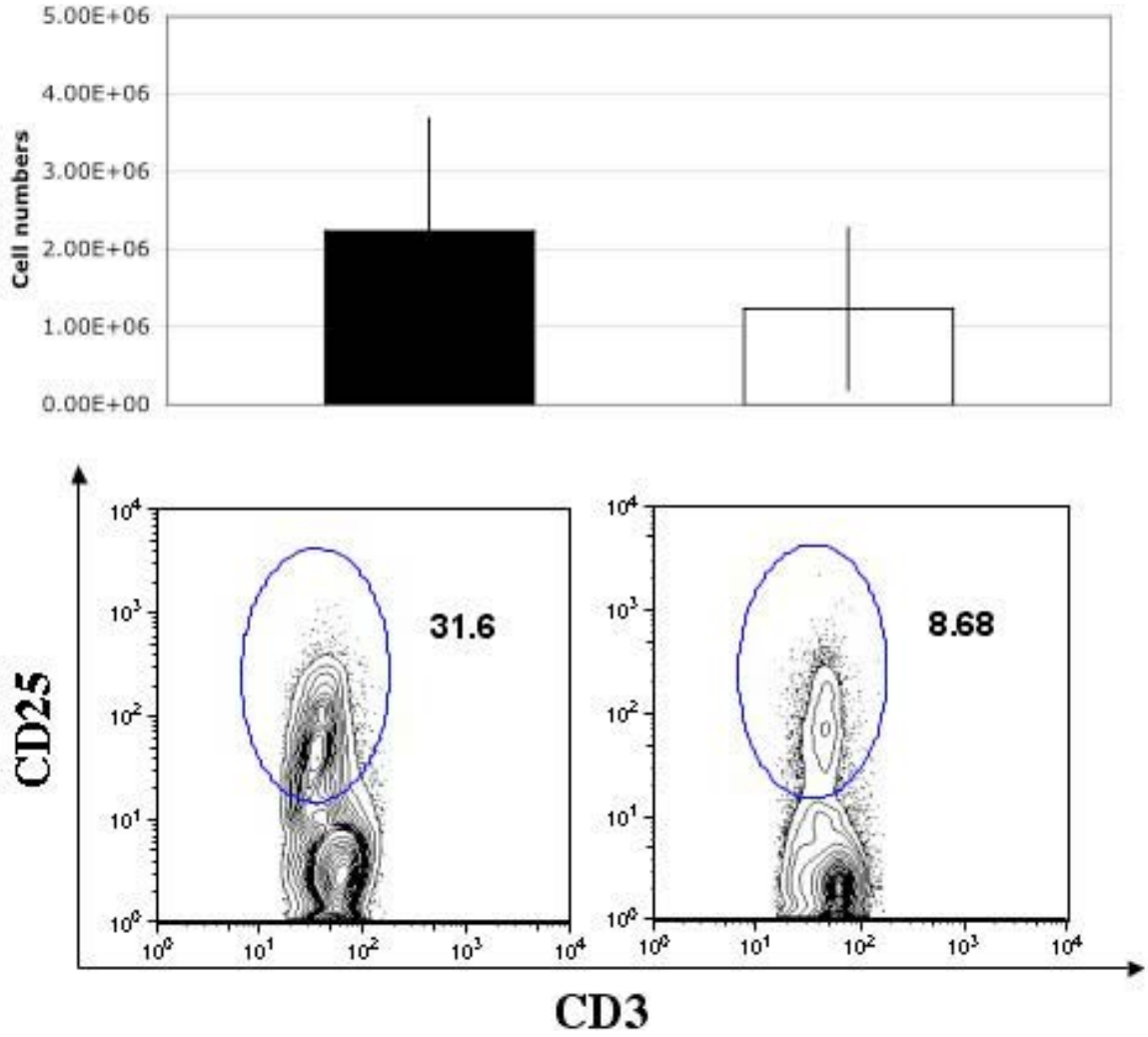

Figure 37: Increased amount of CD4$^+$CD25$^+$ T cells in the spleen of TUB001 animals. Histogram: absolute numbers of CD4$^+$CD25$^+$ T cells in the spleen of TUB001 (filled) or control mice (open). Shown is the mean and standard deviation of 3 mice per group. Contour plots: representative staining example for a TUB001 (left) or a WT control (right). Plots are gated on live CD3$^+$ and CD4$^+$ cells. Numbers represent the frequency of CD25$^+$ cells of all CD4$^+$ cells.

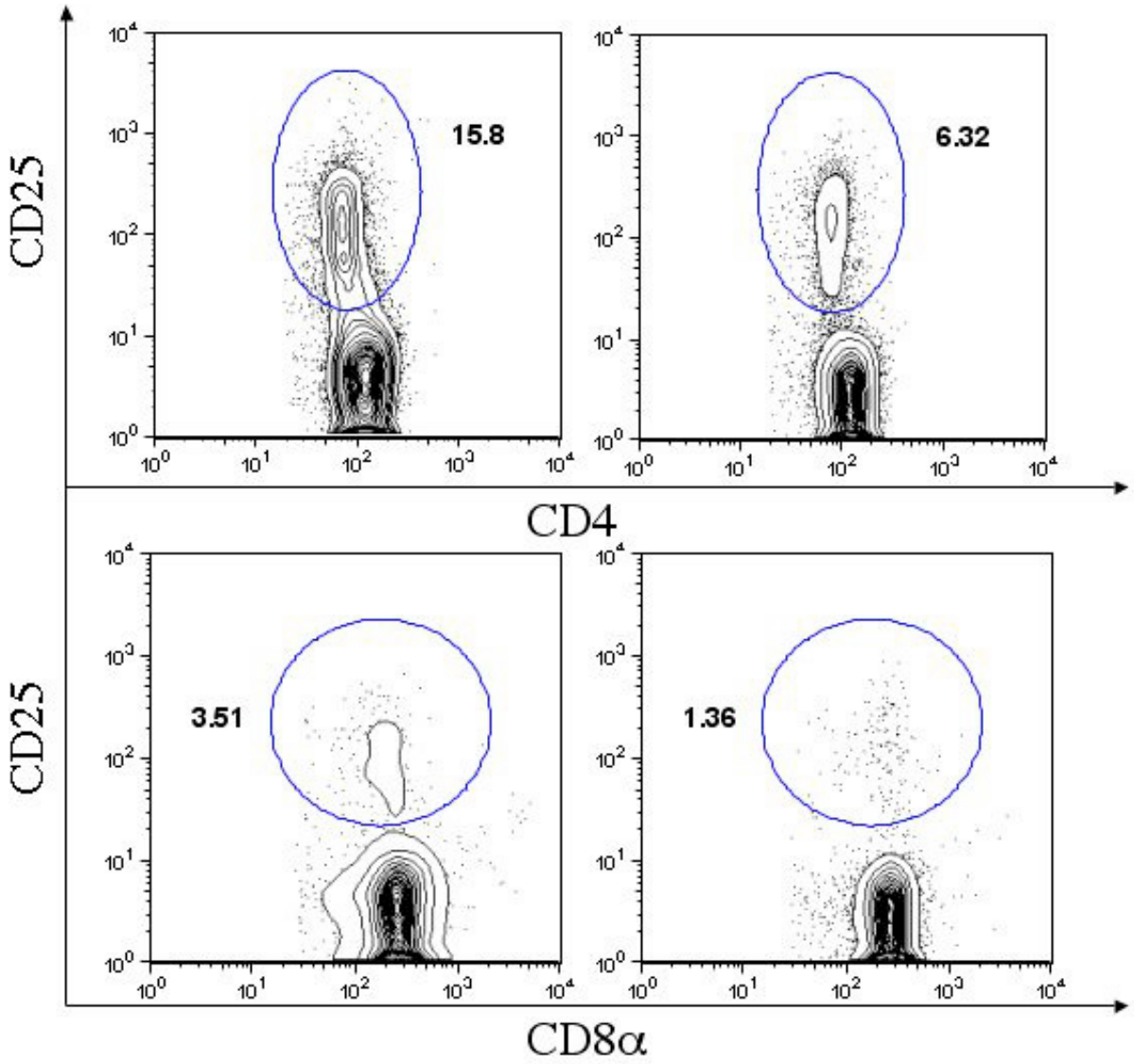

Figure 38: Increased frequency of CD25⁺ T cells in mLN of TUB001 mice.
Increased frequencies of CD4⁺CD25⁺ (upper panel) and CD8⁺CD25⁺ (lower panel) regulatory or activated T cells in the mLNs of TUB001 mice. Representative contour plots of TUB001 (left panel) and age- and sex-matched littermate controls (right panel) are gated on live CD3⁺CD4⁺ (upper) or CD3⁺CD8⁺ (lower) cells.

3.4.5 Disturbed leukocyte development in thymus and bone marrow

TUB001 mice show high numbers of granulocytes and low numbers of B and T cells in the periphery. Therefore, it was important to look at the site of development of those cell types, namely the thymus for T cells and the bone marrow for granulocytes and B cells.

Maturation of T cells in the thymus can be followed by the surface expression of the co-receptors CD4 and CD8 (Janeway et al., 2001). Immature T lymphocytes start from a $CD4^-$ $CD8^-$ (double negative) stage towards $CD4^+CD8^+$ (double positive) cells, before they are

released in the periphery as either $CD4^+$ or $CD8^+$ (single positive) T cells. Analysis of TUB001 thymuses obtained a reduction in the frequency of double positive T cells with a simultaneous increase of double negative T cells, indicating towards an impaired T cell development in TUB001 animals (Figure 39).

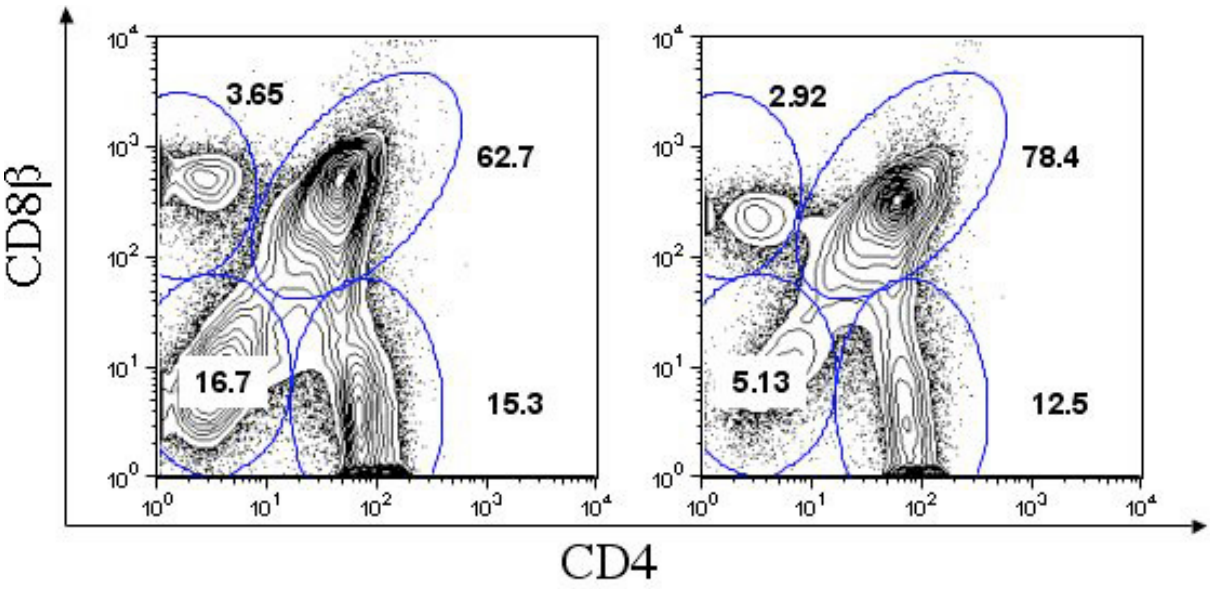

Figure 39: Altered proportions of thymocytes in TUB001 mice.
Lower frequencies within the $CD4^+CD8^+$- with simultaneous increase of the $CD4^-CD8^-$-T cell compartment in the thymus of affected homozygous TUB001 animals. Plots are gated on live thymocytes in 14 weeks old male TUB001 (left) or age-, sex- and strain-matched control animals. Numbers indicate the percentage of respective cell population.

A more detailed characterization of the double negative T cell population for the maturation markers CD44 and CD25 revealed higher percentages of $CD44^{med}CD25^-$ T cells that appear in the last developmental stage of double negative cells before becoming double positive T cells. This finding is further strengthened by the presence of a lower percentage of double negative T cells, which were already able to express a T cell receptor β-chain on the cell surface, Figure 40.

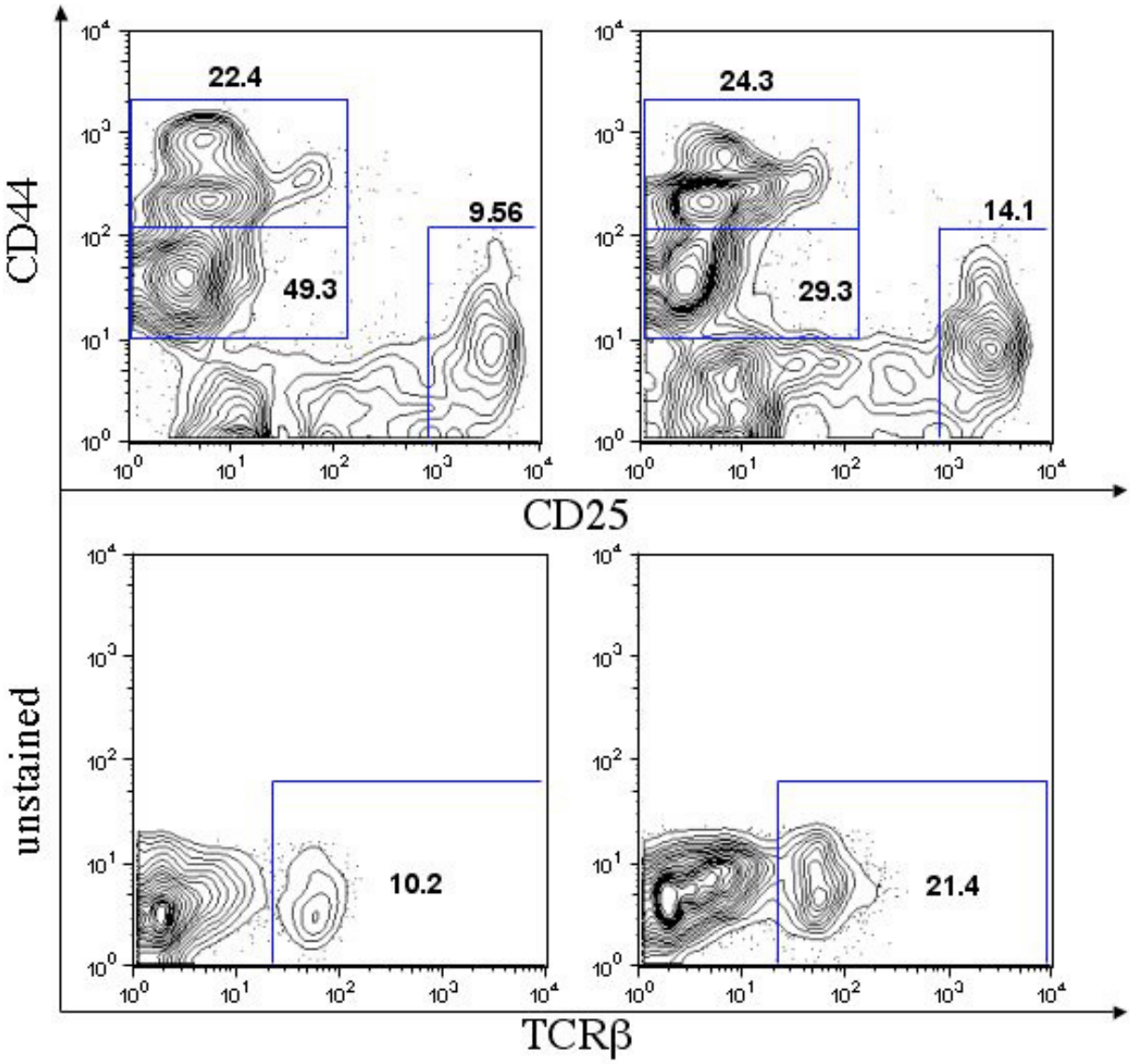

Figure 40: Abnormal expression of maturation markers in the thymus of TUB001 mice. Upper panel: Increased frequency of CD44^{med}CD25^{-} T cells within the CD4^{-}CD8^{-} double negative T cell compartment of homozygous TUB001 mice (left) compared to the WT situation (right). Lower panel: Lower percentage of double negative T cells that already express a functional TCRβ chain on the cell surface in affected TUB001 males (left). Contour plots are gated on CD4^{-}CD8^{-} living thymocytes of 14 weeks old male TUB001 or sex-, age- and strain-matched control animals.

Taken together, the results in the thymus point towards a defect in T cell maturation of TUB001 animals. However, additional experiments have to be performed to clarify whether the T cell development phenotype is a primary consequence of the mutation or a secondary effect, mediated by the systemic inflammation.

With respect to the determination of the origin of the high frequencies of Gr-1$^+$ cells and low frequencies of B cells in blood and spleen, FACS analysis revealed a tremendous increase of Gr-1$^+$ cells in the BM, as illustrated in Figure 41. Nearly all cells in BM of TUB001 homozygous mice express CD11b and Gr-1, whereas other cell populations usually found in the BM, like B220$^+$ B cells, are almost absent. This result could reflect an enhanced production of Gr-1$^+$ cells in the BM, although one cannot rule out that the observed alterations in the BM are caused by defects in migration or reinvasion of Gr-1$^+$ cells to the BM.

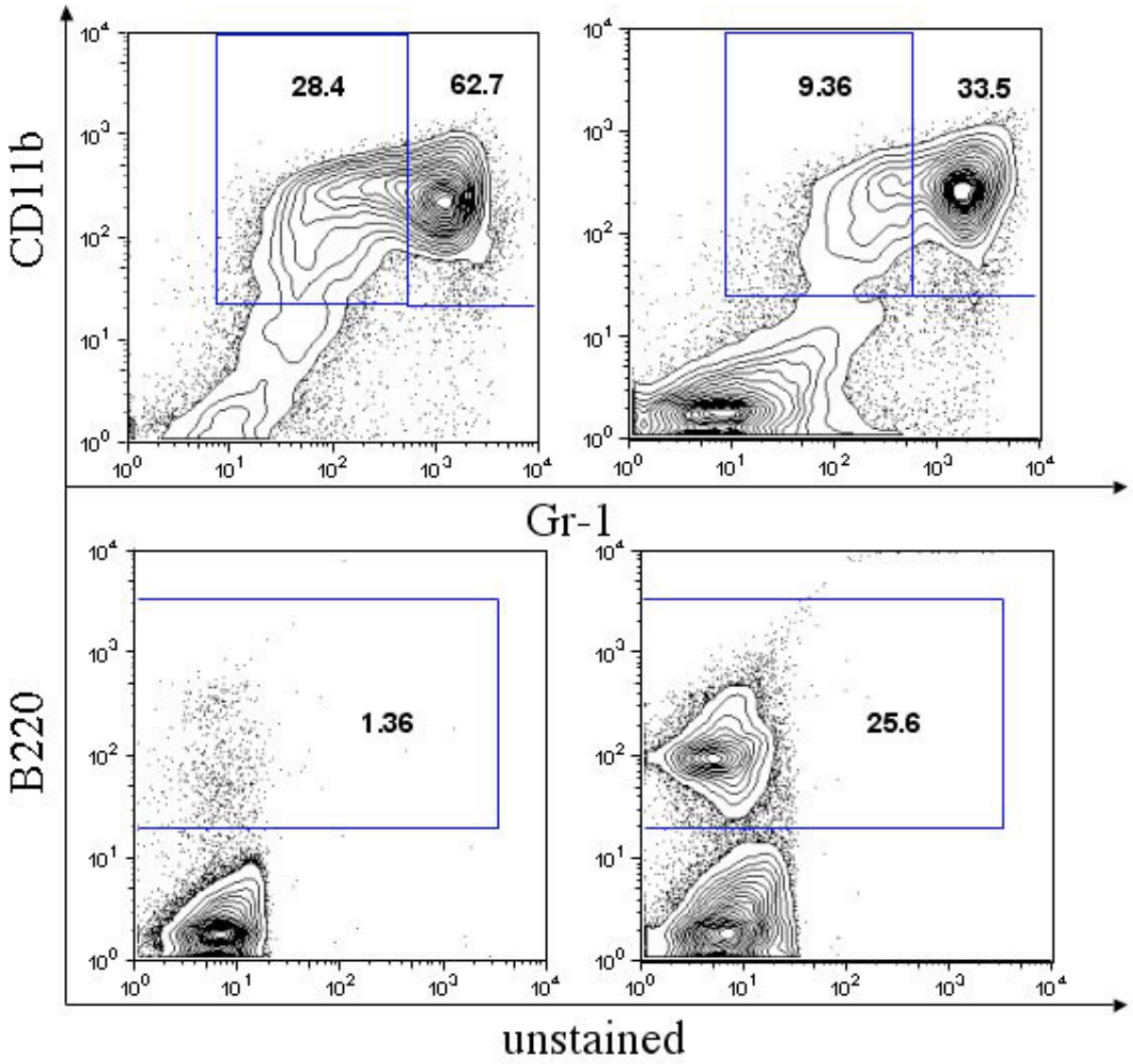

Figure 41: Massive granulocytosis in the bone marrow of TUB001 animals.
Typical FACS staining result for a TUB001 (14 weeks, male, left) and a strain-, age- and sex-matched control mouse (right). Numbers indicated the frequency of Gr-1$^+$CD11b$^+$ or Gr-1^{med}CD11b$^+$ cells (upper row) or the frequency of B220$^+$ cells to the BM (lower row). Contour plots are gated on live bone marrow cells.

In summary, TUB001 mice show an impressive and complex phenotype characterized by a variety of abnormalities, including morphological and immunological changes. Until now, these findings point towards the development of systemic inflammation in TUB001 mice, which subsequently results in ectopic calcifications and causes the defective composition of several lymphoid tissues. However, additional investigations, especially the genotyping of the mutation, are needed to confirm this hypothesis and to determine the initial trigger that causes the inflammations.

4 Discussion

With this PhD work, novel mouse phenotyping protocols were established for the detection of immunodeficiencies in naïve mice, as well as after specific challenge with a live pathogen. When strictly controlling for environmental-, strain-dependent- and gender-mediated-factors, these assay systems were shown to be highly reliable, robust and easily transferable to high-throughput measurements, which was best demonstrated by the identification of 25 novel mutant lines after screening of more than 5000 ENU mutagenized mice. A newly identified mutant mouse line, TUB001, may represent a unique animal model for an inherited human disease, confirming the scientific power of ENU mutagenesis in combination with standardized mouse phenotyping.

4.1. Immunological mouse phenotyping

For the successful identification of single individuals with immunodeficiencies out of cohorts of mice, technical, environmental, or endogenous factors that can influence the results have to be minimized. This includes first a strict definition of the analyzed groups of animals in terms of age, strain and gender. This is for example demonstrated in Figure 10, which shows large differences in the composition of the cellular compartments and the concentrations of several immunoglobulin subclasses in the peripheral blood of male or female mice from C57BL/6, BALB/c and C3H/HeJ inbred strains. Without gender-matching, the variability of some parameters would become extremely large and the sensitivity for identification of outliers will decrease substantially. Additional experiments, which were not directly part of this thesis work, analyzing large cohorts of mice furthermore provided evidence that several immunological parameters in the peripheral blood show even in sex- and strain-matched cohorts of animals relatively high variations when mice are derived from different animal areas (inside the GSF). These results underline once more the importance of well-controlled groups; in order to keep environmental exposures as identical as even possible, housing should be done in the same room or hygiene treat of an animal facility. In mixtures of mice with respect to age, gender or genetic background, it will be impossible to judge, which values are lying outside the normal range. Another important aspect for standardized immunological phenotyping is to critically evaluate the variability and sensitivity for each single parameter, which can differ substantially. The natural variability of distinct parameters even in age-, sex- and strain-matched groups is quite high. This observation could be

supported, for example, by the percentage of $DX5^+$ cells in peripheral blood. This value showed a high standard deviation in all tested groups of mice, regardless of sex or strain (Figure 10). This high natural variability could serve as an explanation, why during the ENU screen of naïve mice altered values for $DX5^+$ cells could be annotated only for 4 variants (Figure 12) and none of these phenotypes could be confirmed by backcrossing (Figure 13). Furthermore, for high quality immunological phenotyping, permanent monitoring of the health status of the tested animals is crucial, as it is obvious that during an ongoing infection or after recovery, several parameters of the immune system can be significantly altered (see chapter 3.3.3 and (Merrick et al., 1997)).

Besides the reduction of external and endogenous factors to a minimum, the proper choice of the screening assays and the standardization of the technical performance determines its usefulness for standardized mouse phenotyping. Immunological research has a vast array of tools to identify immunodeficiencies, often derived from diagnostic methods applied in the clinic, like immunoelectrophoresis for the detection of serum proteins (Ouchterlony, 1962), immunohistochemistry to visualize the cellular structures and content of certain tissues (Falini and Taylor, 1983) or technologies from the molecular biology like the polymerase chain reaction (Eisenstein, 1990). The handling of very high sample numbers in a blood-based screening procedure requires robust, easy and fast detection assays with a high sensitivity, specificity and reproducibility. This is especially important for ENU screens, where many animals have to be tested to enlarge the probability to identify mutant mice with unpredictable phenotypes (Soewarto et al., 2003). FACS analysis for the cellular compartment (Baumgarth and Roederer, 2000) as well as ELISA for soluble factors in the plasma (Flaswinkel et al., 2000) have turned out to be appropriate methods for mouse immunophenotyping. For the analysis of immunoglobulin isotypes or cytokines, novel technologies occurred, which might outdate the present dominance of ELISA based measurements. The usage of bead array based systems like the Luminex X-map© technology has several advantages over traditional methods (Fulton et al., 1997), mostly due to its power to allow the simultaneous analysis of up to 100 different analytes in a single and relatively small amount of body fluid/plasma/serum with high sensitivity (see chapter 3.1.1). By further implementation of high-tech machinery at the GMC, for example a 96-well pipetting robot (Quadra3, Tomtec, USA) or loader systems for automated acquisition of FACS samples (MAS and HTS, Becton Dickinson, USA), the applied screening assays could be adapted to high-throughput requirements. Furthermore, the definition of and strict compliance to standard operation procedures (SOP – see chapter 2.2.1) guarantee a minimization of human errors and therein

the generation of reliable results, as proven for this immunological phenotyping protocol by the consistent finding in two independent measurements of more than 90 variants (Figure 12).

4.2 ENU mutagenesis

In the last decade, ENU mutagenesis has emerged as a very powerful tool to generate new mutant mouse lines. This strategy has and will help to improve our understanding in a variety of different fields of biological research (Rastan et al., 2004) in assigning defined functions to different genes (Nadeau et al., 2001; Nolan et al., 2000a). Alone within the Munich ENU Screen, more than 600 mutant lines with unique phenotypes could be identified (http://www.gsf.de/ieg/groups/enu/mutants/index.html, 2004). Mutants derived from ENU screens represent a valuable source for biological and medical science as they can even serve as models for several human diseases like diabetes (Inoue et al., 2004), cataract (Graw et al., 2001), or deafness (Vreugde et al., 2002). The description of several ENU mutants, which elucidated the major role of certain molecules in distinct immunological signaling pathways (Hoebe et al., 2003b), for the development of immunological cell populations (Garcia-Martinez et al., 2004) or regulation of the immune response (Jun et al., 2003), underlines the importance of mutagenesis also for the field of immunology (Beutler et al., 2004).

4.2.1 ENU screening of naïve mice

Application of standardized phenotyping protocols facilitated the analysis of approximately 5000 offspring of ENU treated founders during this PhD work. The success of this screen is underlined by the identification and establishment of 24 new mutant mouse lines with abnormalities in many different compartments and cell populations of the immune system (Figure 13). Additional 25 variants are still at the stage of confirmation cross, potentially further increasing the amount of novel mutant mouse lines. Despite these impressive numbers, one cannot rule out that several mutants have been missed during the screening. This could be due to the limitation of the screen to a certain immunological compartment (peripheral blood) and a single defined time point (12 weeks). Based on these settings, this screen potentially missed mutations, which neither result in a detectable phenotype in the peripheral blood, nor develop their phenotype at a later age.

In-depth analysis of these novel mutant mouse lines is necessary to fully elucidate the effects of distinct mutations on the entire organism and to judge the potential use of certain mutants

as models for human diseases. A more detailed analysis of ENU mutants includes extensive phenotyping to uncover all consequences and pathways affected by the mutation, not only for immunology but also for other physiological aspects of the organism. A very promising approach for comprehensive phenotyping represents the establishment of the GMC, where scientists from 13 different fields of research are brought together under one roof to systematically analyze in close collaboration mutant mouse lines for abnormalities in a variety of different issues (http://www.mouseclinic.de).

In addition to improve the understanding of the phenotype of a given ENU mutant line, approaches have to be initiated to identify the responsible mutation(s). In our case, genotyping is already in progress for the mutants TUB001, TUB006 and TUB010. This procedure is still a time consuming task, as the phenotype bearing animals have to be out-crossed two times to a different genomic background, before homologous recombination events between the original founder- and the host-genome occur, which subsequently allows to identify the mutated genomic region by micro-satellites or single nucleotide polymorphisms (SNP). Nevertheless, big advances in genotyping result from the publication of the complete mouse genome sequence (Gregory et al., 2002), what allows the generation of SNP maps with high resolution (Lindblad-Toh et al., 2000) facilitating the mapping of certain genomic regions (Shifman and Darvasi, 2004) or help to develop new mapping strategies (Beier and Herron, 2004).

4.2.2 Immunological challenge screen

Since the information available from current human and mouse resources is by no means sufficient for understanding the complexity of genetic interactions involved in immunological homeostasis or effective immune regulation, there is an urgent need for new experimental models correlating with defined human diseases of the immune system (Buer and Balling, 2003). As described before, ENU mutagenesis is a powerful tool for the generation of mutant mouse lines, which can help to uncover new genes or to annotate novel functions to already known genes. However, identification of mutants out of a large cohort of naïve mutagenized mice is limited to those phenotypes, which are detectable under resting conditions, whereas mutations in genes only activated under challenging conditions will remain unrecognized. Especially screening of naïve mice does not provide information about an individual mouse to cope with an infection or to generate and maintain effective protection, one of the main functions of the immune system. Therefore, first efforts have been undertaken to screen for

ENU mutants under challenge conditions like *in vitro* stimulation of cells with TLR ligands (Hoebe et al., 2003a) or different immunization strategies and subsequent measuring of humoral immune responses (Vinuesa and Goodnow, 2004).

4.2.2.1 *L.m.* challenge screen

The results of this PhD work suggest that a novel advanced challenging approach using the *L.m.* infection model might be provided, fulfiling most of the specific requirements for the successful screening of ENU treated mice with defects in either the innate and/or the adaptive immune response. The big advantage of this experimental challenge system is the fact that the pathogen is a bacterium. ENU mutants with an increased susceptibility for *Listeria* either during primary or secondary infection can be easily rescued by antibiotic treatment (Wong and Pamer, 2003b), preventing the loss of these interesting mutants (Figure 19). It turned out that the concentrations of GOT (Figure 14) and IFNγ (Figure 15) measured at day 3 after primary infection, which are readily detectable in the blood plasma via enzyme assays or Bio-Plex based methods, correlate very well with the severity of infection and the ability of the mouse to control replicating bacteria during the innate immune response. The identification of a novel epitope, $p60_{117\text{-}125}$, presented on H2-K^k MHC-I molecules allowed to monitor the strength of the adaptive immune response against *L.m.* infection in C3H mice used in the Munich ENU screen (Soewarto et al., 2000). Robust frequencies of $p60_{117\text{-}125}$-Tetramer$^+$ T cells were detectable in the peripheral blood at day 7 after primary infection (Figure 18), a method that can be easily transferred to high-throughput measurements. As it is known that WT mice develop very effective protection against reinfection with *L.m.*, which is mediated mainly by Ag-specific $CD8^+$ T cells (Harty and Bevan, 1992), the *Listeria* challenge screen could also be useful for the identification of mutant mice with defects in the establishment or maintenance of protective immunity. For this type of screening, recall infection with higher doses of *L.m.* and subsequent detection GOT and IFNγ on day 2 and Ag-specific T cells at day 5 after infection enables the assessment of the ability of the ENU mutagenized mice to develop an effective secondary immune response against *Listeria*.

4.2.2.2 Influence of dosage and gender for *L.m.* infection

Minimization of endogenous and environmental factors as well as standardized phenotyping protocols are needed for the realization of a meaningful *Listeria*-based challenge screen. A very important aspect for successfully identifying mutagenized mice with altered immune

responses to *Listeria* infection is the exact control of the infection dose, because many of the measured parameters are sensitive to the original amount of infecting pathogens (Figure 14 and 15). Insufficient control of the infection dose would cause high variability in the parameters, making it impossible to distinguish between a phenotype bearing mutant or a mouse that received a too low/high dose of *L.m.*. Furthermore, in most cases the screening procedure cannot be repeated with the same mouse, since the maturation of the adaptive immune system after the first contact with *Listeria* influences all subsequent experiments. This makes it essential to develop highly reliable and reproducible infection procedures, especially for the first challenge. To solve the problem of controlling the original infection dose, in our experience counting of live bacteria under a microscope and application of the pathogen i.p. are the most reliable and consistent ways of infection, which turned out to be also most independent from the technical skills of the person performing the experiment.

Besides the amount of *L.m.* applied for infection, the results of this PhD work indicate an important role of the gender of *Listeria* infected mice with respect to severity and outcome of the disease. Surprisingly, the sex dependent susceptibility pattern found for murine infection with *L.m.* is inversed when compared to what is known for most other infection models, although similar experimental findings of a higher resistance in male individuals have been described for some other human pathogens including Leishmania (Giannini, 1986), Toxoplasma (Roberts et al., 1995), Babesia (Aguilar-Delfin et al., 2001) and Pseudomonas (Guilbault et al., 2002), indicating that this phenotype might not be unique to *L.m.* infection but is part of a broader biological phenomenon. Since infection with *L.m.* has become one of the most commonly used infection models in immunological research, it is likely that insufficient control for gender-influence substantially contributed to controversial results generated by different laboratories using the same infection model. The dramatic sex-dependent differences in the immune response and outcome of disease described in this thesis point out the importance of using sex-matched groups of animals for immunological studies as well as for challenge screens. To further elucidate the molecular and cellular bases for this unusual susceptibility pattern, it has been shown for *L.m.* infection that several cytokines like INFγ, TNFα, IL-1, IL-6 and IL-12 are intimately involved in the development of an effective immune response. Since INFγ seems to be essential for the resolution of *L.m.* infection (Buchmeier and Schreiber, 1985), this interpretation correlates well with the finding of higher values of INFγ in the more resistant males (Figure 24). In contrast, IL-10 is known to be a potent immunosuppressor with an ability, among other functions, to suppress Th1 immune responses (Moore et al., 1993). Therefore, it is very likely that the increase of IL-10 in

females (Figure 24) is responsible for the impaired INFγ production, resulting in higher susceptibility of female mice. This interpretation is strongly supported by the finding that in IL-10 deficient mice, male and female mice handle the infection equally well (Figure 25 A), and that INFγ levels in IL-10 deficient females are restored to similar values of WT males (Figure 25 B). Sex hormones can substantially affect the expression of distinct cytokines, for example estrogen down-regulates INFγ and TNFα, but stimulates IL-10 (Salem, 2004), providing a potential explanation for the observed differences in resistance against *L.m.* between males and females. However, both innate and adaptive responses are necessary for the establishment of sterilizing immunity after *L.m.* infection (Busch et al., 1999). Surprisingly, even though a clear-cut difference during the early phase of infection could be shown regarding resistance and cytokine production between the sexes, the quality of the Ag-specific $CD8^+$ (Figure 27) or $CD4^+$ primary T cell responses seems to be unaffected by the sex in the *Listeria* infection system. Although there are also hints for the influence of certain hormones, e.g. testosterone on $CD4^+$ T cells (Liva and Voskuhl, 2001), on the adaptive immune system, our results somehow suggest a more prominent effect of sex hormones on the regulation of innate immunity after *L.m.* infection. Nevertheless, further investigations are needed to elucidate the molecular mechanisms behind the hormone-cytokine interplay and to determine the cellular origin for the differential level of IL-10 in male and female mice in Listeriosis. In addition, it might be interesting to determine the potential influence of gender on the protective recall immune response.

Regardless of gender, the immunosuppressive function of IL-10 on T cell activation or proliferation has been demonstrated *in vivo* by enhanced T cell responses in IL-10 deficient mice for several infection models (Liu et al., 2003; Roers et al., 2004), as well as for Th1 cytokine secretion in the *L.m.* system (Dai et al., 1997). At least the report by Dai et al. seems to be in direct contrast to our observations (chapter 3.3.7) of reduced, primary Ag-specific T cell responses in IL-10 deficient mice, reflected by lower frequencies and numbers of $Tetramer^+$ $CD8^+$ T cells in both sexes (Figure 28). Taking into account that the size of an Ag-specific T cell population in part correlates with the amount of available antigen during the primary phase, and that effective T cell priming only requires a short time span of approximately 24h (Wong and Pamer, 2003a), the described phenotype in IL-$10^{-/-}$ mice could also be due to differences in bacterial load. Previous reports demonstrated for example an inhibition of innate immune mechanisms by IL-10 (Moore et al., 1993), e.g. macrophage effector function (Takakura et al., 2002). IL-10 deficient mice are characterized by an enhanced innate immune response with a more rapid Ag-clearance. This could potentially

result in less effective T cell priming and subsequently lower amounts of *Listeria*-specific T cells. But to fully elucidate the influence of IL-10 on the Ag-specific adaptive immune response against *L.m.*, more experiments are needed, like infections with serial dilutions of the infection dosages.

A better understanding of the mechanisms determining susceptibility and resistance to infections is a prerequisite for future developments of more effective therapies and vaccinations against infectious diseases. Therefore, influences of gender on susceptibility to infection with distinct pathogens as well as the contribution of certain cytokines on the generation of an effective innate or adaptive immunity could be of clinical relevance and represent an interesting target for therapeutic interventions.

4.2.3 Advantages of the *Listeria* infection model

L.m. infection is a very attractive candidate for future ENU challenge screens, as its scientific power lies in the ability to potentially identify mutants with defects in the establishment of protective, adaptive immunity, the main principle behind all vaccination strategies. The investigation of the molecular mechanisms responsible for the development of protective immunity is one of the major goals of contemporary immunological research. Although until now many features of Ag-specific immunity have been identified, like the kinetics of primary and secondary T cell response (Busch et al., 1998b; Harty et al., 1996), affinity maturation of an Ag-specific T cell population between primary and secondary responses (Busch and Pamer, 1999), several surface markers for distinct memory T cell populations (Huster et al., 2004), advanced technologies for isolation of Ag-specific T cells (Knabel et al., 2002), or that T cell help is needed for effective $CD8^+$ recall T cell response (Janssen et al., 2003; Shedlock and Shen, 2003; Sun and Bevan, 2003), the genes involved and molecular mechanisms behind the establishment of protective immunity are still poorly understood. A *L.m.* infection screen of ENU mutagenized mice might provide the big opportunity to uncover new genes involved in these important immunological pathways. Furthermore, the identified genes could become candidates for improved vaccination strategies in the future.

4.3 TUB001 as animal model for an inherited human disease

Mutant mice are most valuable if they closely resemble the phenotype of a defined human diseases. Within this thesis, unexpected but important findings have been obtained by closer investigations of the newly identified ENU mutant mouse line TUB001 (chapter 3.4). The initial primary screening results (elevated immunoglobulins, lymphopenia and granulocytosis in the peripheral blood (Figure 34)) reflected only a small aspect of a quite severe phenotype. Comprehensive and detailed phenotypical analysis of TUB001 mice was carried out to fully elucidate the effects of the mutation on the complete organism. Older animals began to develop inflammatory pseudo-tumors around the chest, crippled back and stiff spine (Figure 30), indicating towards an involvement of the mutated gene in bone morphogenesis. X-ray analysis (Figure 31) and CT-images (Figure 32) of affected offspring confirmed the hypothesis of defective morphology, providing evidence for massive, ectopic calcifications, eventually even bone formation, in the upper abdomen and around the chest region. In addition, histology revealed muscle cell degeneration and strong granulocyte infiltration in the involved tissues (Figure 33). These findings are in concordance with FACS results that point towards a systemic inflammation in TUB001 animals, as shown by extensive granulocytosis and lymphopenia in blood (Figure 34) and spleen (Figure 35). Altogether, the observations in TUB001 animals closely resemble the phenotype of a group of human diseases that is characterized by trauma induced ectopic bone formations, e.g. after surgery. The most aggressive form of these disorders represents the rare, autosomal-dominant inherited disease called Fibrodysplasia Ossificans Progressiva, (FOP) (Connor and Evans, 1982b; Kaplan et al., 1993), in which the patients suffer from spontaneously-developing and progressive ongoing heterotopic ossifications (Connor and Evans, 1982a; Rogers and Geho, 1979). Although the molecular mechanisms of FOP are still unclear, it could be shown that FOP patients have increased levels of BMP4 m-RNA in the fibroproliferative lesions of the affected tissue (Shafritz et al., 1996), and a genome-wide analysis of 4 affected families revealed a linkage of the disease to the 4q27-q31 genomic region in humans. This part of the human genome contains at least one promising candidate gene potentially involved in the pathophysiology of the disease, SMAD1, which is participating in bone morphogenetic pathways (Feldman et al., 2000). As a result of these findings, several mouse lines, transgenic for SMAD1- or BMP4-expression have been generated to serve as animal models for FOP (Guha et al., 2002; Kan et al., 2004), but none of them fully shows the complex phenotype of FOP. Until now, there does not exist a suitable animal model for this human disease.

The TUB001 phenotype resembles most features of the FOP phenotype and can therefore potentially serve as animal model for this severe illness. But still more investigations on the pathophysiology and the constitution of the calcifications/ossifications are needed. Furthermore, analysis of the candidate genes BMP4 and SMAD1, should be performed as soon as possible. In addition, one has to clarify how the findings of more Gr-1$^+$ cells in the BM (Figure 41) and increased frequencies of double negative T cells in thymus (Figure 39) fit into the context of FOP. Genotyping of the TUB001 mutation was initiated during this PhD work.

4.4 Outlook and future perspectives

Over the last decade, mutagenesis approaches in general, and ENU mutagenesis in special, have become a widely accepted and frequently used method for successful generation of new mutant mouse lines. There is no doubt that in combination with gene-trap (To et al., 2004) and gene knock-in/knock-out technology (Austin et al., 2004), mutagenesis will also in the future contribute to the enlargement of the pool of mutant mice (Auwerx et al., 2004; Clark et al., 2004a). Especially by the development of advanced screening strategies for ENU treated mice it will be possible in the future to find mutants with defects in specific physiological functions. Besides the novel *L.m.* infection screen described here (see 3.2), which could help to identify genes involved in the generation and maintenance of a functional immune response, one can also think of advanced mutagenesis trials. As the mapping of the mutated genomic region is still one of the most time extensive tasks of ENU mutagenesis, first efforts have been started to circumvent this problem by using novel strategies for mutagenesis. One alternative represents transposons (Voelker and Dybvig, 1998), which are already applied in plants (Greco et al., 2001) or bacteria for mutagenesis (Stewart et al., 2004). By the development of (retro-)transposonal elements that are also active and jumping in the mammalian genome (Carlson et al., 2003; Clark et al., 2004b; Han and Boeke, 2004), this technology is a promising candidate for future random mutagenesis approaches, as it directly allows the sequencing of the genomic region, where the transposon has been inserted.

However, whereas the generation of mutant mouse lines has been well established and even transferred to large-scale mutant production, the main bottleneck turns out to be the detailed, standardized and comprehensive phenotypic analysis of mice. Even many existing mouse resources have never been fully phenotyped, leaving an enormous source for potential mouse models of human diseases almost untouched. In order to face the challenge of standardized

phenotypic analysis, several research centers around the world have initiated the development of generally accepted protocols for most comprehensive examinations of the mouse like the German Mouse Clinic Munich, Germany, the Eumorphia research program, or the Mouse Clinic Institute Strasbourg, France. To fully elucidate all consequences of certain genetic modifications or variations on the entire organism, these phenotyping centers will become important institutions for biological research. One good example for the scientific impact of these phenotyping centers is the characterization of the complex phenotype of the TUB001 mouse mutant line, described in this thesis. The close and interdisciplinary collaboration of experts from different fields of research at the GMC (immunology, clinical chemistry, morphology and pathology) was a prerequisite to uncover the pathophysiology of TUB001 animals, which subsequently enabled the connection between the TUB001- and FOP-phenotype.

In summary, the data generated in this thesis impressively demonstrate the power of combining well-standardized phenotyping protocols with large-scale mutagenesis approaches to identify mutant mouse lines with immunodeficiencies. Some of the newly described mutant mouse lines closely resemble the phenotype of well-documented human diseases and might serve as important immunological model systems for further investigations.

5 Summary

Although a number of traits for main functions of the immune system, like control of infections, susceptibility to autoimmune diseases or the prevention of cancer development, have been attributed to distinct genes, many of the factors contributing to the preservation of immunological homeostasis or regulation of specific immune functions are unknown. Therefore, several countries have initiated large-scale mutagenesis programs for the generation of new mouse models for *in vivo* analysis of distinct genes or gene functions. One of the main problems in these efforts is the standardized examination, in order to identify mutated mice with even minor alterations of biological parameters. Therefore, main goal of this thesis was the development and subsequent application of immunological screening methods for rapid and reliable identification of immunodeficiencies in individual mutant mice.

A standardized immunological screen was established to identify single mutants out of cohorts of ENU mutagenized mice with defects in immunological parameters under constant resting conditions, combining high throughput sample management with sensitive screening protocols. Basic requirements for the successful identification of abnormal phenotypes were well-controlled groups of mice, e.g. sex-, strain- and age-matched, and the robustness of the screening assays, which was achieved by strictly defined standard operation procedures for all experimental settings, including data acquisition and analysis. Since a newly identified immunodeficient ENU mutant has to be kept alive for further geno- and phenotyping, methods were limited to non-mouse-consuming assays, mainly based on the analysis of small volume blood samples. The cellular composition of the peripheral blood, determined by a complex FACS staining pattern, as well as measurement of immunoglobulin isotype concentrations and testing for the potential presence of autoimmune antibodies, performed by Bio-Plex and ELISA, turned out to be suitable for a sensitive and reproducible identification of mice with immunological alterations. Application of this screen on approximately 5000 ENU mutagenized mice allowed the identification of more than 80 variants, in which significantly altered immunological parameters could be identified, and for 21 of these variants germ line transmission was confirmed. Forty-five variants are still in the process of confirmation cross.

Since several immune functions are believed to be turned on specifically under challenge conditions, like the activation of innate and adaptive immune responses during pathogen invasion, effective mutations in these induction-dependent pathways are likely to be missed

when analyzing naïve mice. Therefore, we tested an *in vivo* challenge model using live bacteria in an advanced immunological screen to specifically identify mutants, which carry defective genes important for protective innate and adaptive immune responses.

For this infectious challenge screen, the bacterium *Listeria monocytogenes* (*L.m.*) was chosen as infecting agent, because of several specific advantages over other pathogens. For example the loss of ENU mutagenized mice with increased susceptibility towards *L.m.* infection can be prevented by antibiotic treatment, and there are many tools available for investigating innate and adaptive immune responses in mice against *L.m.*. Main task was to develop novel assay systems to measure the severity of infection under high-throughput conditions from blood samples, as well as to adapt antigen-specific T cell analysis to C3H mice, used in the ENU screen in Munich.

We identified INFγ concentrations and GOT enzyme activity in plasma samples to directly correlate with severity and progression of disease during the early phase of infection. With the identification of a novel H2-K^k restricted *Listeria* epitope $p60_{117\text{-}125}$, we succeeded to transfer the MHC-I Tetramer technology to C3H mice for Ag-specific T cell analysis. Measurement of the severity of recall infections allows determination of the ability to generate and maintain a functional and effective memory T cell response.

During establishment and standardization of the *L.m.* infection screen we made the surprising observation that gender strongly influences resistance towards infection. More detailed analysis revealed that females are more susceptible and respond with significantly higher plasma values of the immunosuppressive Interleukin 10. The interpretation that IL-10 is involved in the sex dependent susceptibility pattern was supported by experiments with IL-10 deficient mice, which demonstrated equal resistance between male and female individuals.

The scientific importance of ENU mutagenesis and standardized phenotyping lies especially in the identification of new mutant mouse lines, which can potentially serve as models for human diseases. One of the newly identified lines in this thesis, TUB001, had been followed up in more detail, because of the severity of the immunological disorders, comprising strong granulocytosis and lymphopenia in numerous organs. With age, TUB001 mice develop stiff extremities and calcifications mainly around the chest and upper abdomen. This phenotype is similar to a group of human diseases characterized by ectopic ossification. TUB001 mice closely resembles the most systemic form called Fibrodysplasia ossificans progressiva. Mapping of the genetic mutation causing the TUB001 phenotype was initiated and will hopefully lead to a better understanding of the pathophysiology of this disease in the near future.

6 References

Aguilar-Delfin, I., Homer, M. J., Wettstein, P. J., and Persing, D. H. (2001). Innate resistance to Babesia infection is influenced by genetic background and gender. Infect Immun *69*, 7955-7958.

Altare, F., Durandy, A., Lammas, D., Emile, J. F., Lamhamedi, S., Le Deist, F., Drysdale, P., Jouanguy, E., Doffinger, R., Bernaudin, F.*, et al.* (1998). Impairment of mycobacterial immunity in human interleukin-12 receptor deficiency. Science *280*, 1432-1435.

Altman, J. D., Moss, P. A., Goulder, P. J., Barouch, D. H., McHeyzer-Williams, M. G., Bell, J. I., McMichael, A. J., and Davis, M. M. (1996). Phenotypic analysis of antigen-specific T lymphocytes. Science *274*, 94-96.

Appleby, M. W., and Ramsdell, F. (2003). A forward-genetic approach for analysis of the immune system. Nat Rev Immunol *3*, 463-471.

Austin, C. P., Battey, J. F., Bradley, A., Bucan, M., Capecchi, M., Collins, F. S., Dove, W. F., Duyk, G., Dymecki, S., Eppig, J. T.*, et al.* (2004). The knockout mouse project. Nat Genet *36*, 921-924.

Auwerx, J., Avner, P., Baldock, R., Ballabio, A., Balling, R., Barbacid, M., Berns, A., Bradley, A., Brown, S., Carmeliet, P.*, et al.* (2004). The European dimension for the mouse genome mutagenesis program. Nat Genet *36*, 925-927.

Badovinac, V. P., Hamilton, S. E., and Harty, J. T. (2003). Viral infection results in massive CD8+ T cell expansion and mortality in vaccinated perforin-deficient mice. Immunity *18*, 463-474.

Balling, R. (1998). Modelsysteme Maus. In Lehrbuch der Genetik, W. Seyffert, ed. (Stuttgart, Gustav Fischer Verlag), pp. 309-322.

Baumgarth, N., and Roederer, M. (2000). A practical approach to multicolor flow cytometry for immunophenotyping. J Immunol Methods *243*, 77-97.

Beier, D. R., and Herron, B. J. (2004). Genetic mapping and ENU mutagenesis. Genetica *122*, 65-69.

Bergmeyer, H. U., and Horder, M. (1980). International federation of clinical chemistry. Scientific committee. Expert panel on enzymes. IFCC document stage 2, draft 1; 1979-11-19 with a view to an IFCC recommendation. IFCC methods for the measurement of catalytic concentration of enzymes. Part 3. IFCC method for alanine aminotransferase. J Clin Chem Clin Biochem *18*, 521-534.

Bergmeyer, H. U., Horder, M., and Rej, R. (1986). International Federation of Clinical Chemistry (IFCC) Scientific Committee, Analytical Section: approved recommendation (1985) on IFCC methods for the measurement of catalytic concentration of enzymes. Part 3. IFCC method for alanine aminotransferase (L-alanine: 2-oxoglutarate aminotransferase, EC 2.6.1.2). J Clin Chem Clin Biochem *24*, 481-495.

Beutler, B., Hoebe, K., and Shamel, L. (2004). Forward genetic dissection of afferent immunity: the role of TIR adapter proteins in innate and adaptive immune responses. C R Biol *327*, 571-580.

Boyse, E. A. (1977). The increasing value of congenic mice in biomedical research. Lab Anim Sci *27*, 771-781.

Bruton, O. C. (1952). Agammaglobulinemia. Pediatrics *9*, 722-728.

Bruton, O. C., Apt, L., Gitlin, D., and Janeway, C. A. (1952). Absence of serum gamma globulins. AMA Am J Dis Child *84*, 632-636.

Buchmeier, N. A., and Schreiber, R. D. (1985). Requirement of endogenous interferon-gamma production for resolution of *Listeria monocytogenes* infection. Proc Natl Acad Sci U S A *82*, 7404-7408.

Buer, J., and Balling, R. (2003). Mice, microbes and models of infection. Nat Rev Genet *4*, 195-205.

Busch, D. H., Kerksiek, K., and Pamer, E. G. (1999). Processing of *Listeria monocytogenes* antigens and the *in vivo* T-cell response to bacterial infection. Immunol Rev *172*, 163-169.

Busch, D. H., and Pamer, E. G. (1998). MHC class I/peptide stability: implications for immunodominance, *in vitro* proliferation, and diversity of responding CTL. J Immunol *160*, 4441-4448.

Busch, D. H., and Pamer, E. G. (1999). T cell affinity maturation by selective expansion during infection. J Exp Med *189*, 701-710.

Busch, D. H., Pilip, I., and Pamer, E. G. (1998a). Evolution of a complex T cell receptor repertoire during primary and recall bacterial infection. J Exp Med *188*, 61-70.

Busch, D. H., Pilip, I. M., Vijh, S., and Pamer, E. G. (1998b). Coordinate regulation of complex T cell populations responding to bacterial infection. Immunity *8*, 353-362.

Carlson, C. M., Dupuy, A. J., Fritz, S., Roberg-Perez, K. J., Fletcher, C. F., and Largaespada, D. A. (2003). Transposon mutagenesis of the mouse germline. Genetics *165*, 243-256.

Chalfie, M., and Au, M. (1989). Genetic control of differentiation of the Caenorhabditis elegans touch receptor neurons. Science *243*, 1027-1033.

Clark, A. T., Goldowitz, D., Takahashi, J. S., Vitaterna, M. H., Siepka, S. M., Peters, L. L., Frankel, W. N., Carlson, G. A., Rossant, J., Nadeau, J. H., and Justice, M. J. (2004a). Implementing large-scale ENU mutagenesis screens in North America. Genetica *122*, 51-64.

Clark, K. J., Geurts, A. M., Bell, J. B., and Hackett, P. B. (2004b). Transposon vectors for gene-trap insertional mutagenesis in vertebrates. Genesis *39*, 225-233.

Conlan, J. W., and North, R. J. (1991). Neutrophil-mediated dissolution of infected host cells as a defense strategy against a facultative intracellular bacterium. J Exp Med *174*, 741-744.

Connor, J. M., and Evans, D. A. (1982a). Fibrodysplasia ossificans progressiva. The clinical features and natural history of 34 patients. J Bone Joint Surg Br *64*, 76-83.

Connor, J. M., and Evans, D. A. (1982b). Genetic aspects of fibrodysplasia ossificans progressiva. J Med Genet *19*, 35-39.

Dai, W. J., Kohler, G., and Brombacher, F. (1997). Both innate and acquired immunity to *Listeria monocytogenes* infection are increased in IL-10-deficient mice. J Immunol *158*, 2259-2267.

Denny, P., and Justice, M. J. (2000). Mouse as the measure of man? Trends Genet *16*, 283-287.

Egger, G., Liang, G., Aparicio, A., and Jones, P. A. (2004). Epigenetics in human disease and prospects for epigenetic therapy. Nature *429*, 457-463.

Eisenstein, B. I. (1990). The polymerase chain reaction. A new method of using molecular genetics for medical diagnosis. N Engl J Med *322*, 178-183.

Falini, B., and Taylor, C. R. (1983). New developments in immunoperoxidase techniques and their application. Arch Pathol Lab Med *107*, 105-117.

Feldman, G., Li, M., Martin, S., Urbanek, M., Urtizberea, J. A., Fardeau, M., LeMerrer, M., Connor, J. M., Triffitt, J., Smith, R.*, et al.* (2000). Fibrodysplasia ossificans progressiva, a heritable disorder of severe heterotopic ossification, maps to human chromosome 4q27-31. Am J Hum Genet *66*, 128-135.

Fischer, A. (2001). Primary immunodeficiency diseases: an experimental model for molecular medicine. Lancet *357*, 1863-1869.

Fischer, A. (2002). Natural mutants of the immune system: a lot to learn! Eur J Immunol *32*, 1519-1523.

Fischer, A. (2004). Human primary immunodeficiency diseases: a perspective. Nat Immunol *5*, 23-30.

Flaswinkel, H., Alessandrini, F., Rathkolb, B., Decker, T., Kremmer, E., Servatius, A., Jakob, T., Soewarto, D., Marschall, S., Fella, C.*, et al.* (2000). Identification of immunological relevant phenotypes in ENU mutagenized mice. Mamm Genome *11*, 526-527.

Fulton, R. J., McDade, R. L., Smith, P. L., Kienker, L. J., and Kettman, J. R., Jr. (1997). Advanced multiplexed analysis with the FlowMetrix system. Clin Chem *43*, 1749-1756.

Garcia-Martinez, L. F., Appleby, M. W., Staehling-Hampton, K., Andrews, D. M., Chen, Y., McEuen, M., Tang, P., Rhinehart, R. L., Proll, S., Paeper, B.*, et al.* (2004). A novel mutation in CD83 results in the development of a unique population of CD4+ T cells. J Immunol *173*, 2995-3001.

Gellin, B. G., and Broome, C. V. (1989). Listeriosis. Jama *261*, 1313-1320.

Giannini, M. S. (1986). Sex-influenced response in the pathogenesis of cutaneous leishmaniasis in mice. Parasite Immunol *8*, 31-37.

Glass, A. S., and Dahm, R. (2004). The zebrafish as a model organism for eye development. Ophthalmic Res *36*, 4-24.

Graw, J., Klopp, N., Loster, J., Soewarto, D., Fuchs, H., Becker-Follmann, J., Reis, A., Wolf, E., Balling, R., and Habre de Angelis, M. (2001). Ethylnitrosourea-induced mutation in mice leads to the expression of a novel protein in the eye and to dominant cataracts. Genetics *157*, 1313-1320.

Greco, R., Ouwerkerk, P. B., Sallaud, C., Kohli, A., Colombo, L., Puigdomenech, P., Guiderdoni, E., Christou, P., Hoge, J. H., and Pereira, A. (2001). Transposon insertional mutagenesis in rice. Plant Physiol *125*, 1175-1177.

Gregory, S. G., Sekhon, M., Schein, J., Zhao, S., Osoegawa, K., Scott, C. E., Evans, R. S., Burridge, P. W., Cox, T. V., Fox, C. A.*, et al.* (2002). A physical map of the mouse genome. Nature *418*, 743-750.

Guha, U., Gomes, W. A., Kobayashi, T., Pestell, R. G., and Kessler, J. A. (2002). *In vivo* evidence that BMP signaling is necessary for apoptosis in the mouse limb. Dev Biol *249*, 108-120.

Guilbault, C., Stotland, P., Lachance, C., Tam, M., Keller, A., Thompson-Snipes, L., Cowley, E., Hamilton, T. A., Eidelman, D. H., Stevenson, M. M., and Radzioch, D. (2002). Influence of gender and interleukin-10 deficiency on the inflammatory response during lung infection with Pseudomonas aeruginosa in mice. Immunology *107*, 297-305.

Han, J. S., and Boeke, J. D. (2004). A highly active synthetic mammalian retrotransposon. Nature *429*, 314-318.

Harty, J. T., and Bevan, M. J. (1992). CD8+ T cells specific for a single nonamer epitope of *Listeria monocytogenes* are protective *in vivo*. J Exp Med *175*, 1531-1538.

Harty, J. T., Lenz, L. L., and Bevan, M. J. (1996). Primary and secondary immune responses to *Listeria monocytogenes*. Curr Opin Immunol *8*, 526-530.

Hoebe, K., Du, X., Georgel, P., Janssen, E., Tabeta, K., Kim, S. O., Goode, J., Lin, P., Mann, N., Mudd, S.*, et al.* (2003a). Identification of Lps2 as a key transducer of MyD88-independent TIR signalling. Nature *424*, 743-748.

Hoebe, K., Du, X., Goode, J., Mann, N., and Beutler, B. (2003b). Lps2: a new locus required for responses to lipopolysaccharide, revealed by germline mutagenesis and phenotypic screening. J Endotoxin Res *9*, 250-255.

Hoebe, K., Georgel, P., Rutschmann, S., Du, X., Mudd, S., Crozat, K., Sovath, S., Shamel, L., Hartung, T., Zahringer, U., and Beutler, B. (2005). CD36 is a sensor of diacylglycerides. Nature *433*, 523-527.

Houwen, B. (1992). Reticulocyte maturation. Blood Cells *18*, 167-186.

Hozumi, K., Negishi, N., Suzuki, D., Abe, N., Sotomaru, Y., Tamaoki, N., Mailhos, C., Ish-Horowicz, D., Habu, S., and Owen, M. J. (2004). Delta-like 1 is necessary for the generation of marginal zone B cells but not T cells *in vivo*. Nat Immunol *5*, 638-644.

Hrabe de Angelis, M., and Balling, R. (1998). Large scale ENU screens in the mouse: genetics meets genomics. Mutat Res *400*, 25-32.

Hrabe de Angelis, M., McIntyre, J., 2nd, and Gossler, A. (1997). Maintenance of somite borders in mice requires the Delta homologue DII1. Nature *386*, 717-721.

http://www.gsf.de/ieg/groups/enu/mutants/index.html (2004). The ENU-Mouse Mutagenesis Screen Project (German Human Genome Project).

Huster, K. M., Busch, V., Schiemann, M., Linkemann, K., Kerksiek, K. M., Wagner, H., and Busch, D. H. (2004). Selective expression of IL-7 receptor on memory T cells identifies early CD40L-dependent generation of distinct CD8+ memory T cell subsets. Proc Natl Acad Sci U S A *101*, 5610-5615.

Inoue, M., Sakuraba, Y., Motegi, H., Kubota, N., Toki, H., Matsui, J., Toyoda, Y., Miwa, I., Terauchi, Y., Kadowaki, T.*, et al.* (2004). A series of maturity onset diabetes of the young, type 2 (MODY2) mouse models generated by a large-scale ENU mutagenesis program. Hum Mol Genet *13*, 1147-1157.

International-Human-Genome-Sequencing-Consortium (2004). Finishing the euchromatic sequence of the human genome. Nature *431*, 931-945.

Jackson, I. J. (1994). Molecular and developmental genetics of mouse coat color. Annu Rev Genet *28*, 189-217.

Jackson, I. J., and Bennett, D. C. (1990). Identification of the albino mutation of mouse tyrosinase by analysis of an *in vitro* revertant. Proc Natl Acad Sci U S A *87*, 7010-7014.

Janeway, C. A., Travers, P., Walport, M., and Shlomchik, M. (2001). Immunobiology: the immun system in health and disease, 5ed edn (New York, Garland Publishing).

Janssen, E. M., Lemmens, E. E., Wolfe, T., Christen, U., von Herrath, M. G., and Schoenberger, S. P. (2003). CD4+ T cells are required for secondary expansion and memory in CD8+ T lymphocytes. Nature *421*, 852-856.

Jiang, Y. H., Bressler, J., and Beaudet, A. L. (2004). Epigenetics and human disease. Annu Rev Genomics Hum Genet *5*, 479-510.

Joshi, A. (2003). Evolutionary genetics: the Drosophila model. J Genet *82*, 77-78.

Jouanguy, E., Altare, F., Lamhamedi-Cherradi, S., and Casanova, J. L. (1997). Infections in IFNGR-1-deficient children. J Interferon Cytokine Res *17*, 583-587.

Jun, J. E., Wilson, L. E., Vinuesa, C. G., Lesage, S., Blery, M., Miosge, L. A., Cook, M. C., Kucharska, E. M., Hara, H., Penninger, J. M.*, et al.* (2003). Identifying the MAGUK protein Carma-1 as a central regulator of humoral immune responses and atopy by genome-wide mouse mutagenesis. Immunity *18*, 751-762.

Justice, M. J., Carpenter, D. A., Favor, J., Neuhauser-Klaus, A., Hrabe de Angelis, M., Soewarto, D., Moser, A., Cordes, S., Miller, D., Chapman, V.*, et al.* (2000). Effects of ENU dosage on mouse strains. Mamm Genome *11*, 484-488.

Justice, M. J., Noveroske, J. K., Weber, J. S., Zheng, B., and Bradley, A. (1999). Mouse ENU mutagenesis. Hum Mol Genet *8*, 1955-1963.

Kan, L., Hu, M., Gomes, W. A., and Kessler, J. A. (2004). Transgenic mice overexpressing BMP4 develop a fibrodysplasia ossificans progressiva (FOP)-like phenotype. Am J Pathol *165*, 1107-1115.

Kaplan, F. S., Tabas, J. A., Gannon, F. H., Finkel, G., Hahn, G. V., and Zasloff, M. A. (1993). The histopathology of fibrodysplasia ossificans progressiva. An endochondral process. J Bone Joint Surg Am *75*, 220-230.

Kaufmann, S. H. (1995). Immunity to intracellular microbial pathogens. Immunol Today *16*, 338-342.

Kawai, T., Adachi, O., Ogawa, T., Takeda, K., and Akira, S. (1999). Unresponsiveness of MyD88-deficient mice to endotoxin. Immunity *11*, 115-122.

Kern, F., Faulhaber, N., Frommel, C., Khatamzas, E., Prosch, S., Schonemann, C., Kretzschmar, I., Volkmer-Engert, R., Volk, H. D., and Reinke, P. (2000). Analysis of CD8 T cell reactivity to cytomegalovirus using protein-spanning pools of overlapping pentadecapeptides. Eur J Immunol *30*, 1676-1682.

Knabel, M., Franz, T. J., Schiemann, M., Wulf, A., Villmow, B., Schmidt, B., Bernhard, H., Wagner, H., and Busch, D. H. (2002). Reversible MHC multimer staining for functional isolation of T-cell populations and effective adoptive transfer. Nat Med *8*, 631-637.

Kuhn, R., Lohler, J., Rennick, D., Rajewsky, K., and Muller, W. (1993). Interleukin-10-deficient mice develop chronic enterocolitis. Cell *75*, 263-274.

Kuhn, R., Schwenk, F., Aguet, M., and Rajewsky, K. (1995). Inducible gene targeting in mice. Science *269*, 1427-1429.

Kursar, M., Bonhagen, K., Fensterle, J., Kohler, A., Hurwitz, R., Kamradt, T., Kaufmann, S. H., and Mittrucker, H. W. (2002). Regulatory CD4+CD25+ T cells restrict memory CD8+ T cell responses. J Exp Med *196*, 1585-1592.

Lee, J. W., Lee, E. J., Hong, S. H., Chung, W. H., Lee, H. T., Lee, T. W., Lee, J. R., Kim, H. T., Suh, J. G., Kim, T. Y., and Ryoo, Z. Y. (2001). Circling mouse: possible animal model for deafness. Comp Med *51*, 550-554.

Lee, M. P. (2003). Genome-wide analysis of epigenetics in cancer. Ann N Y Acad Sci *983*, 101-109.

Lengeling, A., Pfeffer, K., and Balling, R. (2001). The battle of two genomes: genetics of bacterial host/pathogen interactions in mice. Mamm Genome *12*, 261-271.

Leonard, W. J. (2001). Cytokines and immunodeficiency diseases. Nat Rev Immunol *1*, 200-208.

Lindblad-Toh, K., Winchester, E., Daly, M. J., Wang, D. G., Hirschhorn, J. N., Laviolette, J. P., Ardlie, K., Reich, D. E., Robinson, E., Sklar, P.*, et al.* (2000). Large-scale discovery and genotyping of single-nucleotide polymorphisms in the mouse. Nat Genet *24*, 381-386.

Liu, X. S., Xu, Y., Hardy, L., Khammanivong, V., Zhao, W., Fernando, G. J., Leggatt, G. R., and Frazer, I. H. (2003). IL-10 mediates suppression of the CD8 T cell IFN-gamma response to a novel viral epitope in a primed host. J Immunol *171*, 4765-4772.

Liva, S. M., and Voskuhl, R. R. (2001). Testosterone acts directly on CD4+ T lymphocytes to increase IL-10 production. J Immunol *167*, 2060-2067.

Ma, J., Xu, J., Madaio, M. P., Peng, Q., Zhang, J., Grewal, I. S., Flavell, R. A., and Craft, J. (1996). Autoimmune lpr/lpr mice deficient in CD40 ligand: spontaneous Ig class switching with dichotomy of autoantibody responses. J Immunol *157*, 417-426.

Maecker, H. T., Dunn, H. S., Suni, M. A., Khatamzas, E., Pitcher, C. J., Bunde, T., Persaud, N., Trigona, W., Fu, T. M., Sinclair, E.*, et al.* (2001). Use of overlapping peptide mixtures as antigens for cytokine flow cytometry. J Immunol Methods *255*, 27-40.

Mak, T. W., Penninger, J. M., and Ohashi, P. S. (2001). Knockout mice: a paradigm shift in modern immunology. Nat Rev Immunol *1*, 11-19.

Merrick, J. C., Edelson, B. T., Bhardwaj, V., Swanson, P. E., and Unanue, E. R. (1997). Lymphocyte apoptosis during early phase of *Listeria* infection in mice. Am J Pathol *151*, 785-792.

Moore, K. W., O'Garra, A., de Waal Malefyt, R., Vieira, P., and Mosmann, T. R. (1993). Interleukin-10. Annu Rev Immunol *11*, 165-190.

Nadeau, J. H., Balling, R., Barsh, G., Beier, D., Brown, S. D., Bucan, M., Camper, S., Carlson, G., Copeland, N., Eppig, J.*, et al.* (2001). Sequence interpretation. Functional annotation of mouse genome sequences. Science *291*, 1251-1255.

Nichols, K. E. (2000). X-linked lymphoproliferative disease: genetics and biochemistry. Rev Immunogenet *2*, 256-266.

Nolan, P. M., Peters, J., Strivens, M., Rogers, D., Hagan, J., Spurr, N., Gray, I. C., Vizor, L., Brooker, D., Whitehill, E.*, et al.* (2000a). A systematic, genome-wide, phenotype-driven mutagenesis programme for gene function studies in the mouse. Nat Genet *25*, 440-443.

Nolan, P. M., Peters, J., Vizor, L., Strivens, M., Washbourne, R., Hough, T., Wells, C., Glenister, P., Thornton, C., Martin, J.*, et al.* (2000b). Implementation of a large-scale ENU mutagenesis program: towards increasing the mouse mutant resource. Mamm Genome *11*, 500-506.

Noveroske, J. K., Weber, J. S., and Justice, M. J. (2000). The mutagenic action of N-ethyl-N-nitrosourea in the mouse. Mamm Genome *11*, 478-483.

O'Brien, M. C., and Bolton, W. E. (1995). Comparison of cell viability probes compatible with fixation and permeabilization for combined surface and intracellular staining in flow cytometry. Cytometry *19*, 243-255.

Ouchterlony, O. (1962). Quantitative immunoelectrophoresis. Acta Pathol Microbiol Scand *Suppl 154*, 252-254.

Pamer, E. G., Sijts, A. J., Villanueva, M. S., Busch, D. H., and Vijh, S. (1997). MHC class I antigen processing of *Listeria monocytogenes* proteins: implications for dominant and subdominant CTL responses. Immunol Rev *158*, 129-136.

Pandolfi, P. P., Roth, M. E., Karis, A., Leonard, M. W., Dzierzak, E., Grosveld, F. G., Engel, J. D., and Lindenbaum, M. H. (1995). Targeted disruption of the GATA3 gene causes severe abnormalities in the nervous system and in fetal liver haematopoiesis. Nat Genet *11*, 40-44.

Payet, M. E., Woodward, E. C., and Conrad, D. H. (1999). Humoral response suppression observed with CD23 transgenics. J Immunol *163*, 217-223.

Plitz, T., Huffstadt, U., Endres, R., Schaller, E., Mak, T. W., Wagner, H., and Pfeffer, K. (1999). The resistance against *Listeria monocytogenes* and the formation of germinal centers depend on a functional death domain of the 55 kDa tumor necrosis factor receptor. Eur J Immunol *29*, 581-591.

Purtilo, D. T., Grierson, H. L., Davis, J. R., and Okano, M. (1991). The X-linked lymphoproliferative disease: from autopsy toward cloning the gene 1975-1990. Pediatr Pathol *11*, 685-710.

Rajewsky, K., Gu, H., Kuhn, R., Betz, U. A., Muller, W., Roes, J., and Schwenk, F. (1996). Conditional gene targeting. J Clin Invest *98*, 600-603.

Rastan, S., Hough, T., Kierman, A., Hardisty, R., Erven, A., Gray, I. C., Voeling, S., Isaacs, A., Tsai, H., Strivens, M.*, et al.* (2004). Towards a mutant map of the mouse--new models of neurological, behavioural, deafness, bone, renal and blood disorders. Genetica *122*, 47-49.

Rinchik, E. M., Bangham, J. W., Hunsicker, P. R., Cacheiro, N. L., Kwon, B. S., Jackson, I. J., and Russell, L. B. (1990). Genetic and molecular analysis of chlorambucil-induced germ-line mutations in the mouse. Proc Natl Acad Sci U S A *87*, 1416-1420.

Roberts, C. W., Cruickshank, S. M., and Alexander, J. (1995). Sex-determined resistance to Toxoplasma gondii is associated with temporal differences in cytokine production. Infect Immun *63*, 2549-2555.

Roers, A., Siewe, L., Strittmatter, E., Deckert, M., Schluter, D., Stenzel, W., Gruber, A. D., Krieg, T., Rajewsky, K., and Muller, W. (2004). T cell-specific inactivation of the interleukin 10 gene in mice results in enhanced T cell responses but normal innate responses to lipopolysaccharide or skin irritation. J Exp Med *200*, 1289-1297.

Rogers, J. G., and Geho, W. B. (1979). Fibrodysplasia ossificans progressiva. A survey of forty-two cases. J Bone Joint Surg Am *61*, 909-914.

Rogner, U. C., and Avner, P. (2003). Congenic mice: cutting tools for complex immune disorders. Nat Rev Immunol *3*, 243-252.

Russell, W. L., Kelly, E. M., Hunsicker, P. R., Bangham, J. W., Maddux, S. C., and Phipps, E. L. (1979). Specific-locus test shows ethylnitrosourea to be the most potent mutagen in the mouse. Proc Natl Acad Sci U S A *76*, 5818-5819.

Sakaguchi, S. (2000). Regulatory T cells: key controllers of immunologic self-tolerance. Cell *101*, 455-458.

Salem, M. L. (2004). Estrogen, A Double-Edged Sword: Modulation of TH1- and TH2-Mediated Inflammations by Differential Regulation of TH1/TH2 Cytokine Production. Curr Drug Targets Inflamm Allergy *3*, 97-104.

Schubart, D. B., Rolink, A., Schubart, K., and Matthias, P. (2000). Cutting edge: lack of peripheral B cells and severe agammaglobulinemia in mice simultaneously lacking Bruton's tyrosine kinase and the B cell-specific transcriptional coactivator OBF-1. J Immunol *164*, 18-22.

Schutt, C., Eggers, G., Schroder, I., Kruse, H., Schulz, M., and Blau, H. J. (1983). [Discrepancy between the clinical and immunologic picture of *in vitro* diagnosis during transfer factor therapy in a patient with Wiscott-Aldrich syndrome]. Folia Haematol Int Mag Klin Morphol Blutforsch *110*, 677-684.

Seyama, K., Nonoyama, S., Gangsaas, I., Hollenbaugh, D., Pabst, H. F., Aruffo, A., and Ochs, H. D. (1998). Mutations of the CD40 ligand gene and its effect on CD40 ligand expression in patients with X-linked hyper IgM syndrome. Blood *92*, 2421-2434.

Shafritz, A. B., Shore, E. M., Gannon, F. H., Zasloff, M. A., Taub, R., Muenke, M., and Kaplan, F. S. (1996). Overexpression of an osteogenic morphogen in fibrodysplasia ossificans progressiva. N Engl J Med *335*, 555-561.

Shedlock, D. J., and Shen, H. (2003). Requirement for CD4 T cell help in generating functional CD8 T cell memory. Science *300*, 337-339.

Shifman, S., and Darvasi, A. (2004). Mouse inbred strain sequence information and Yin-Yang crosses for QTL fine mapping. Genetics.

Shultz, L. D. (1991). Immunological mutants of the mouse. Am J Anat *191*, 303-311.

Sijts, A. J., Pilip, I., and Pamer, E. G. (1997). The *Listeria monocytogenes*-secreted p60 protein is an N-end rule substrate in the cytosol of infected cells. Implications for major histocompatibility complex class I antigen processing of bacterial proteins. J Biol Chem *272*, 19261-19268.

Smith, L. J. (2004). Paroxysmal nocturnal hemoglobinuria. Clin Lab Sci *17*, 172-177.

Soewarto, D., Blanquet, V., and Hrabe de Angelis, M. (2003). Random ENU mutagenesis. Methods Mol Biol *209*, 249-266.

Soewarto, D., Fella, C., Teubner, A., Rathkolb, B., Pargent, W., Heffner, S., Marschall, S., Wolf, E., Balling, R., and Hrabe de Angelis, M. (2000). The large-scale Munich ENU-mouse-mutagenesis screen. Mamm Genome *11*, 507-510.

Sokolowski, M. B. (2001). Drosophila: genetics meets behaviour. Nat Rev Genet *2*, 879-890.

Stewart, P. E., Hoff, J., Fischer, E., Krum, J. G., and Rosa, P. A. (2004). Genome-wide transposon mutagenesis of Borrelia burgdorferi for identification of phenotypic mutants. Appl Environ Microbiol *70*, 5973-5979.

Strober, W., and Chua, K. (2000). Common variable immunodeficiency. Clin Rev Allergy Immunol *19*, 157-181.

Sun, J. C., and Bevan, M. J. (2003). Defective CD8 T cell memory following acute infection without CD4 T cell help. Science *300*, 339-342.

Takakura, R., Kiyohara, T., Murayama, Y., Miyazaki, Y., Miyoshi, Y., Shinomura, Y., and Matsuzawa, Y. (2002). Enhanced macrophage responsiveness to lipopolysaccharide and CD40 stimulation in a murine model of inflammatory bowel disease: IL-10-deficient mice. Inflamm Res *51*, 409-415.

To, C., Epp, T., Reid, T., Lan, Q., Yu, M., Li, C. Y., Ohishi, M., Hant, P., Tsao, N., Casallo, G.*, et al.* (2004). The Centre for Modeling Human Disease Gene Trap resource. Nucleic Acids Res *32 Database issue*, D557-559.

Traver, D., Herbomel, P., Patton, E. E., Murphey, R. D., Yoder, J. A., Litman, G. W., Catic, A., Amemiya, C. T., Zon, L. I., and Trede, N. S. (2003). The zebrafish as a model organism to study development of the immune system. Adv Immunol *81*, 253-330.

Van de Vijver, G., Van Speybroeck, L., and De Waele, D. (2002). Epigenetics: a challenge for genetics, evolution, and development? Ann N Y Acad Sci *981*, 1-6.

van der Pouw Kraan, T. C., Kasperkovitz, P. V., Verbeet, N., and Verweij, C. L. (2004). Genomics in the immune system. Clin Immunol *111*, 175-185.

Venter, J. C., Adams, M. D., Myers, E. W., Li, P. W., Mural, R. J., Sutton, G. G., Smith, H. O., Yandell, M., Evans, C. A., Holt, R. A.*, et al.* (2001). The sequence of the human genome. Science *291*, 1304-1351.

Vihinen, M., Mattsson, P. T., and Smith, C. I. (2000). Bruton tyrosine kinase (BTK) in X-linked agammaglobulinemia (XLA). Front Biosci *5*, D917-928.

Vinuesa, C. G., and Goodnow, C. C. (2004). Illuminating autoimmune regulators through controlled variation of the mouse genome sequence. Immunity *20*, 669-679.

Voelker, L. L., and Dybvig, K. (1998). Transposon mutagenesis. Methods Mol Biol *104*, 235-238.

Vreugde, S., Erven, A., Kros, C. J., Marcotti, W., Fuchs, H., Kurima, K., Wilcox, E. R., Friedman, T. B., Griffith, A. J., Balling, R.*, et al.* (2002). Beethoven, a mouse model for dominant, progressive hearing loss DFNA36. Nat Genet *30*, 257-258.

Waterston, R. H., Lindblad-Toh, K., Birney, E., Rogers, J., Abril, J. F., Agarwal, P., Agarwala, R., Ainscough, R., Alexandersson, M., An, P.*, et al.* (2002). Initial sequencing and comparative analysis of the mouse genome. Nature *420*, 520-562.

Wong, P., and Pamer, E. G. (2003a). CD8 T cell responses to infectious pathogens. Annu Rev Immunol *21*, 29-70.

Wong, P., and Pamer, E. G. (2003b). Feedback regulation of pathogen-specific T cell priming. Immunity *18*, 499-511.

World-Health-Organization (2003). The World Health Report 2003 - Shaping the Future (Geneva, World Health Organization).

Wurst, W., Rossant, J., Prideaux, V., Kownacka, M., Joyner, A., Hill, D. P., Guillemot, F., Gasca, S., Cado, D., Auerbach, A., and et al. (1995). A large-scale gene-trap screen for insertional mutations in developmentally regulated genes in mice. Genetics *139*, 889-899.

Zhang, Y., Ma, C., Delohery, T., Nasipak, B., Foat, B. C., Bounoutas, A., Bussemaker, H. J., Kim, S. K., and Chalfie, M. (2002). Identification of genes expressed in C. elegans touch receptor neurons. Nature *418*, 331-335.

Zhu, J., Min, B., Hu-Li, J., Watson, C. J., Grinberg, A., Wang, Q., Killeen, N., Urban, J. F., Jr., Guo, L., and Paul, W. E. (2004). Conditional deletion of Gata3 shows its essential function in T(H)1-T(H)2 responses. Nat Immunol *5*, 1157-1165.

7 Acknowledgements

I would like to take the opportunity to thank all the people supporting me during this thesis, either scientifically or concerning private issues.

First of all I would like to acknowledge all the people of the Busch laboratory, in particular the team working together with me for nearly 3 years at the GMC (GSF, Neuherberg). I would like to thank the technicians, Christine Fürmann, Florian Schleicher and Kerstin Kutzner for their excellent technical assistance and the friendly atmosphere in the laboratory, as well as Dr. S. Kalaydjiev for fruitful scientific discussions and his practical support during the last years. I also credit the coordinators of the GMC Dr. V. Gailus-Durner and Dr. H. Fuchs and the head of the Institute of Experimental Genetics, Prof. Dr. M. Hrabe de Angelis, for the productive scientific environment at the GMC.
Furthermore, I would like to acknowledge our partners at the GBF in Braunschweig, Dr. A. Lenggeling and Dr. B. Pasche, for the collaboration in the project of sex dependent susceptibility against *L.m.* infection. Many thanks to Sandra Kunder and Prof. Dr. L. Quintilla-Fend from the Institute for Pathology at the GSF for the help with the histological analysis of the TUB001 mouse, to Dr. Helmut Fuchs of the Institute of Experimental Genetics at the GSF for his efforts concerning X-ray and computer tomography experiments, Dr M. Klempt for the help with the GOT/GPT assays and to Dr. S. Wagner and Dr. D. Michels from the Institute of Experimental Genetics for the organization of the ENU treatment of mice.
Especially I would like to thank Prof. Dr. D.H. Busch, who gave me the opportunity to carry out this PhD in his laboratory and his excellent support. I would like to thank him for always finding time for discussions, providing new ideas and giving the needed feedback for the progress of this project.

Finally, I would like to thank the people in my private environment for their assistance, namely Christine and my friends Sebastian, René and Wolfgang. Last but not least, many thanks to my brother and above all to my parents, who supported me not only during this thesis but also during my whole studies.